PHYSICAL REVIEW
LETTERS

VOLUME 5 DECEMBER 15, 1960 NUMBER 12

ISOTOPIC COMPOSITION OF SILVER IN AN IRON METEORITE*

V. Rama Murthy
School of Science and Engineering, University of California, La Jolla, California
(Received November 21, 1960)

The recent discovery of radiogenic Xe^{129} in Richardton chondrite by Reynolds[1] has emphasized the importance of a search for extinct radioactivities. Several such possible nuclides have been suggested.[2,3] As part of a program of investigating the isotopic composition and abundances of several elements in meteorites, the isotopic composition of silver in the troilite of Toluca iron meteorite was determined and this paper discusses the results.

Pd^{107} is an extinct radioactive nuclide which decays to Ag^{107}. The half-life of this decay is reported to be 7.5×10^6 years by Sullivan.[4] During the formation and separation of silicate and metal phases of meteorites, Pd will be incorporated into the metal phase because of its siderophile nature. Goldschmidt[5] classified silver as both a siderophile and chalcophile though the observational data for the meteorites are unreliable. Thermodynamic calculations assuming ideal solution laws for Ag_2S in troilite and silver in iron-nickel substantiate a siderophile classification. However, ideal solution laws may not apply because elemental silver forms a two-liquid system with molten iron and hence the calculations must indicate a more siderophile character than is actually the case. Silver, therefore, is likely to be fractionated from Pd in the metal phase. If the formation of the metal phase of meteorites happened within a few half-lives of Pd^{107} after the end of nucleosynthesis, because of the above-mentioned fractionation between Pd and Ag, the metallic phase is likely to show an enrichment of Ag^{107} as a result of decay of Pd^{107}. During the subsequent cooling of the metal phase and formation of the troilite nodules, it is possible that the Ag^{107}-enriched silver from the metal phase was concentrated in the troilite.

Silver was extracted from the troilite of Toluca meteorite by ion exchange techniques (to be published elsewhere). A few micrograms of Ag were isolated and mounted on a tantalum filament as Ag_2S and a drop of 2% NH_4NO_3 was added to the filament. The mass spectrometer used was a 12-in. radius and 60°-deflection instrument built by Nuclide Analysis Associates.

The results of measurement of the isotopic composition of silver in Toluca troilite and of silver from reagent grade Baker and Adams $AgNO_3$ are given in Table I. The data are reported as measured in both cases without any corrections. It is possible that our mass spectrometer has a systematic mass discrimination in the range of silver isotopes, but this will not affect a comparison of terrestrial silver with

Table I. Isotopic compositions of silver in Toluca troilite and terrestrial silver.

Sample	Ag^{107}/Ag^{109}	No. of ratios
Toluca troilite		
Run I	1.097 ± 0.002	14
Run II	1.100 ± 0.002	15
Run III	1.094 ± 0.002	20
Average	1.097 ± 0.002	
Reagent $AgNO_3$ - I	1.076 ± 0.002	22
Reagent $AgNO_3$ - II	1.072 ± 0.002	18

meteoritic silver; any systematic discrimination would affect both measurements equally.

The isotopic composition of Ag in Toluca troilite was measured as three sets of data, each set comprising 14 to 20 ratios of Ag^{107}/Ag^{109}, during a six-hour run of stable emission. The mean value of Ag^{107}/Ag^{109} in Toluca troilite is 1.097 $\pm$ 0.002. Our measurement of Ag^{107}/Ag^{109} ratio of terrestrial Ag, using reagent grade $AgNO_3$, is within experimental error the same as the value of 1.0756 for the Ag standard of the National Bureau of Standards and several other samples of terrestrial Ag as carefully measured by Shields, Craig, and Dibeler.[6]

Hess, Marshall, and Urey[7] analyzed the composition of silver in Toluca troilite and found that silver in this meteorite was very similar to terrestrial silver. However, their estimated experimental error was large enough to mask the 2% enrichment of Ag^{107}/Ag^{109} ratio in Toluca troilite, reported in this work.

The excess Ag^{107} in Toluca troilite may have been caused by selective fractionation of the light isotope of Ag into the troilite during long period of cooling of the iron phase, estimated by Urey[8] to be of the order of 10^7 - 10^8 years, or, by some nuclear processes during the last stages of nucleosynthesis, in the solar system.[9] However, if the excess Ag^{107} in the Toluca troilite is attributed to the decay of Pd^{107}, the time interval, Δt, between the end of nucleosynthesis and the formation of iron meteorites can be estimated.

In the "sudden synthesis" model, which postulates element formation in one event, Δt is given by

$$\Delta t = \tau_{107}[\ln(Pd^{105}/Ag^{107*}) + \ln(Pd^{107}/Pd^{105})],$$

where τ_{107} is the mean life of Pd^{107}, (Pd^{105}/Ag^{107*}) is the ratio of Pd^{105} to radiogenic Ag^{107} in the meteorite, and (Pd^{107}/Pd^{105}) is the ratio of these isotopes at the end of nucleosynthesis. The Pd content of Toluca iron meteorite is reported to be 4.72 ppm by Goldberg, Uchiyama, and Brown.[10] Judging from the cosmic abundance curve of Suess and Urey[11] at Pd mass region, the ratio of the abundances of two neighboring odd-mass nuclides, Pd^{107}/Pd^{105}, can be taken to be about unity. The silver content of iron meteorites is not well known. Hess, Marshall, and Urey report less than 0.2 ppm in the Canyon Diablo iron and Lovering[12] reports less than 0.5 ppm in three troilites including Toluca. Assuming a silver content of 0.1 ppm in Toluca iron, Δt in the "sudden synthesis" model is about 8.4×10^7 years.

In the more commonly accepted "continuous synthesis" model of Burbidge, Burbidge, Fowler, and Hoyle,[13] the Pd^{107} abundance at the end of nucleosynthesis is expected to be in steady-state proportions. In this model, Δt is given by

$$\Delta t = \tau_{107}[\ln(Pd^{105}/Ag^{107*}) + \ln(Pd^{107}/Pd^{105}) + \ln(\tau_{107}/T)].$$

The value of Δt in this model is 10^7 years. This estimate of Δt is perhaps not very significant because the half-life of Pd^{107} is short compared to the total time span of nucleosynthesis, T, of the order of 10^{10} years. The abundance of Pd^{107} at the end of nucleosynthesis will depend to a large extent only on the production of this isotope in the last supernova. On this basis, assuming a Pd^{107}/Pd^{105} ratio of 0.1 at the end of a "continuous model" nucleosynthesis, Δt is about 4.5×10^7 years. This estimate of Δt is similar to the value of 4×10^7 years obtained for Canyon Diablo iron by Anders and Stevens[14] using the Pb^{205}-Tl^{205} decay scheme. These estimates of Δt are still not precise enough to evaluate the role of many other shorter lived radioactivities in the early development of meteorites and other planets.

Further work is in progress to look for this effect in other iron meteorites, particularly those which are rich in Pd.

I wish to thank Professor H. C. Urey, University of California, La Jolla, for helpful discussions.

*Work supported by the U. S. Atomic Energy Commission.

[1]J. H. Reynolds, Phys. Rev. Letters 4, 8 (1960).
[2]T. P. Kohman, Ann. N. Y. Acad. Sci. 62, 503 (1953).
[3]H. C. Urey, Proc. Natl. Acad. Sci. (U.S.) 41, 127 (1955).
[4]W. H. Sullivan, Trilinear Chart of Nuclides (U. S. Government Printing Office, Washington, D. C., 1957).
[5]V. M. Goldschmidt, Geochemistry (Clarendon Press, Oxford, 1954).
[6]W. R. Shields, D. N. Craig, and V. H. Dibeler (unpublished work, 1960).
[7]D. C. Hess, R. R. Marshall, and H. C. Urey, Science 126, 1291 (1957).
[8]H. C. Urey, Astrophys. J. 124, 625 (1956).
[9]W. A. Fowler (private communication).
[10]E. Goldberg, A. Uchiyama, and H. Brown, Geochim. et Cosmochim. Acta 2, 1 (1951).
[11]H. E. Suess and H. C. Urey, Revs. Modern Phys. 28, 58 (1956).
[12]J. F. Lovering, Geochim. et Cosmochim. Acta 12,

253 (1957).
[13]E. M. Burbidge, G. R. Burbidge, W. A. Fowler, and F. R. S. Hoyle, Revs. Modern Phys. 29, 547 (1957).
[14]E. Anders and C. M. Stevens, J. Geophys. Research 65, 3043 (1960).

HELIUM II IN ROTATION*

John D. Reppy, David Depatie, and C. T. Lane
Department of Physics, Yale University, New Haven, Connecticut
(Received November 21, 1960)

In a recent experiment,[1] Pellam has reported some measurements concerned with the velocity field of He II when contained in a simply connected vessel subject to steady rotation about its vertical axis of symmetry. These results are interesting, and unexpected, since they are contrary to the predictions of any current theory of liquid helium. We felt it important, therefore, to examine the problem using a different approach.

In our experiment the helium is contained in a light cylindrical glass vessel (bucket) which can be given an angular velocity about the vertical axis. The volume occupied by the helium was approximately 2.5 cm in diameter by 11 cm in depth. The bucket and its contents are suspended from a Beams type magnetic bearing, the whole system being enclosed in a high vacuum. Under these circumstances the parasitic rotational drag on the system was less than 5×10^{-6} dyne cm which, for our purposes, was negligible.

The procedure consists in giving the system, initially at rest, a sudden (~1/2 sec) rotational impulse and thence allowing it to coast freely. Observations are then made of the angular velocity of the system as a function of time and Fig. 1 shows two typical results, one above and the other below the λ point. As seen, the velocity of the system decreases with time and eventually reaches a steady value. Since angular momentum is conserved, the slow-down of the system must mean that the liquid, initially at rest, is slowly accelerated into rotation by the walls of the bucket. The "reaction time" is sharply temperature dependent, being the faster the higher the temperature, and this indicates that the mechanism of interaction between bucket and liquid is different for the normal and superfluid components of the helium.

Control experiments show that no appreciable angular momentum is transmitted to the liquid in the very short initial period during which the system is being brought into rotation. Hence a simple calculation, making use of readily measured

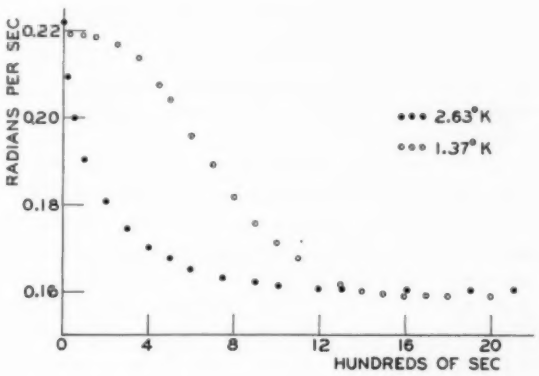

FIG. 1. The angular velocity of the system, subject to no external torques, as a function of time. Two runs are shown, for He I and He II, respectively, illustrating the very different types of interaction in the two fluids.

constants, permits us to find the angular momentum acquired by the helium in reaching its equilibrium state.

The result, in all cases, shows that this angular momentum is always classical to within an average experimental error of about five percent. By classical is meant that, at equilibrium, the helium is rotating in solid body type motion with the same angular velocity which the bucket then possesses—a situation which would also occur in the case of an ordinary viscous fluid. This behavior, of course, is precisely that predicted for a pure superfluid by the Onsager-Feynman[2] vortex line theory and this theory has met with some success in accounting for a variety of other superfluid experiments.

Figure 2 is a plot of the ratio of the angular momentum so measured (L) to the classical value (L_C) as a function of temperature. The above ratio is identical to Pellam's ρ_{eff}/ρ and his results are therefore included on the same graph for comparison.

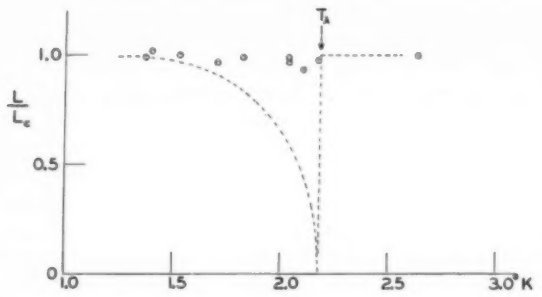

FIG. 2. The angular momentum of the helium (L) compared to the classical value (L_C) as a function of temperature. Circles are the present experiment and the dashed curve is Pellam's result (reference 1). The rotational velocity in all runs was near 2 rpm.

The most obvious difference between our technique and that of Pellam lies in the fact that his Rayleigh disk provides a semimicroscopic measure of the velocity field whereas ours provides an average over such a field. But this fact alone can hardly explain the vast difference in results which the two experiments show. It must be pointed out that earlier experiments on angular momentum by Hall[3] and Walmsley and Lane[4] are at variance with both of the above experiments and, of course, with the theory. Plausible, though not entirely certain, reasons can be advanced to explain this discrepancy with our present result but not, at all obviously, with Pellam's.

The present experiment is the only one of those cited which is in concordance with current theories of He II. Further, our method appears to subject the helium to much less extraneous disturbance, such as induced turbulence in the liquid, than do any of the others. We suggest, in consequence, that Pellam's result is possibly connected with some such extraneous effect.

*Assisted by a grant from the National Science Foundation.

[1]J. R. Pellam, Phys. Rev. Letters 5, 189, 282(E) (1960).

[2]R. P. Feynman, Progress in Low-Temperature Physics, edited by J. C. Gorter (Interscience Publishers, New York, 1955), Vol. 1.

[3]H. E. Hall, Trans. Roy. Soc. (London) 250, 359 (1957).

[4]R. H. Walmsley and C. T. Lane, Phys. Rev. 112, 1041 (1958).

MAGNETIC MOMENT OF TRANSITION METAL ATOMS IN DILUTE SOLUTION AND THEIR EFFECT ON SUPERCONDUCTING TRANSITION TEMPERATURE

B. T. Matthias, M. Peter, H. J. Williams, A. M. Clogston, E. Corenzwit, and R. C. Sherwood
Bell Telephone Laboratories, Murray Hill, New Jersey
(Received November 15, 1960)

We have found a decisive experiment which shows the conditions under which the magnetic moment of a transition metal atom remains localized when in dilute solution in another transition metal. We have correlated this effect with a drastic lowering of the superconducting transition temperature in a particular superconductor.

Some time ago a series of observations was reported which showed that the superconducting transition temperature of various metals and alloys could be greatly decreased by the presence of small amounts of rare earth metals.[1] This effect has been identified as due to an exchange interaction between the conduction electrons and the localized f-shell electrons.[2] In contrast to this behavior, it has been reported that the addition of transition metal impurities raises the superconducting temperature of titanium by an order of magnitude[3] and that of zirconium somewhat less.[4] In the case of the fifth column elements vanadium and niobium, dilute transition-metal impurities lower the transition temperature in a way strictly in accord with the electron concentration.[5] This behavior is consistent with the fact that even large concentrations of iron dissolved in Ti, V, or Nb do not show any magnetic interaction or temperature-dependent susceptibility. As far as we are aware no localized moment has been observed for a transition-metal impurity in dilute solution in another transition metal of the fourth or fifth column.

In this paper we now report a strong lowering of the transition temperature of the superconducting alloy $Mo_{0.8}Re_{0.2}$ by the solution of small amounts of metals belonging to the first-row transition series. These experiments are re-

conciled to those previously reported by showing that the 3*d* metals in dilute solution in metals of the fourth row acquire a magnetic moment abruptly between the fifth and sixth columns. This result is consistent with the fact that very dilute solutions of iron in palladium are known to become ferromagnetic with an effective moment for the iron exceeding two Bohr magnetons per atom.[6]

The sixth column element Mo is not a superconductor. To study the effects of 3*d* impurities upon transition metals in the sixth column and beyond, we have therefore made use of the molybdenum-rhenium alloys whose high superconducting transition temperatures were discovered by Hulm.[7] This temperature decreases linearly with iron concentration at a rate of 22° per atomic percent Fe. In these concentrations the addition of nonmagnetic elements has little effect. The specific depression is about 150 times greater in $Mo_{0.8}Re_{0.2}$ than in the neighboring elements Nb and V.

Susceptibility measurements have been made on the $Mo_{0.8}Re_{0.2}$ alloys with iron as an impurity which show a Curie-Weiss law for the susceptibility.[8] The constant c in the relation $\chi = c/(T-T_C)$ is plotted in Fig. 1 as a function of concentration.

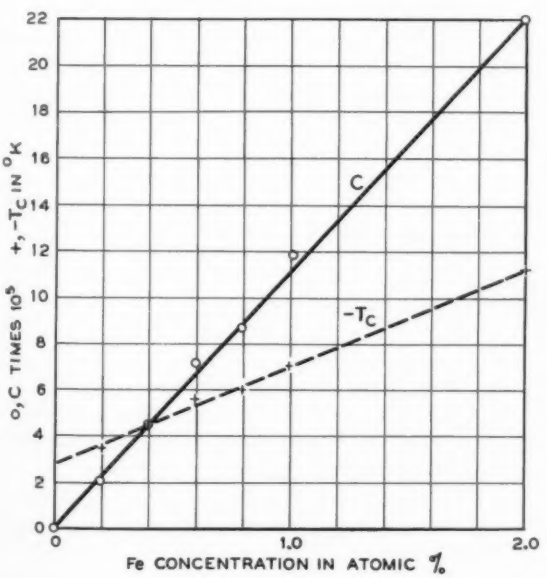

FIG. 1. The constant c in $\chi = c/(T-T_C)$ corresponds to $2.3\mu_B$ per atom of iron in $Mo_{0.8}Re_{0.2}$. T_C is negative and a smooth function of concentration (broken line).

From it we derive $p = g[S(S+1)]^{1/2} = 3.2$, which for $S = 1$ leads to a saturation moment of $2.3\mu_B$ per iron. We conclude that the lowering of the transition temperature of $Mo_{0.8}Re_{0.2}$ by these impurities is due to an exchange interaction with the localized spin and is analogous to the effects produced by rare earth ions in lanthanum and other metals and alloys.[1] We have also plotted in Fig. 1 the Curie temperature T_C which turns out to be negative and a smooth function of the concentration.

Both niobium and molybdenum crystallize in a body-centered cubic structure and form a continuous series of solid solutions. The presence of a localized moment for iron atoms dissolved in $Mo_{0.8}Re_{0.2}$, and the absence of such a moment in Nb, suggests that a localized moment will appear somewhere in the series between Nb and Mo. In Fig. 2 we show the effective magnetic moment per iron atom, p, as a function of Mo concentration, obtained from susceptibility data taken on Nb - Mo solid solutions containing 1 atomic percent iron. An appreciable moment appears first at 50% Mo. The Nb - Mo alloys up

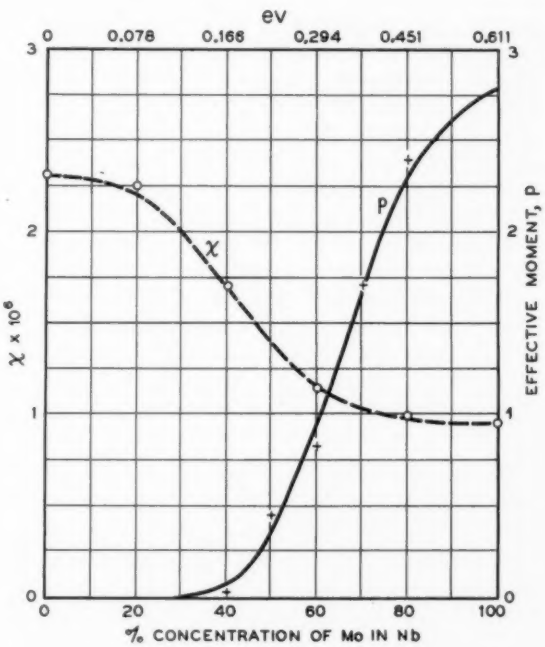

FIG. 2. Effective magnetic moment per iron atom, p, in Nb-Mo solutions containing 1 atomic percent Fe. The broken line gives the susceptibility at 300° in the absence of Fe. From it is derived the energy scale explained in the text.

to 30% Nb remain superconducting and no appreciable reduction in T_S due to the iron was observed in the present experiments, consistent with the conclusion advanced above.

We have also plotted in Fig. 2 the susceptibility χ per gram of the Nb - Mo alloys without iron. If we assume that the susceptibility measures the density of states at the Fermi surface, we may relate an increase in the average number of electrons per atom N to an increase in the Fermi energy E_F by the relation $\Delta E_F = \mu_B^2 \Delta N / \chi M_0 A$, where M_0 is the mass of an atom of unit atomic weight and A is the average atomic weight. The energy scale derived in this way is shown in Fig. 2.

The sharp rise in magnetic moment per atom seen in Fig. 2 is a remarkable new phenomenon and provides some insight into the electronic structure of iron present as an impurity in the Nb - Mo crystal. A possible interpretation of the observations is the following. Each iron atom has 5 d states. Following suggestions by Mott and Stevens[9] that apply to the bcc structure, we may assume that 3 of these states of symmetry t_{2g} become part of the conduction band of the host lattice. The remaining two states of symmetry e_g we suppose to be only weakly coupled to surrounding wave functions and therefore essentially localized. For the alloys of less than 50% Mo we assume that the Fermi level lies below the e_g states and no moment is observed. Above 80% Mo we suppose that the Fermi level has crossed these states and that they are occupied by two electrons whose spins align according to Hund's rule to give the observed moment. The antiparallel spin states will be split off by exchange and correlation energy so that they lie above the Fermi surface and are unoccupied. From the energy scale in Fig. 2 we may estimate the effective width of the e_g band to be about 0.3 ev.

[1]B. T. Matthias, H. Suhl, and E. Corenzwit, Phys. Rev. Letters 1, 92 (1958).

[2]H. Suhl and B. T. Matthias, Phys. Rev. 114, 977 (1959).

[3]B. T. Matthias, V. B. Compton, H. Suhl, and E. Corenzwit, Phys. Rev. 115, 1957 (1959).

[4]B. T. Matthias and E. Corenzwit, Phys. Rev. 100, 626 (1955).

[5]G. Busch and J. Müller, Proceedings of the Kamerlingh Onnes Conference on Low-Temperature Physics, Leiden, 1958 [Suppl. Physica 24, S152 (1958)]. The explanation given by Busch and Müller for lowering of the transition temperature in V-Fe alloys has since been withdrawn (private communication).

[6]J. Crangle, Phil. Mag. 5, 335 (1960).

[7]J. K. Hulm, Phys. Rev. 98, 1539 (1955).

[8]Our samples were prepared by arc-furnace melting under an argon atmosphere. Our calculations are based on the percentage of iron added to the melt. While the linearity of the plot in Fig. 1 indicates internal consistency, there remains some uncertainty as to the calibration due to the possibility of iron losses from the melt.

[9]N. F. Mott and K. W. H. Stevens, Phil. Mag. 2, 1364 (1957).

EFFECT OF SPIN-ORBIT SPLITTING ON THE FERMI SURFACES OF THE HEXAGONAL-CLOSE-PACKED METALS*

Morrel H. Cohen and L. M. Falicov
Institute for the Study of Metals, University of Chicago, Chicago, Illinois
(Received November 14, 1960)

All theories of the electronic properties of metals and alloys having the hexagonal-close-packed (hcp) structure have supposed that the energy gaps vanish across the hexagonal face of the first Brillouin zone.[1,2] The simple argument based on the vanishing of the structure factor put forward first by Jones[3] was not correct for a general potential. A rigorous basis for the sticking together of the bands was provided by the symmetry properties and time-reversal arguments of Herring.[4] These were generalized to include spin-orbit coupling by Elliott for various crystal structures.[5] In particular, one sees from his results that the degeneracy is removed at the point H and along the symmetry lines S and S', but not at A and L nor along the line R (Fig. 1). The implications of Elliott's work for the electronic properties of hcp metals and alloys appear to have been overlooked. Two questions arise: How big is the splitting, and what modification of the existing theories is required?

We have extended Elliott's analysis to a general point in the plane, and have found, as expected, the degeneracy to be lifted. Near A the splitting

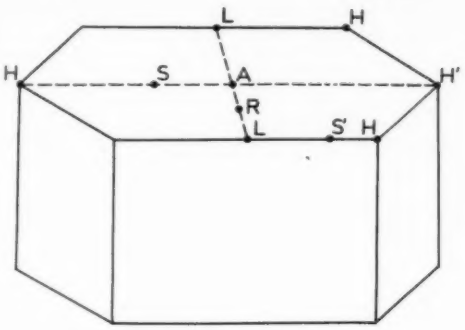

FIG. 1. The first Brillouin zone for hcp structures, showing points and lines of symmetry in the hexagonal face.

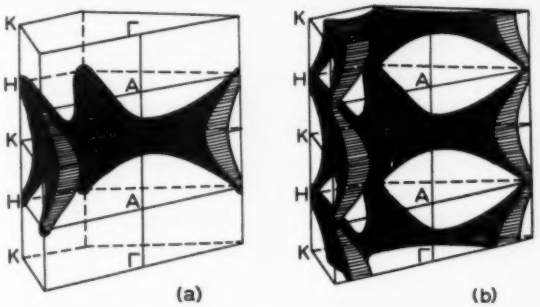

FIG. 2. The change in the connectivity properties of the Fermi surface of magnesium due to spin-orbit coupling. Diagram (a) shows the "without spin" case and (b) the surface in the second band when spin-orbit coupling is taken into account.

is very small because it is required to vanish by symmetry along the three lines R intersecting at A. The splitting increases from A along S initially as $(\Delta k)^3$ towards a maximum value for the entire plane at H.

We have calculated numerical values of the splittings at H for magnesium using the results of a previous orthogonal plane wave (OPW) calculation of the band structure.[6] A six-OPW approximation to the wave function was used; fewer OPW's would not have yielded the correct order of magnitude, more would have required an inappropriate amount of computation. The results are listed in Table I.

From the detailed wave functions one would have anticipated the splitting to be small for H_3, and for H_1 and H_2 to be somewhat greater than half the spin-orbit-coupling parameter for a $3p$ electron in atomic Mg (5×10^{-3} ev from the term values[7] of the configuration $3s3p\ ^3P_J$). Both are found to be the case. Approximately the same

Table I. The energies at H in magnesium.

Without spin		With spin	
Level	Energy (ev)	Levels	Splitting (ev)
H_2	9.33	H_4+H_6 H_8	2.83×10^{-3}
H_1	9.63	H_8 H_9	2.86×10^{-3}
H_3	12.22	H_5+H_7 H_9	3.1×10^{-5}

Fermi level at about $E_F=9.25$ ev.

ratios of splittings in the crystal to atomic spin-orbit-coupling parameter should hold for the other hcp metals: Be, Zn, Cd, and Tl. For these metals, therefore, the spin-orbit splittings are 0.05, 9.5, 28, and 129 times as large as the corresponding splittings for Mg.

No major changes of existing alloy theories are required because the spin-orbit splitting vanishes at the center of the hexagonal face and is very small in a sizable region around the center. However, the topological features of the Fermi surfaces of the pure metals are fundamentally changed, and the double zone scheme ordinarily used in their representation is no longer valid. Without spin-orbit coupling, that piece of the Fermi surface corresponding to holes in the first and second bands in Mg[8] and Zn[2] is multiply connected with infinite extent normal to the c axis but not parallel to it [Fig. 2(a)]. With such a Fermi surface the observed lack of saturation of the magnetoresistance for fields normal to the c axis[8,9] could not be understood. The spin-orbit splitting, however, separates the small pockets of holes in the first band from the region of holes in the second and causes the latter to extend infinitely along the c axis [Fig. 2(b)]. This explains the observed magnetoresistance, because now open orbits exist for all directions of magnetic field normal to the hexad axis.

*This research was supported in part by the Office of Naval Research.

[1]N. F. Mott and H. Jones, The Theory of the Pro-

perties of Metals and Alloys (Clarendon Press, Oxford, 1936), p. 161.

[2]W. A. Harrison, Phys. Rev. 118, 1190 (1960).

[3]H. Jones, Proc. Roy. Soc. (London) A147, 396 (1934).

[4]C. Herring, Phys. Rev. 52, 361 (1937); J. Franklin Inst. 233, 525 (1942).

[5]R. J. Elliott, Phys. Rev. 96, 280 (1954).

[6]L. M. Falicov, thesis submitted to the University of Cambridge, England, 1960; and to be published.

[7]Charlotte E. Moore, Atomic Energy Levels, National Bureau of Standards Circular No. 467 (U. S. Government Printing Office, Washington, D. C., 1949).

[8]Mg: N. E. Alekseevskii and Yu. P. Gaidukov, J. Exptl. Theoret. Phys. U.S.S.R. 38, 1720 (1960).

[9]Zn: B. I. Verkin, doctoral dissertation, Khar'kov State University, 1956 (unpublished); I. M. Lifshitz and V. G. Peschanskii, J. Exptl. Theoret. Phys. U.S.S.R. 35, 1251 (1958) [translation: Soviet Phys. – JETP 8(35), 875 (1959)].

VOIGT EFFECT IN SEMICONDUCTORS

S. Teitler and E. D. Palik
U. S. Naval Research Laboratory, Washington, D. C.
(Received October 10, 1960)

Double refraction of an electromagnetic wave passing through an isotropic substance under the influence of a static magnetic field in a direction normal to the direction of propagation is known as the Voigt effect.[1] We take as the equation of motion for an electron in the conduction band,

$$\frac{d^2\vec{r}}{dt^2}+(1/\tau)\frac{d\vec{r}}{dt}=-(e/m^*)\left(\vec{E}+\frac{d\vec{r}}{dt}\times\vec{H}\right), \quad (1)$$

where $\vec{r}$ is the displacement vector of the electron, τ is the mean collision time of the electron, $\vec{E}$ is the incident radiation field, $\vec{H}$ is the external magnetic field, and m^* is the effective mass of the electron.

A straightforward classical calculation using Maxwell's equations yields, using unrationalized cgs units,

$$2n_\perp^2=\epsilon-4\pi\sigma_0\tau/\beta[(\alpha/\beta)^2+\omega^2\tau^2]+\left\{\left(\epsilon-\frac{4\pi\sigma_0\tau}{\beta[(\alpha/\beta)^2+\omega^2\tau^2]}\right)^2+\frac{16\pi^2\sigma_0^2\alpha^2}{\omega^2\beta^4[(\alpha/\beta)^2+\omega^2\tau^2]^2}\right\}^{1/2}, \quad (2a)$$

$$2K_\perp^2=-\epsilon+4\pi\sigma_0\tau/\beta[(\alpha/\beta)^2+\omega^2\tau^2]+\left\{\left(\epsilon-\frac{4\pi\sigma_0\tau}{\beta[(\alpha/\beta)^2+\omega^2\tau^2]}\right)^2+\frac{16\pi^2\sigma_0^2\alpha^2}{\omega^2\beta^4[(\alpha/\beta)^2+\omega^2\tau^2]^2}\right\}^{1/2}, \quad (2b)$$

where the magnetic permeability has been assumed equal to one, $n_\perp$ is the index of refraction for radiation with electric vector normal to both the magnetic field and the direction of propagation, $K_\perp$ is the extinction coefficient in the normal direction, and

$$\alpha=1+\{\omega^2\omega_c^2\tau^2/[\omega^2+(\omega^2-\omega_p^2)^2\tau^2]\},$$

$$\beta=1-\{\omega_c^2(\omega^2-\omega_p^2)\tau^2/[\omega^2+(\omega^2-\omega_p^2)^2\tau^2]\},$$

$$\sigma_0=Ne^2\tau/m^*,\ \omega_c=eH/m^*c,\ \omega_p^2=4\pi Ne^2/m^*\epsilon,$$

with N equal to the free electron concentration.

For radiation with electric vector parallel to the magnetic field, the index of refraction, $n_\parallel$, and the extinction coefficient, $K_\parallel$, follow immediately from Eqs. (2) by setting $\alpha=\beta=1$.

The phase shift between components parallel and normal to the magnetic field when incident radiation of wavelength λ traverses a substance of thickness d in a direction normal to the magnetic field is

$$\delta=2\pi d(n_\parallel-n_\perp)/\lambda. \quad (3)$$

This phase shift takes a particularly simple form

when

$$\omega\tau >> 1, \quad \omega > \omega_c, \quad \omega > \omega_p,$$

i.e.,

$$\delta = \frac{Nde^4H^2\lambda^3}{4\pi^2\epsilon^{1/2}m^{*3}c^8}\left[\frac{\omega^2}{\omega^2 - \frac{1}{2}\omega_p^2}\right]\left[\frac{\omega^2}{\omega^2 - \omega_p^2 - \omega_c^2}\right], \quad (4)$$

where we have taken (ω_p^2/ω^2) and ω_c^2/ω^2 to be small quantities of the same order of magnitude, X. Equation (4) is correct to terms of order X^3.

To check Eq. (4) experimentally we used a sample of n-type InAs with carrier concentration of $10^{17}/\text{cm}^3$ which is thereby extrinsic at room temperature. The mobility was in excess of 2×10^4 $\text{cm}^2/\text{volt-sec}$. Under experimental conditions employed, the validity of Eq. (4) is assured. Also since $\omega\tau >> 1$, this sample had the added convenience that away from the cyclotron resonance region, there was essentially no difference between $K_\perp$ and $K_\parallel$ to complicate the double-refraction experiment. Infrared radiation at various wavelengths in the region 14μ - 19μ and plane polarized at an angle of 45° to the magnetic field with a pile-of-plates polyethylene polarizer was incident on the InAs at room temperature in a direction normal to the magnetic field. We detected circularly polarized radiation with a CsI Fresnel rhomb and a second polyethylene polarizer as a function of magnetic field. Fields as high as 70 kilogauss were used. A typical result is shown in Fig. 1. The first peak, which signifies a phase shift of $\pi/2$, occurred in all cases before the cyclotron resonance absorption began and may be used directly in Eq. (4). The same results were obtained when the direction of the varying field was reversed, thereby indicating that the double refraction is an even function of the magnetic field. While the occurrence of extrema in the observation of circularly polarized radiation is unaffected by any difference in extinction coefficients, a correction for the changing background due to cyclotron resonance absorption must be made. In the raw data as shown in Fig. 1, this cyclotron resonance absorption makes it difficult to assign a reliable magnetic field to the minimum.

In order to establish the properties of the double refraction we restricted ourselves to the use of the first maxima which are essentially unaffected by cyclotron resonance absorption. The effective-mass ratio obtained by inserting these data into Eq. (4) is plotted in Fig. 2, as a function of magnetic field. The intercept at 0.0313 for zero magnetic field is consistent with the low-field Faraday-rotation effective-mass ratio obtained for the same sample. This compares with an effective-mass ratio of 0.023 obtained on pure InAs by cyclotron resonance.[2] This indicates that we are measuring an effective mass substantially above the bottom of the nonparabolic energy band, which is to be expected since our sample is relatively impure. This is consistent with Austin's[3] result of 0.043 for the effective-mass ratio in a more impure sample of InAs with a carrier concentration of $1.04\times10^{18}/\text{cm}^3$. The slope of the effective-mass ratio curve of Fig. 2 is also consistent with the slope of the effective-mass ratio versus magnetic field for cyclotron resonance data for pure material.[2]

In preliminary experiments on InSb we have

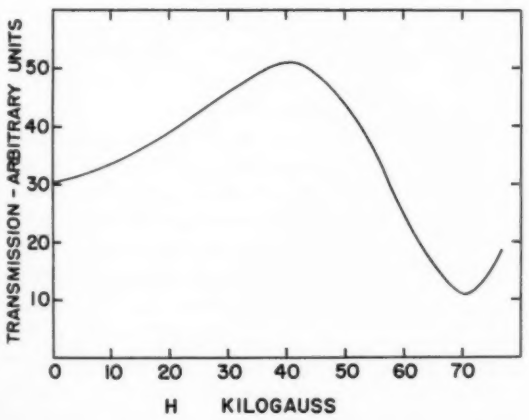

FIG. 1. Transmission of InAs versus magnetic field at 17.9 microns, illustrating Voigt effect.

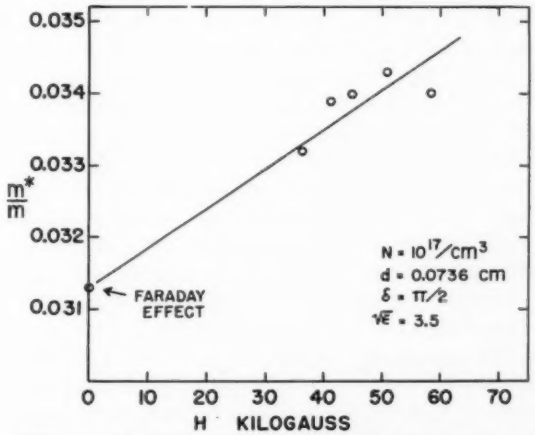

FIG. 2. Variation of effective-mass ratio with magnetic field for InAs at room temperature.

also obtained the Voigt effect using the above procedure. However, for more general application to semiconductors with heavier masses, it is desirable to modify the procedure. This is so because the phase shifts are less than $\pi/2$ for wavelengths for which the materials are transparent and for the available static magnetic fields. We again start with radiation polarized 45° to the magnetic field but now observe the major axis, the ratio of axes, and the orientation of the resultant elliptically polarized radiation due to double refraction for a fixed magnetic field and wavelength by rotating a linear polarizer before the detector.

Recently Gurevič et al.[4] have independently discussed magnetic double refraction properties of semiconductors which may be similar to those considered in the present Letter.

We gratefully acknowledge many informative discussions with Dr. R. F. Wallis of this Laboratory. We also acknowledge an interesting discussion concerning magneto-optic effects with Dr. R. A. Toupin.

[1]See, e. g., H. A. Lorentz, The Theory of Electrons (G. E. Stechert Company, New York, 1916), 2nd ed., p. 164.

[2]E. D. Palik and R. F. Wallis (to be published).

[3]I. G. Austin, J. Electronics and Control 8, 167 (1960).

[4]L. D. Gurevič, I. P. Ipatova, and Z. I. Uricky, International Conference on Semiconductor Physics, Prague, 1960 (unpublished).

EFFECT OF LANDAU LEVELS UPON TUNNEL CURRENTS IN INDIUM ANTIMONIDE

A. G. Chynoweth, R. A. Logan, and P. A. Wolff
Bell Telephone Laboratories, Murray Hill, New Jersey
(Received November 7, 1960)

It has already been shown[1-3] that when a magnetic field, H, is applied to an InSb Esaki junction there is a reduction in the tunnel current due to the change in the tunnelling probability that arises primarily through the increase in the energy gap with H. An additional effect has now been observed at low temperatures, namely, an oscillation of the tunnel current with H.

The junctions used in this work were made by alloying pellets of 0.1% Cd in In into n-type InSb containing an average excess donor density of 10^{17} cm^{-3}. The excess acceptor concentration on the p side was estimated to be 10^{18} cm^{-3}. Results obtained from two junctions are described in this paper; one was an Esaki junction, the other a backwards diode. Although these junctions were made from the same crystal, it is believed that the well-known inhomogeneities in the donor concentration were responsible for the observed spread in the junction characteristics. Results basically similar to those described here were obtained with several other junctions.

Current-voltage characteristics taken at 4°K showed that as H was increased from zero to 85 000 gauss, the tunnel current underwent an oscillation superimposed on the decrease of current noted previously. The oscillations were observed with $H \| E$, the junction field, and not with $H \perp E$. For more detailed studies, a constant current was passed through the junction and the potential drop across the junction was plotted continuously as a function of H on an X-Y recorder. (Plotting voltage was virtually equivalent to plotting current since the current was roughly proportional to the bias for small changes in the latter.) Figure 1 shows the results obtained with the Esaki junction at small

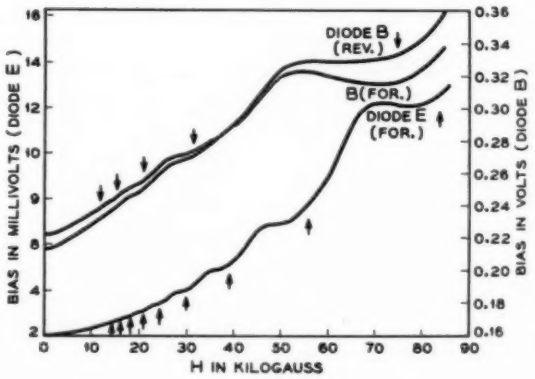

FIG. 1. The bias required to maintain a constant tunnel current as a function of magnetic field for two different junctions: Junction E was an Esaki diode; junction B was a backwards diode. The oscillations in bias are attributed to the Landau levels in the conduction band.

forward bias and with the backwards diode at larger biases, the forward bias being such as to operate the junction in the excess current range. It is apparent that as H increases, small voltage oscillations appear, that the amplitudes and field spacings of these oscillations increase with H, and that the oscillations are similar for both forward and reverse biases.

To establish whether the oscillations were caused by a series magnetoresistance effect, the location of the phonon-bump on the current-voltage characteristics was examined as a function of H using equipment[4] that automatically plotted (d^2I/dV^2) against V. At $H=0$ the phonon bump occurred at a forward bias of 24.5 ± 0.5 mv, in agreement with other measurements,[5] and it remained at this value to within 1.0 mv up to the highest values of H, thereby eliminating series resistance effects as the cause of the voltage fluctuations. This is in line with previous observations.[2]

It is possible to ascribe the oscillations to the oscillatory variation in the density of electrons available for tunnelling brought about by the Landau quantization in the conduction band on the n-type side. At low biases most of the tunnelling transitions are to and from energy levels located near the Fermi levels on both sides of the junction. For electrons and light holes the density of states at the Fermi surface is proportional to

$$\sum_n \frac{(2\epsilon_F + \epsilon_G)}{\{(\epsilon_F + \epsilon_G)\epsilon_F - \epsilon_G[(n+\frac{1}{2})\hbar\omega_c \pm \mu g H]\}^{1/2}}, \quad (1)$$

where ϵ_F is the Fermi energy, ϵ_G the energy gap, ω_c the cyclotron frequency, and μg the spin moment. This function has a sharp maximum whenever the bottom of a Landau sub-band crosses the Fermi level and thereby gives rise to fluctuations in the tunnel current.

Expression (1) predicts that if H^{-1} for the nth maximum is plotted against n, a straight line should result. Such plots are shown for the two junctions in Fig. 2 where it is apparent that very good straight lines are obtained. The slope of the line, which is proportional to $m^* \epsilon_F(\epsilon_F + \epsilon_G)/\epsilon_G$, is greater for the Esaki junction than for the backwards junction by a factor of 2.4. This ratio can also be estimated from the current densities of the two diodes. At small biases, the current density in the Esaki junction was 70 times that of the backwards diode so that the junction width constants differed by about 470 A whereas their average width was about 1440 A. Hence, the

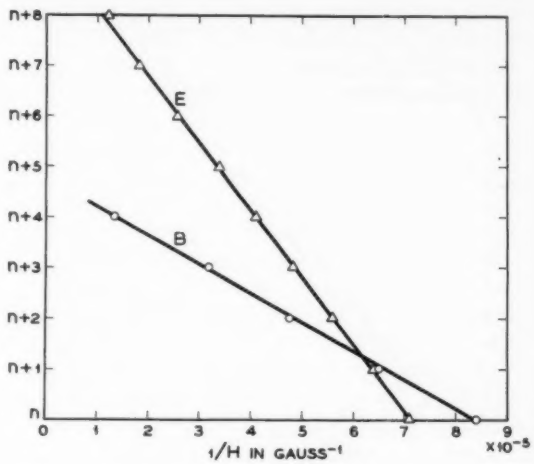

FIG. 2. Plots of the oscillation number versus H^{-1} derived from the curves of Fig. 1.

donor concentration for the Esaki junction was about 2.5 times that for the backward junction, thereby making the predicted ratio of the slopes about 1.9, in reasonable agreement with the observed value. The values of m^* derived from the two lines of Fig. 2 were equal to within ±5%, their average value of $0.011 m_0$ being in reasonable agreement with other determinations of the electron mass at the bottom of the conduction band,[6] considering the uncertainties in the estimates of ϵ_F.

These data show that the oscillations in the tunnel current are due to fluctuations in level density of the Fermi surface in the n-type sides of the diodes only. It is important to realize that these current maxima [see Eq. (1)] are due to carriers whose energy is entirely transverse to the junction field. Thus the observation of oscillations indicates that an appreciable fraction of the tunnel current is carried by electrons whose velocity is, initially, perpendicular to the field. In electron-light hole tunnelling, this transverse energy must be conserved. From the known band structure of InSb, and noting that the Fermi energy on the n side (0.05 - 0.10 ev) is considerably greater than that (0.02 ev) on the p side, it is, therefore, impossible (in our junctions) for a carrier with entirely transverse energy to tunnel from the Fermi surface in the conduction band to the light-hole band. Thus, the observed oscillations must be due to electron-heavy hole tunnelling, in which case the selection rules are re-

laxed and the dependence of the amplitude of the oscillations on H will not be simple.

Some remarks can be made on the absence of a second component in the oscillations contributed by Landau levels in the valence band. Because of instrumental limitations, fields of 15 kgauss or more are required for the observation of the electron Landau levels. Hence, those for the heavy holes would require considerably higher fields. Another factor tending to obscure the Landau levels on the p side will be the greater scattering frequency due to the relatively greater impurity concentration. On the other hand, it might be possible, in principle, to detect oscillations in the tunnel current of electrons from well below the Fermi level in the conduction band to the Fermi surface in the light-hole band. However, these have not been observed, the probable reason being that at the fields at which oscillations can just be detected (~15 kgauss), the maximum energy of the light-hole band is already lower than the Fermi energy in the valence band.

In the case of $E \parallel H$, the infinite degeneracy of Landau states is responsible for the sharp peaks in the density of states. In the $E \perp H$ geometry, this degeneracy is broken since the energy of a Landau level now depends upon the position of the electron in the plane normal to H. Thus the density of states will vary with H in the perpendicular geometry, so accounting for the absence of oscillations.

The fact that, to within experimental error, the Landau spacings at the Fermi level in the conduction band determine the current oscillations at relatively high biases implies that the tunnel current is still dominated by transitions to or from states close to the Fermi level on the n side.

The authors are grateful to J. K. Galt for providing the magnet facility, and to W. L. Feldmann, J. F. Gilbert, and H. W. Dail for assistance with the experiments.

[1]L. Esaki and P. J. Price (private communications).
[2]A. G. Chynoweth, R. A. Logan, and D. E. Thomas, Bull. Am. Phys. Soc. 5, 374 (1960).
[3]A. R. Calawa, R. H. Rediker, B. Lax, and A. L. McWhorter, Phys. Rev. Letters 5, 55 (1960).
[4]This equipment was developed by D. E. Thomas.
[5]R. N. Hall, J. H. Racette, and H. Ehrenreich, Phys. Rev. Letters 4, 456 (1960).
[6]S. D. Smith, T. S. Moss, and K. W. Taylor, J. Phys. Chem. Solids 11, 131 (1959).

LOW-TEMPERATURE TRANSPORT IN "SPLIT p-GERMANIUM"

Seymour H. Koenig and John J. Hall
International Business Machines Watson Research Laboratory, Columbia University, New York, New York
(Received November 28, 1960)

By measuring conductivity and Hall mobility of p-Ge at low temperature under large strains ($>10^{-3}$), we have been able to determine the sign, the ratio, and the approximate magnitude of the two deformation potentials that describe the change, under shear, of the valence band. In addition we have been able to verify that the velocity dependence of the hole-acceptor recombination cross section is independent of the acceptor ground-state energy over a limited range, in agreement with the prediction of the trap mechanism proposed by Lax.[1]

When germanium is subjected to a shear stress the valence band, normally 4-fold degenerate (including spin) at the Brillouin zone center, splits into two doubly degenerate bands separated by an energy $\delta\mathcal{E}$.[2-5] In a neighborhood within an energy $\ll \delta\mathcal{E}$ of each (new) band edge, the surfaces of constant energy are ellipsoids of revolution about the stress direction, and the effective masses are functions of the geometry of the strain, and not its magnitude.[2,3,5]

For a uniaxial stress χ in either the $\langle 100\rangle$ or $\langle 111\rangle$ directions, the splitting is given by

$$\delta\mathcal{E}_{100} = 2\Delta_{100} = 2S_{11}(1+\lambda)|b\chi| = 4S_{11}(1+\lambda)|D_u\chi|/3 = 2|b|\epsilon_{100} = 2.44\times10^{-12}|\chi b| \text{ ergs}, \quad (1a)$$

$$\delta\mathcal{E}_{111} = 2\Delta_{111} = \sqrt{3}S_{44}|d\chi|/3 = 2S_{44}|D_u'\chi|/3 = \sqrt{3}|d|\epsilon_{111}S_{44}/(S_{11}+2S_{12}+S_{44}) = 0.838\times10^{-12}|\chi d| \text{ ergs}, \quad (1b)$$

and $b = -2D_u/3$; $d = -2D_u'/\sqrt{3}$. Here b is the deformation potential constant (for hole energies) appropriate to a strain of tetragonal symmetry (with respect to the conventional cubic basis) as

defined by Pikus and Bir[3] (PB); d is the similar constant for a deformation of rhombohedral symmetry. D_u and D_u' are similar constants defined (for electron energies) by Kleiner and Roth[4] (KR). The definitions used are those in Eq. (2) and Table I of KR, rather than their verbal description of D_u and D_u', which is apparently inconsistent with these. S_{11}, S_{12}, S_{44} are the elastic compliance constants, and λ the Poisson ratio. ϵ_{100} and ϵ_{111} are the respective longitudinal components of strain that result from the stress χ.[6] The relation to the notation of other authors is given in Table I of Price and Kao.[7]

Sufficiently large stresses may be applied to germanium so that at low temperatures ($\lesssim 10°K$), $\delta\mathcal{E} \gg kT$. In this limit only one band is appreciably populated; the Hall mobility then becomes independent of strain. Figure 1 shows the strain dependence of the Hall mobility for two samples of 20 ohm cm p-type Ge cut from the same crystal, one $\langle 111\rangle$ oriented, the other $\langle 100\rangle$. The abscissa scale was chosen so that if $b=d$, it would be proportional to $\delta\mathcal{E}$ for both samples. The saturation of the mobility is clearly indicated. From these data, a ratio $|d/b| = 2.1 \pm 15\%$ or $|D_u'/D_u| = 3.6$ is obtained. This result is a factor of ~2 less than the estimates made by PB[3] and KR[4] from piezoresistance data. It is difficult to obtain any precise value for d from the present data. However, if one assumes that when the mobility is at 90% saturation, $\delta\mathcal{E} \sim 3kT$, then $d \simeq 1$ ev.

According as the sign of b and d, the relevant effective-mass ellipsoid is either oblate or prolate.[3] To determine the signs we have crudely measured the transverse conductivity under saturation strain for both samples by making a two-terminal measurement of the resistance between the Hall contacts. For the $\langle 100\rangle$ case, $\mu_\parallel/\mu_\perp > 1$ corresponding[3] to $b<0$ or $D_u>0$, ignoring the (unlikely) possibility of an extremely large scattering anisotropy. Similarly, for the $\langle 111\rangle$ case, $\mu_\parallel/\mu_\perp < 1$ corresponding to $d<0$ or $D_u'>0$. These results agree with the signs of the estimates made by KR[4] and those which may be deduced from PB.[3] It is interesting to note, however, that the work of Hensel and Feher[5] yields the opposite signs for the corresponding valence band deformation potentials in silicon.[8] (Actually only the signs of the products dD and bB are here determined experimentally, where D and B are the conventional matrix elements of the spin-orbit interaction; but the signs of D and B are presumed known.[8,5])

If $\delta\mathcal{E}$ can be made sufficiently large, the acceptor ground state will be formed from Bloch states near the edge of the upper of the two split bands. The effective-mass approximation as extended to the prolate case by Keyes,[9] using the masses calculated by Pikus and Bir,[3] and assuming that the dielectric constant remains isotropic, gives for the saturation activation energy ϵ the value 4.25×10^{-3} ev for a $\langle 100\rangle$ stress. Figure 2 shows a plot of reciprocal Hall constant vs strain for the $\langle 100\rangle$ orientation at $T = 6°K$. The maximum stress on the $\langle 100\rangle$ sample, which corresponds to a strain of 0.7×10^{-2}, was limited by the available apparatus. (This corresponds to

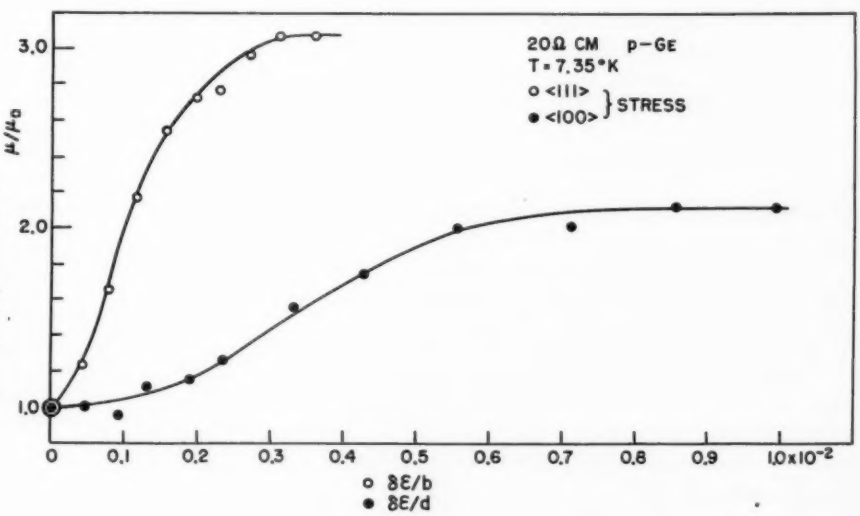

FIG. 1. Hall mobility (normalized to zero strain value) vs strain for a $\langle 100\rangle$ and $\langle 111\rangle$ oriented sample of p-Ge. The abscissa scale is in units of the strain-dependent splitting of the valence band at the zone center divided by the appropriate deformation potential [see Eq. (1)]. The strains at saturation are $>10^{-3}$.

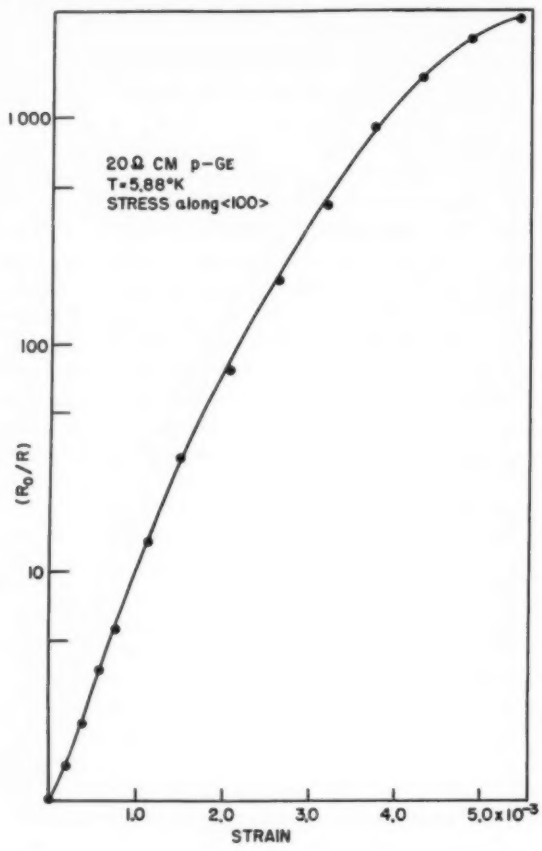

FIG. 2. Reciprocal Hall constant vs strain. The variation is due to a change in impurity activation energy which, in terms of the effective-mass approximation, is caused by a large reduction in at least one component of the mass tensor.

$\delta\mathcal{E} \sim 7\times10^{-3}$ ev.) It would appear from the data that the condition $\epsilon \ll \delta\mathcal{E}$ has almost been reached. The activation energy measured at this strain is 6.8×10^{-3} ev. Whether there is indeed a discrepancy with the predictions of the effective-mass approximation remains to be determined. For a $\langle 111 \rangle$ stress, the reciprocal mass tensor is oblate; the calculated ϵ in this case is 5.0×10^{-3} ev.[10]

This "new" semiconductor, "split p-germanium," has a unique application in hot electron problems for values of strain and electric field such that $\delta\mathcal{E} \gg kT_e$ where T_e is the electron "temperature." The nonlinear current-voltage relation[11] should then be independent of strain (except for a strain-dependent scale factor in the current caused by the varying activation energy) until impact ionization of neutral impurities makes a significant contribution to the current density. The electric field at which this occurs has been a matter of conjecture for some time.[12] However, it is now possible, by varying the strain, to vary continuously the impurity activation energy, without changing any transport parameters. Figure 3 shows recorder traces of

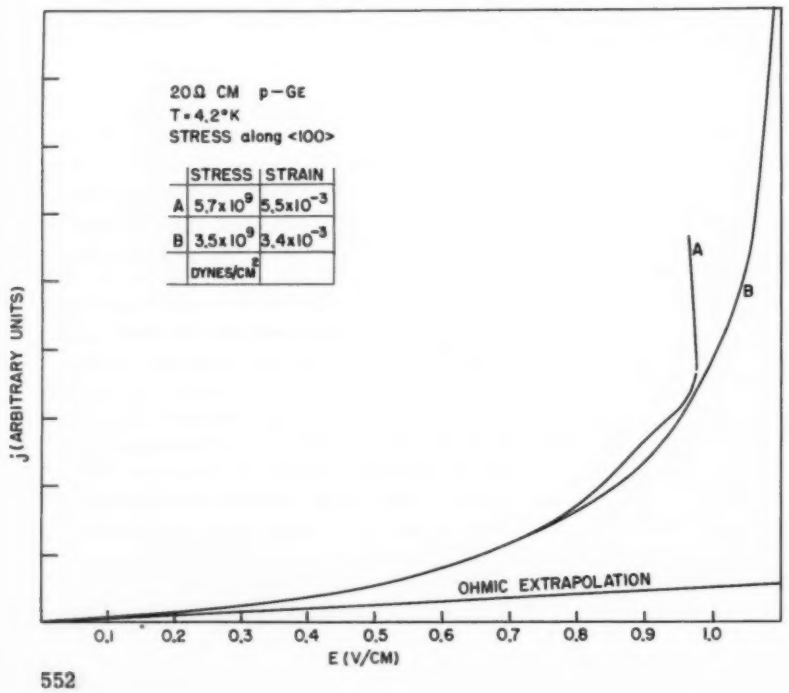

FIG. 3. Variation of current with electric field for two values of strain sufficiently large so that the transport parameters are strain independent but the activation energy not. The two curves diverge when impact ionization of neutral impurities begins to contribute appreciably to the carrier density. (The current scales have been adjusted to compensate for the activation energy change by making the curves overlap in the Ohmic range.)

current density vs electric field for two large values of strain; the current sensitivity has been adjusted to compensate for the activation energy change (~20%). There is overlap of the two curves for a considerable range of electric field where the nonlinearity in conductivity is due to the velocity dependence of the recombination coefficient σ.[12] It is seen that σ varies by a factor of 3.5 over this range. The (velocity-dependent) recombination cross section is expected to be dependent, not on the acceptor ground-state energy, but rather on a continuum of states ~kT above the valence band edge,[1] which depends in this case on the parameters of the upper band. This expectation is here confirmed experimentally, and is additional strong confirmation that the cascade recombination mechanism of Lax is operative.

We are indebted to Rodney Brown for computational assistance and to Peter J. Price for discussions.

[1]M. Lax, Phys. Rev. 119, 1502 (1960).
[2]E. N. Adams, Chicago Midway Laboratories Report CML-TN-P8, 1954 (unpublished); Phys. Rev. 96, 803 (1954).
[3]G. E. Pikus and G. L. Bir, Soviet Phys.– Solid State 1, 136 (1959); 1, 1502 (1960).
[4]W. H. Kleiner and L. M. Roth, Phys. Rev. Letters, 2, 334 (1959).
[5]J. C. Hensel and G. Feher, Phys. Rev. Letters 5, 307 (1960).
[6]Our Eq. (1b) differs by a factor of 2 from Eq. (3) of reference 5 in a direction which suggests that these authors lost the perennial factor that enters into the change from tensor to six-vector notation for the strain tensor.
[7]P. J. Price and Y. Kao, IBM J. Research Develop. (to be published).
[8]W. Kohn, in Solid-State Physics, edited by F. Seitz and D. Turnbull (Academic Press, New York, 1957), Vol. 5, p. 257.
[9]R. W. Keyes, IBM J. Research Develop. (to be published).
[10]W. Kohn and J. M. Luttinger, Phys. Rev. 98, 915 (1955).
[11]See, for example, S. H. Koenig, J. Phys. Chem. Solids, 8, 227 (1959).
[12]S. H. Koenig, International Conference on Solid-State Physics in Electronics and Telecommunications, Brussels, June, 1958 (Academic Press, New York, 1960) Vol. 1, p. 422.

POLARIZATION OF THE CONDUCTION ELECTRONS IN THE FERROMAGNETIC METALS*

A. J. F. Boyle, D. St. P. Bunbury, and C. Edwards
The Physical Laboratories, University of Manchester, Manchester, England
(Received November 15, 1960)

It has recently been proposed[1] that the polarization of the 4s conduction electrons in Fe, Co, and Ni is antiparallel to that of the electrons in the unfilled 3d shell; this is the reverse of the usual assumption. There are few ways in which this polarization is manifested. One, however, is in the effective magnetic field at a nucleus, which acts through the contact interaction with the 4s electrons. The magnitude of this field has been given by Marshall[2] as

$$H_c = (8\pi/3)\xi_s |\psi(0)|_A^2 \mu n p, \qquad (1)$$

where μ is the Bohr magneton, $\xi_s|\psi(0)|_A^2$ is the average probability density of a 4s conduction electron evaluated at the nucleus [$|\psi(0)|_A^2$ being the free atom value], n is the number of conduction electrons per atom, and p is their polarization. The sign of the field is positive, i.e., parallel to the direction of magnetization, if the polarization of the 4s electrons is parallel to the 3d polarization.

Hanna et al.[3,4] have measured the magnitude and sign of the field at the Fe nucleus in iron by observing the Zeeman splitting of the 14-kev transition in Fe^{57} and obtain the value -3×10^5 koe. In this case, however, there are other contributions to the field beside H_c; mainly those due to the electrons of the same atom, i.e., the polarized 3d electrons. These other contributions almost certainly outweigh the effect of the field H_c alone (H_c is probably of the order of 50 to 100 koe), and it is therefore difficult to draw any conclusion concerning its sign.

In an attempt to measure H_c directly, dilute (1%) solid solutions of Sn in the ferromagnetic metals (Fe, Co, and Ni) have been prepared. Since Sn is basically diamagnetic, we expect that there will be no contribution to the field at the Sn nucleus from its own inner electrons and that the field will be given simply by

$$H_s = (4\pi/3)M + H_c, \qquad (2)$$

where $|\psi(0)|_A^2$ in (1) is the appropriate value for a Sn atom. Since H_c is due to an over-all polarization of the conduction electrons, the other terms should remain those appropriate to the solvent atoms.[5]

The Zeeman splitting of the 24-kev transition in Sn^{119} was observed[6] using the Mössbauer effect.[7,8] The transmission through the absorber (the alloy) of the radiation emitted by a moving source was measured as a function of the velocity of the source. The velocity spectrometer has been described in detail elsewhere.[9] The temperature of both the source and absorber were maintained around 100°K. Figures 1, 2, and 3 show the transmission spectra obtained for Fe and Ni and Co. Each member of the doublet is an unresolved triplet caused by the splitting of the excited $\frac{3}{2}^+$ state, while the doublet separation is due mainly to the splitting of the ground $\frac{1}{2}^+$ state. The field strengths H_S listed in Table I were derived using the known values of the magnetic moments. (The excited state moment has been measured as 0.83 ± 0.03 nuclear magneton.[9])

The shifts listed in the table refer to the displacement of the spectra towards negative velocity and are almost entirely due to the chemical shift.[10] In this case, where the source was metallic tin, the magnitude of the shift should be proportional to $(\xi_S - \xi_{Sn})|\psi(0)|_{Sn}^2$; ξ_{Sn} and ξ_S refer to metallic tin and the solvent metal, respectively.

Table I. Results derived from the velocity spectra of the absorption of 24-kev γ rays from Sn^{119m} in absorbers containing 1% of Sn^{119} dissolved in Fe, Co, and Ni. The shift is the displacement of the spectra towards negative velocity due to chemical effects, H_S is the field at the Sn nucleus, and $(4\pi/3)M$ is the usual Lorentz field.

Solvent	Shift (mm/sec)	H_S (koe)	$(4\pi/3)M$	$H_S - (4\pi/3)M$
Fe	1.1	-81 ± 4	7.5	-88
Co	1.1	-20.5 ± 1.5	6.1	-26.5 ± 1.5
Ni	1.1	$+18.5 \pm 1$	2.0	$+16.5 \pm 1$

The sign of H_S was determined by placing each absorber in a transverse magnetic field of about 7 koe; the magnetization direction is now parallel to the external field. A positive field was observed only in the case of Ni. The final values

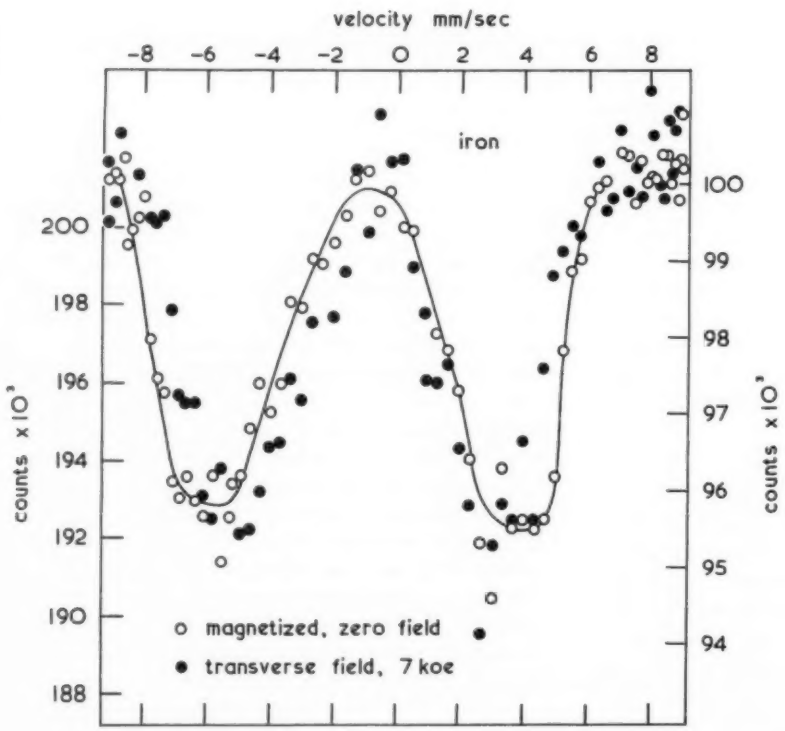

FIG. 1. The absorption spectra obtained with 1% Sn^{119} in Fe. Left scale, o; right scale, •.

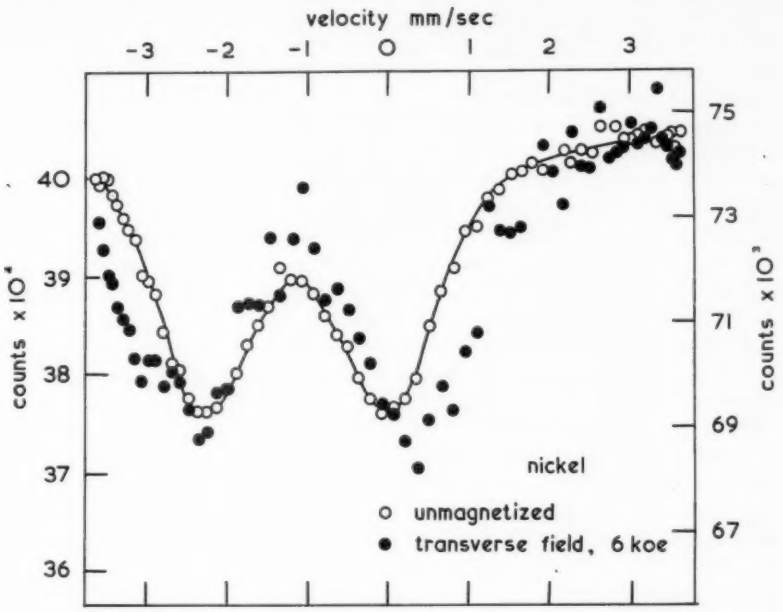

FIG. 2. The absorption spectra obtained with 1% Sn^{119} in Ni. Left scale, o; right scale, •.

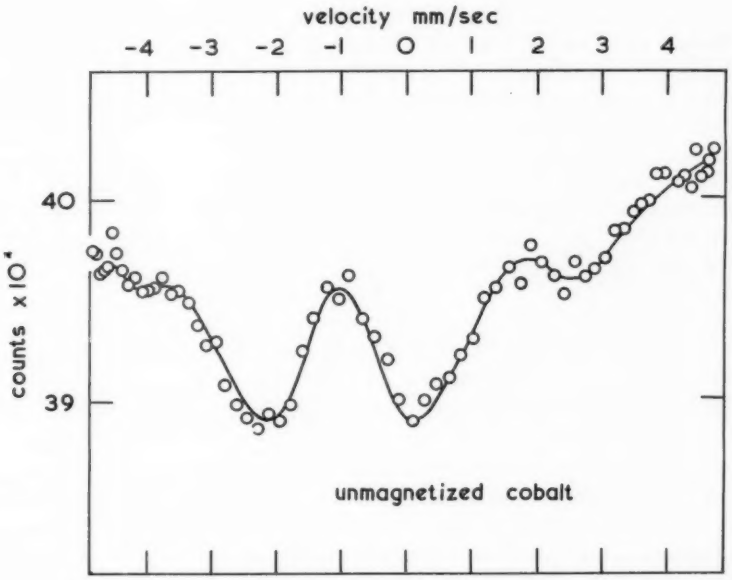

FIG. 3. The absorption spectrum obtained with 1% Sn^{119} in Co.

of $[H_S - (4\pi/3)M]$ are listed in the table, where the values of M have been corrected for the quenching of the atomic moments by the added valence electrons of Sn. This is most significant in Ni, and, since it will occur predominantly amongst the nearest neighbors, will undoubtedly result in a lowered value of the observed field.

The results are obviously inconsistent with the existence of the single field H_c; firstly because of the different signs and secondly because of the relative magnitudes of the fields. Since p is very closely proportional to M,[2] the expression (1) for H_c can be written simply, $H_c = \text{const}\ \xi_S M$. Further, we can conclude from the chemical

shifts that ξ_S is practically constant for Fe, Co, and Ni, and therefore H_C will be roughly proportional to M.

There is another mechanism[11] by which an effective field might be produced at the Sn nucleus in this situation. The wave function for the 4s electrons of the Sn atom will overlap with those of the 3d electrons of the surrounding solvent atoms, and the polarization of the latter will result in a change in the relative spatial distribution of the 4s electrons in respect of their spin orientation. In the region of the Sn nucleus, electrons with spin antiparallel to the 3d polarization will predominate, producing a negative effective field H_p.

Evidence for the existence of such a field is provided by the results for Co (Fig. 3) which indicate the presence of a second field of -50 koe with the same chemical shift. X-ray analysis of the sample showed that both cubic and hexagonal structures were present in the rough proportion 40:60. Since neither ξ_S nor p depends on the structure, the two values of the field cannot be associated with H_C; however, since the distribution of the 3d orbitals will probably differ for the two structures,[12] H_p would also differ.

We have no estimate of H_p, but its magnitude should depend not only on M but also on the mean radius of the 3d shell and thus will decrease more rapidly from Fe to Ni than does the field H_C which depends only on M. In the absence of any further contributions, combination of such a field H_p with a positive value of H_C would therefore provide a qualitative interpretation of the present results.

It is interesting to compare the present results for the field at a Sn nucleus in Fe with those of Samoilov et al.[13] From measurements of the nuclear polarization these authors obtain values of 250 koe and 280 koe, respectively, for the field at In^{114} and Sb^{122} dissolved in Fe.

We are indebted to Dr. C. Johnson for drawing our attention to the results of Samoilov et al. and we are grateful to many people for valuable discussion, particularly Dr. Lomer, Dr. W. Marshall, Dr. S. F. Edwards, and Dr. H. E. Hall. Much helpful advice in the preparation of the alloys has been given by Dr. J. Stubbles. We would also like to thank Dr. J. Zussman for performing the x-ray analysis.

---

*Supported financially by the Department of Scientific and Industrial Research.

[1]For a review article see C. Herring, Suppl. J. Appl. Phys. 31, 3S (1960).

[2]W. Marshall, Phys. Rev. 110, 1280 (1958).

[3]S. S. Hanna, J. Heberle, C. Littlejohn, G. J. Perlow, R. S. Preston, and D. H. Vincent, Phys. Rev. Letters 4, 177 (1960).

[4]S. S. Hanna, J. Heberle, G. J. Perlow, R. S. Preston, and D. H. Vincent, Phys. Rev. Letters 4, 513 (1960).

[5]D. R. Teeters, thesis, University of California, Berkeley, 1955 (unpublished).

[6]Separated Sn^{119} used in the preparation of the alloys was supplied by the Chemistry Division, Atomic Energy Research Establishment, Harwell.

[7]R. L. Mössbauer, Z. Physik 151, 125 (1959).

[8]A. J. F. Boyle, D. St. P. Bunbury, C. Edwards, and H. E. Hall, Proc. Phys. Soc. (London) (to be published).

[9]A. J. F. Boyle, D. St. P. Bunbury, and C. Edwards (to be published).

[10]O. C. Kistner and A. W. Sunyar, Phys. Rev. Letters 4, 412 (1960).

[11]D. A. Goodings and V. Heine, Phys. Rev. Letters 5, 370 (1960).

[12]J. B. Goodenough, Phys. Rev. 120, 67 (1960).

[13]V. N. Samoilov, V. V. Skliarevsky, and E. P. Stepanov, Soviet Phys. —JETP 11(38), 261 (1960).

STIMULATED INFRARED EMISSION FROM TRIVALENT URANIUM

P. P. Sorokin and M. J. Stevenson
Research Center, International Business Machines Corporation, Yorktown, New York
(Received November 28, 1960)

Schawlow and Townes[1] have proposed the extension of maser techniques to generate coherent light in the visible and infrared regions of the electromagnetic spectrum. Recently Maiman[2] and Collins et al.[3] obtained stimulated emission of radiation in chromium-doped Al_2O_3 in the R_1 transition from the ^2E metastable state to the ground state. The oscillation was achieved by inverting the population of the metastable state relative to the ground state by a sufficient amount to overcome the losses in the optical cavity. Since this required approximately 10^{18} - 10^{19} ions in the metastable state, very high optical pumping power was necessary to achieve inversion.

This Letter describes the characteristics of stimulated emission from trivalent uranium ions substituted for divalent calcium ions in calcium fluoride. The crystals were grown by a technique similar to that described by Galkin and Feofilov.[4] In contrast to the case of the ruby optical maser, the oscillation takes place in a transition from a metastable state to a level approximately 515 cm^{-1} above the ground state. At low temperatures this state is depopulated by at least a factor of 10^{10} relative to the ground state. The general condition for stimulated emission is that the number of excited ions in the metastable state must exceed the number of ions in the lower state by a certain amount Δn sufficient to overcome the cavity losses. In trivalent uranium this condition will be achieved at low temperatures when the population of the metastable state is approximately equal to Δn since the population of the lower state is negligible. The value Δn may be generally much less than the number of ions in the ground state. It was indeed observed that the pumping power necessary to achieve stimulated emission was lower by about a factor of 500 compared to ruby.

Figure 1 shows the pertinent energy levels of the trivalent uranium ion when substituted for calcium in the CaF_2 lattice.[4] The ion has several strong absorption bands in the visible and near infrared wavelength regions. The strongest absorption bands are in the green and blue, and as a result the crystals have a pale to deep red color and thus show a striking resemblance to ruby. Very strong fluorescence is observed in the infrared region between 2.0 and 2.6 microns

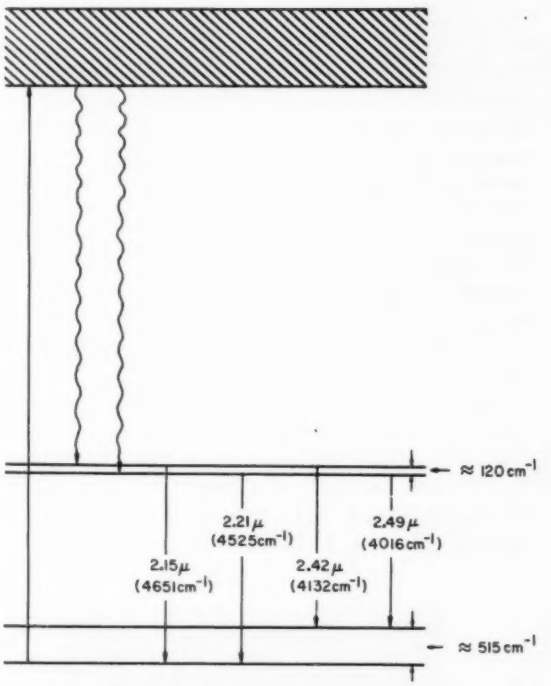

FIG. 1. Energy level diagram of trivalent uranium in calcium fluoride based on the paper by Galkin and Feofilov. Broad-band pumping light applied in the blue and green visible spectrum causes transitions to excited bands, one of which is depicted in the figure. These pumping transitions are followed by rapid, nonradiative transitions to the two metastable levels shown.

when exciting radiation is applied in the range of the absorption bands. The room temperature fluorescence spectrum consists of four peaks. The two shorter wavelength peaks coincide with the absorption peaks and therefore are resonance lines. The two longer wavelength peaks represent emissions to a state located approximately 515 cm^{-1} above the ground state. The longest wavelength emission occurs from the lower metastable state and is the transition in which the maser oscillations are observed.

A single crystal of calcium fluoride with 0.05 mole percent uranium was cut into a cylindrical shape 3/8 in. in diameter and $1\frac{1}{2}$ in. long. The ends were polished flat to one-twentieth of a sodium wavelength and parallel to fifteen seconds

of arc. Silver films were evaporated on both ends, with one end left completely opaque and the other end left with a 1.5% transmission. A protective SiO coating was applied over the silver to prevent oxidation. The sample was placed in a specially constructed liquid helium Dewar and was cooled without being in actual contact with the liquid helium. A pulsed xenon discharge lamp excited the vertically positioned sample through a side port in the Dewar. The infrared radiation generated in the sample was coupled out through the 1.5% transmitting end face and was detected by a lead sulfide detector through a top port. Either a 2.5-micron interference filter or a Perkin-Elmer monochromator was used to isolate the infrared radiation from the lamp background. The response time of the detector was approximately 40 microseconds for decaying radiation.

Figure 2 shows typical oscilloscope traces of the detector response to the intense monochromatic stimulated emission when the pump power is set above the threshold value. The signal during the first 450 microseconds of Fig. 2(a) is due primarily to the scattered light from the xenon flash lamp plus a small but undetermined amount of spontaneous radiation. Oscillation begins where the rapidly rising, almost vertical, trace is observed and always occurs when the pumping power reaches the same critical level. Fig. 2(b) shows the same detector output with reduced gain and expanded time scale. The ratio between the stimulated emission and the background light was measured to be in excess of 1000, which means that the spontaneous emission is less than the stimulated emission by a factor of several thousand. This ratio is larger than that observed for the ruby maser, which conforms to the expectation of smaller spontaneous emission in the infrared as compared with the visible spectral region. The spectral width of the maser pulse was substantially less than the resolving power of the monochromator. The beam was confined to an angle of approximately

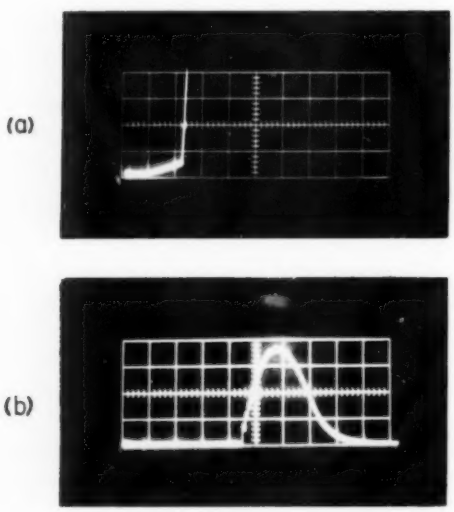

Fig. 2. (a) Detector response above threshold showing the onset of oscillation after 450 μsec. A filter with a bandwidth of 0.1 micron and centered at 2.5 microns is inserted before the detector. The sweep speed is 200 μsec/division. (b) Detector response with the conditions as in 2(a) except that the oscilloscope gain is reduced by a factor of 500 and the sweep speed is 100 μsec/division.

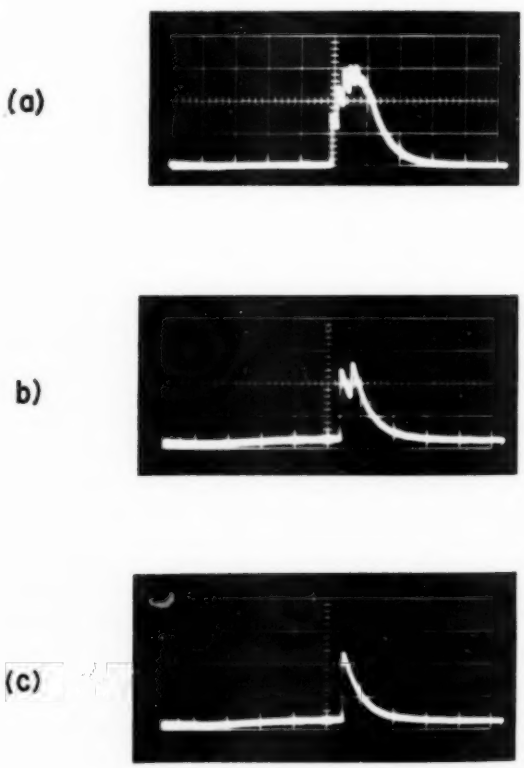

FIG. 3. Relaxation oscillations at varying pump power levels. The time scale is 100 μsec/division. Trace (a) shows the maser output with pump power about 1.5% above threshold. Traces (b) and (c) are taken at powers barely above threshold.

0.01 radian.

An interesting feature of the maser output shown in Fig. 2(b) is the presence of relaxation oscillations, previously also observed in less detail by Collins et al. in ruby. The number of observed spikes decreases rapidly as the power input into the exciting xenon lamp is lowered towards the threshold value until at barely above threshold only a single spike oscillation occurs. Figure 3 illustrates this phenomenon. The single spike takes place at exactly the peak of the pulse output of the xenon lamp, while the multiple spikes begin earlier because the exciting power reaches the threshold value at an earlier point. The spacing between the oscillations increases as the xenon lamp input power is brought closer to threshold. These features seem consistent with the explanation offered by Collins et al. for the relaxation oscillations in the ruby optical maser, perhaps complicated by contributions from several frequency modes within the inhomogeneously broadened line as suggested by G. J. Lasher of this laboratory.

The favorable energy level structure of trivalent uranium as compared to ruby may result in a strong cw infrared source for research purposes in the near future.

We would like to thank J. Lankard for assistance with the experiments, W. V. Smith and A. H. Nethercot for their continued interest and encouragement, and other members of the laboratory for helpful discussions. Special thanks are due Walter Hargreaves of Optovac, Inc. for cooperating with us in growing the crystals.

[1]A. L. Schawlow and C. H. Townes, Phys. Rev. 112, 1940 (1958).

[2]T. H. Maiman, Nature 187, 493 (1960); British Communications and Electronics 7, 674 (1960).

[3]R. J. Collins, D. F. Nelson, A. L. Schawlow, W. Bond, C. G. B. Garrett, and W. Kaiser, Phys. Rev. Letters 5, 303 (1960).

[4]L. N. Galkin and P. P. Feofilov, Doklady Akad. Nauk S.S.S.R. 114, 745 (1957) [translation: Soviet Phys. – Doklady 2, 255 (1957)].

MOBILITY OF HYDROGEN IONS*

Robert N. Varney
Department of Physics, Washington University, St. Louis, Missouri
(Received November 14, 1960)

Experimental measurements of the drift velocity or mobility of hydrogen ions in the parent gas indicate only a single type of ion, which has consistently been assumed to be H_2^+.[1-3] Rarely, a second ion has been reported,[4,5] but it has always been difficult to observe so that a cloud of suspicion as to its reality has prevailed. Identification of the ion as H^+ seems to be justifiable. The theory of ionic mobilities has been applied by Mason and Vanderslice[6] to hydrogen, and it supports the identification of the ions described above. It predicts also that H_3^+ should be found with a mobility considerably higher than that of either H^+ or H_2^+ or of any observed values reported in references 1-5.

Meanwhile, Stevenson[7] has published some properties of the H_3^+ ion which are listed here:

(1) H_3^+ is formed by the reaction $H_2^+ + H_2 = H_3^+ + H$.

(2) The cross section for this reaction is enormous, approximately 1×10^{-14} cm^2.

(3) The binding energy of H_3^+ is 97 kcal or 4.18 ev (private communication).

(4) H_3^+ ions passing through H_2 gas probably have an enormous charge-exchange cross section, of the same approximate size, 1×10^{-14} cm^2, as for the formation of H_3^+.

(5) The charge-exchange mechanism appears to be an exchange of a proton instead of the more usual exchange of an electron envisaged by the term "charge exchange."

If these findings are correct, and there is every reason to believe they are, then two changes must be made in the theory and interpretation of mobilities of ions in hydrogen.

(1) The H_2^+ ion is never observed in mobility experiments nor will it ever be observed.

(2) The H_3^+ ion has a lower mobility than predicted by Mason and Vanderslice, presumably having the value commonly observed.

The following justifications are offered: The chemical equlibrium constant for the formation reaction for H_3^+ given by Stevenson is so large that there is no possibility of shifting the equilibrium toward the H_2^+ side of the reaction within the bounds of swarm-type experiments, for ex-

ample, by very low pressures. At very high temperatures or very high values of E/p_0, at which equilibrium would be shifted toward the left side, the H_2^+ ion would still not be found as the dissociation of H_2^+ would then prevail. It may be noted that the binding energy of H_2^+ at 2.65 ev is appreciably less than that of H_3^+ quoted as 4.18 ev by Stevenson.

The structure of H_3^+ seems necessarily to be H - H - H. Since H_2 is simply H = H, the exchange of the proton is not surprising. The binding energy of H_2 is very nearly the same as for H_3^+, 4.48 and 4.18 ev, respectively, so that the proton exchange is virtually a resonance phenomenon. The H_3^+ ion passing through H_2 gas is, in effect, the "normal" ion of the parent gas consisting of the parent molecule with an attached proton instead of the parent molecule with a detached electron. The size of the charge-exchange cross section should drastically lower the ionic mobility.

The writer is much indebted to Dr. Stevenson for pointing out the experimental evidence he had obtained and for extensive discussions in which the analysis above was formulated.

---

*Supported by the U. S. Army Office of Ordnance Research.

[1]A. M. Tyndall, The Mobility of Positive Ions in Gases (Cambridge University Press, New York, 1938), p. 70.

[2]D. J. Rose, J. Appl. Phys. 31, 643 (1960).

[3]L. M. Chanin, Thirteenth Annual Gaseous Electronics Conference, October 12-15, 1960 (unpublished).

[4]N. E. Bradbury, Phys. Rev. 40, 508 (1932).

[5]K. B. Persson, Phys. Rev. 106, 191 (1957).

[6]E. A. Mason and J. T. Vanderslice, Phys. Rev. 114, 497 (1959).

[7]D. P. Stevenson, J. Chem. Phys. 29, 282 (1958).

DISSOCIATION OF H_2^+ AND He^- BY ELECTRIC FIELDS

A. C. Riviere and D. R. Sweetman
United Kingdom Atomic Energy Authority, Aldermaston, Berkshire, England
(Received November 28, 1960)

Processes leading to the dissociation of molecular ions have assumed some importance recently in connection with injection into thermonuclear devices. In particular, the dissociation of molecular ions by electric fields (or the equivalent $\vec{v}\times\vec{B}$ field), provides an attractive method of injection of high-energy particles which avoids the use of dense low-temperature plasmas or carbon arcs.

Recent theoretical studies by Hiskes et al.[1-3] have shown that the upper vibrational states of molecular ions may dissociate in electric fields of a few hundred kilovolts/cm. In this paper we describe experiments in which this dissociation has been observed and also an experiment in which the He^- ion was dissociated by an electric field.

The experimental arrangement was basically that described by Sweetman[4] for measuring the H_2^+ dissociation cross section in hydrogen. For the present measurements the gas target chamber was replaced by an electrode system so designed that the ion beam would pass through an electric field of known strength. Figure 1 shows the details of the high-field gap and the field distribution as seen by a particle on the axis and on the periphery of the beam. The ions passed through the gap and the high-voltage electrode,

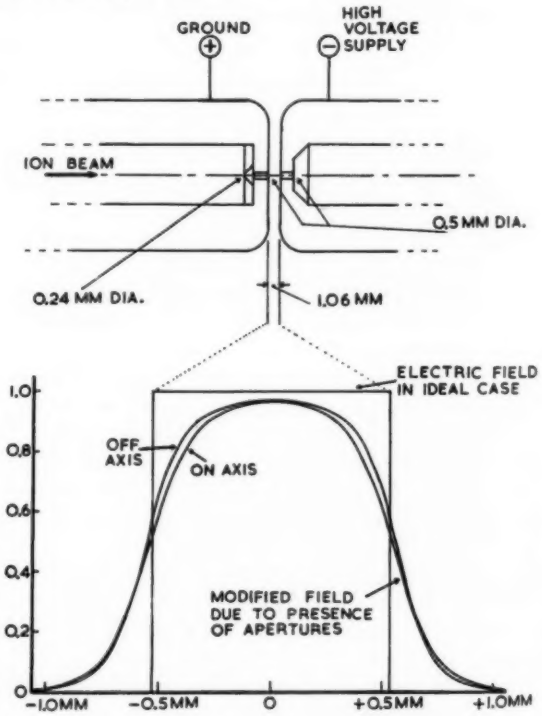

FIG. 1. Details of the high-field gap and electric field distribution.

and then returned to ground potential through a region in which the field was everywhere less than 2% of that in the gap. The ion beam was magnetically analyzed and the individual components were detected by CsI scintillation counters. Coincidences between H^0 and H^+ particles and also between two H^+ particles were recorded so that both modes of dissociation could be studied under low-background conditions.

In the first experiments, H_2^+ ions emerging from an rf ion source were accelerated to 2 Mev in a Van de Graaff electrostatic accelerator before passing into the apparatus. The fraction of the beam dissociated by electric fields up to 5×10^5 volts/cm is shown in Figure 2. The number dissociated increases steadily for fields above 0.70×10^5 volts/cm. The rate of ionizing dissociation (to $H^+ + H^+$) remains constant over this range. This is to be expected since the field strength required to ionize hydrogen atoms is of the order of 10^6 volts/cm,[1] whereas the maximum field strength achieved here was 5×10^5 volts/cm. This result also removes any doubt about possible dissociation due to the deflection of the ion beam on to stops by the applied electric field. No such effect is observed.

In order to increase the population of the uppermost vibrational levels, H_2^+ ions were obtained from H_3^+ ions which had been accelerated to 2.0 Mev and then dissociated by collision with gas molecules. It can be seen that the H_2^+ ions formed by the breakup of H_3^+ ions were dissociated by the field to a much greater extent than those obtained directly from the ion source. This mode of formation evidently results in a considerably greater population of the upper vibrational states.

The calculations of Hiskes[1] show that the uppermost vibrational levels ($v = 17$, 18) with zero rotational energy should be completely dissociated by fields of 6×10^5 and 2×10^5 volts/cm, respectively. A steep rise in the fraction dissociated would be expected at 2×10^5 volts/cm followed by a plateau. In fact the dissociation fraction is seen to rise almost linearly from fields of about 0.7×10^5 volts/cm. According to Hiskes,[1] the presence of rotational energy probably has the effect of reducing the field required for dissociation, and this may account for the lack of distinct steps due to the discrete vibrational states.

The dissociation of HD^+, D_2^+ and other molecular ions is of great interest for thermonuclear experiments and will be investigated in future work.

The effect of an electric field was also tried on He^- and H^- ions at energies of 1.0 Mev and 0.33 Mev, respectively. The results are shown in Fig. 3. The He^- ion has an estimated binding energy of 0.075 ev,[5] and was completely dissociated by a field of 4.5×10^5 volts/cm. The H^- ion has a binding energy of 0.75 ev,[6] and no effect was observed up to the maximum field of 5.4×10^5 volts/cm. Holøien and Midtdal[5] have shown that

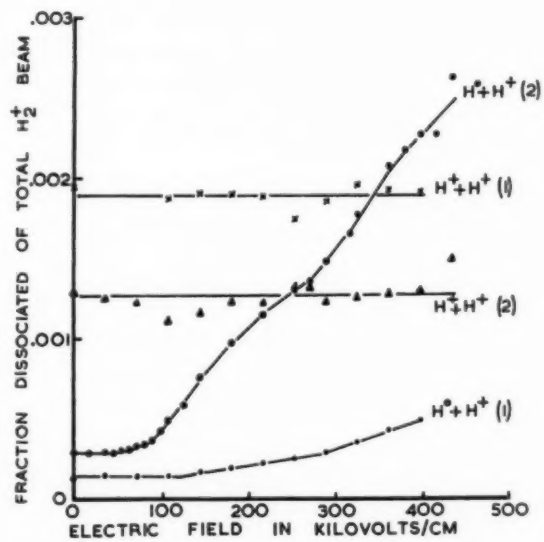

FIG. 2. Dissociation of H_2^+ ions as a function of electric field. Curves (1): H_2^+ ions direct from source. Curves (2): H_2^+ ions obtained from the breakup of H_3^+ ions.

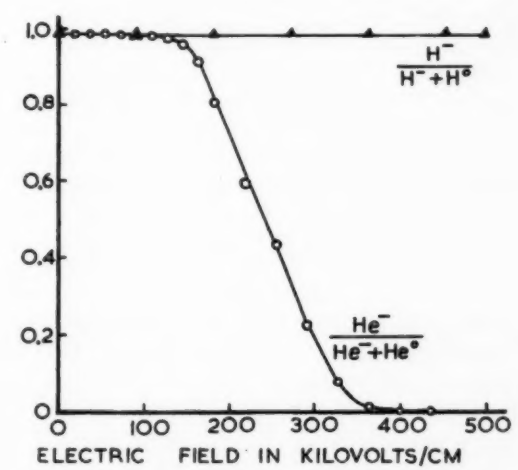

FIG. 3. Dissociation of He^- and H^- as a function of electric field.

the probable configuration of He^- is $(1s\ 2s\ 2p)^4P$, and that autoionization from this state is not allowed. In the absence of an electric field the lifetime of this state is known to be greater than 10^{-5} second.[7] The dissociation of this ion in the electric field may be due to breakdown of the selection rules for autoionization or due to field emission of the electron leaving the He^0 in the $(1s\ 2s)$ metastable state. Further experimental investigations are under way to elucidate this point.

The authors are grateful to Mr. R. E. Bradford, Mr. J. Coupland, and Mr. R. Webster for their help in setting up the apparatus and taking the results.

[1]J. R. Hiskes, University of California Radiation Laboratory Report UCRL-9182, May, 1960 (unpublished).
[2]J. R. Hiskes and J. L. Uretsky, University of California Radiation Laboratory Report UCRL-8255, April, 1958 (unpublished).
[3]J. R. Hiskes, Bull. Am. Phys. Soc. 5, 340 (1960).
[4]D. R. Sweetman, Proc. Roy. Soc. (London) A256, 416 (1960).
[5]E. Holøien and J. Midtdal, Proc. Phys. Soc. (London) A68, 815 (1955).
[6]E. A. Hylleraas and J. Midtal, Phys. Rev. 103, 829 (1956).
[7]D. R. Sweetman, Proc. Phys. Soc. (London) (to be published).

SEARCH FOR A SMALL CHARGE CARRIED BY MOLECULES*

John G. King
Department of Physics and Research Laboratory of Electronics, Massachusetts Institute of Technology, Cambridge, Massachusetts

(Received November 7, 1960; revised manuscript received November 28, 1960)

The suggestion by Lyttleton and Bondi[1] that hydrogen atoms might carry a charge of approximately 2×10^{-18} of an elementary charge has stimulated a number of investigators to undertake experiments designed to measure this charge. At least two methods have been used: atomic beam deflection experiments,[2,3] and the method of Piccard and Kessler.[4] The results published thus far[2-6] are listed in Table I. In this paper preliminary results of a Piccard-Kessler experiment are reported in which hydrogen molecules (and also helium atoms) exhibit a charge that is approximately 40 times less than that required by the hypothesis of Lyttleton and Bondi.

In our experiment the gas whose charge is to be measured is allowed to escape from an electrically insulated metal container connected to an electrometer. While the gas is escaping, a current that can be measured will flow to the container if the gas is charged. The charge on each atom can then be computed, although it is essential to distinguish charge carried by each of the hypothetically charged atoms from charge carried by ions, electrons, and charged dust particles. By passing the escaping gas through a de-ionizer consisting of a coaxial capacitor charged by a

Table I. Upper limit on the charge carried by various molecules.

Molecule	Charge (elementary charge/molecule)	Experimental method
CO_2	$\leq 2\times10^{-19}$	Piccard-Kessler [a]
CsI	$\leq 4\times10^{-13}$	Molecular beam [b]
A	$< 8\times10^{-20}$	Piccard-Kessler [c]
N_2	$< 12\times10^{-20}$	Piccard-Kessler [c]
CsF	$\leq 2\times10^{-14}$	Molecular beam [d]
KF	$\leq 1\times10^{-13}$	Molecular beam [d]
n	$< 6\times10^{-12}$	Molecular beam [e]

[a]See reference 4.
[b]See reference 2.
[c]See reference 5.
[d]See reference 3.
[e]See reference 6.

battery within the container, ions and electrons, because of their relatively high mobilities, can be swept from the gas stream, while atoms carrying the hypothetical charge of 10^{-18} of an elementary charge will be unaffected. Dust particles, which range in size from molecules to visible grains, may be sufficiently massive to pass through the de-ionizer, but their effect is likely to be both erratic and cumulative.

By recording the pressure and the output of the electrometer, both as a function of time, on a two-channel recorder, it is not only possible to measure the total charge carried by the gas, but also to see that the potential-versus-time curve has the expected shape for the flow of a uniformly charged gas. The course to be followed by the experimenter is plain. If the atoms seem to be charged, the computed charge per atom must be independent of all parameters, such as de-ionizer potential and polarity, rate of gas efflux, pressure, bias potential of the container with respect to ground, and, of course, details of apparatus construction and gas handling. It is to be expected that the charge per atom will be different for different gases. On the other hand, if the atoms appear uncharged, it is important to make certain that the electrometer is sensitive during the gas efflux and that mechanisms that might cancel a genuine effect are eliminated. Such cancellation is most likely to occur at the end of the outlet pipe from the container.

Figure 1 is a scale drawing of the apparatus.

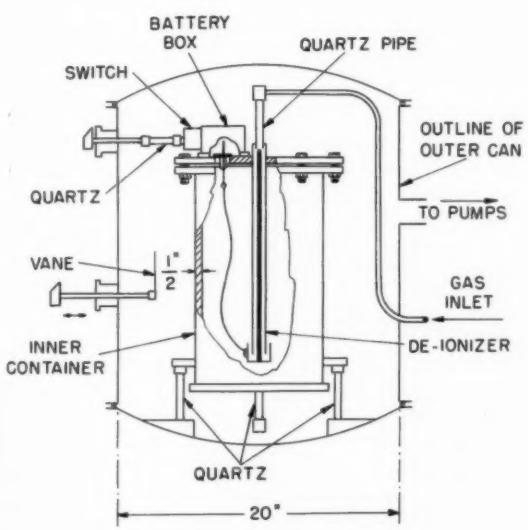

FIG. 1. Scale drawing of the apparatus.

The outer can serves both as a vacuum envelope and as an electrical shield for the container (11.2 liters) which stands on three quartz supports and is filled with gas through a quartz pipe. This quartz pipe is metalized at its ends so that it can be soft-soldered into place. Although it was designed to stand a pressure of 1000 psi, the container was usually operated at a pressure of 265 psi. The outer can was pumped to 10^{-6} mm Hg to prevent electrical leakage and to reduce undesirable thermal effects. The central electrode of the de-ionizer is maintained at ± 90 volts, or zero volts with respect to ground, as determined by the setting of a switch. The approximate contact potential to ground of the container can be determined by a movable vane. The gas that is to be investigated is admitted to the container through a porous bronze filter with 5-μ pores, an electrostatic precipitator, and needle valves for controlling the flow. A pressure transducer generates a signal proportional to the pressure in the container which can be recorded on one channel of a two-channel Sanborn recorder. The gas escapes from the container through an external regulator that maintains constant pressure on a needle valve adjusted to give the desired rate of flow. It was thus possible to obtain a nearly linear drop in pressure in the container with respect to time.

Potential changes of the container with respect to the outer can are measured with a GL5674 electrometer whose output is amplified by a chopper amplifier and recorded on the other channel of the Sanborn recorder. Potential differences of 10^{-4} volt, or currents of approximately 10^{3} electrons per second, can be detected. The time constant is 60 ± 5 sec which agrees with the time constant predicted from independent measurements of the electrometer grid resistance and capacitance, 10^{12} ohms and 60 $\mu\mu$f, respectively. The ground return of the electrometer is connected through a low-impedance voltage supply that makes it possible to place the container at different potentials with respect to the outer can. When the potential of the container was +0.01 volt, moving the vane was found to have negligible effect. Frequent calibrations of the electrometer were made with signals close to the minimum detectable signal introduced at the ground end of the electrometer grid resistor. No consistent dependence of the electrometer sensitivity on the polarity of the calibrated signal, the amount of gas in the container, the polarity of the de-ionizer, or any other parameter was found. Calibrations were also made

while the gas was flowing from the container, and the sensitivity was found to be normal.

The 21 hydrogen and 19 helium runs at 265 psi and 140 sec efflux time (selected only because these parameters were the same) yielded electrometer recordings that are superimposed in Figs. 2(a) and 2(b) normalized at the start of flow. Average curves that were constructed for hydrogen and helium are plotted in Fig. 3. The shaded rectangle, 0.3 mv high and 140 sec long, represents 2.7×10^{5} elementary charges, which is the amount of charge that would be observed if each of the 5.4×10^{24} molecules carried 5×10^{-20} of an elementary charge. The apparent charge per molecule, determined from the average curves, is $(2.5\pm1.5)\times10^{-20}$ elementary charge/molecule for hydrogen, and $(-4\pm2)\times10^{-20}$ elementary charge/molecule for helium. The charge on hydrogen appears to be negative; the charge on helium, to be positive.

None of the recordings looks like the computed curve, (d) of Fig. 3, which was derived from the pressure curve, (a) of Fig. 3. The hydrogen curve goes negative and then positive, and the helium curve has a negative maximum that is too early by 30 sec. If it is assumed that the helium effect is spurious and that whatever produces it is likewise present in the hydrogen runs, the helium curve may be subtracted from the hydrogen curve. This procedure yields a curve (represented by circles in Fig. 3) that is in remarkable agreement with the computed curve. If this agreement is taken to be significant, we obtain a value of $(7\pm2.5)\times10^{-20}$ elementary charge/molecule for hydrogen, and $(0\pm2)\times10^{-20}$ elementary charge/molecule for helium.

The electrometer deflections recorded are still not understood; but the nature of these results, as well as the results of numerous side experiments, eliminates a few of the possible causes for the deflection, such as capacitative effects, piezoelectricity, and thermoelectricity. New and improved apparatus, use of other gases, including deuterium, and wider variations of parameters will provide the answer. In any case, the charge that we found for the hydrogen molecule, by interpreting our experiment in the obvious way, is far less than that required for the hydrogen atom by the hypothesis of Lyttleton and Bondi. A molecular-beam experiment is under way with cesium, but the difficulties of achieving sufficient sensitivity with hydrogen (and later atomic hydrogen) are considerable.

My thanks are due to Professor Jerrold R. Zacharias and Professor E. M. Purcell for valuable discussions, and to Mr. Frank O'Brien

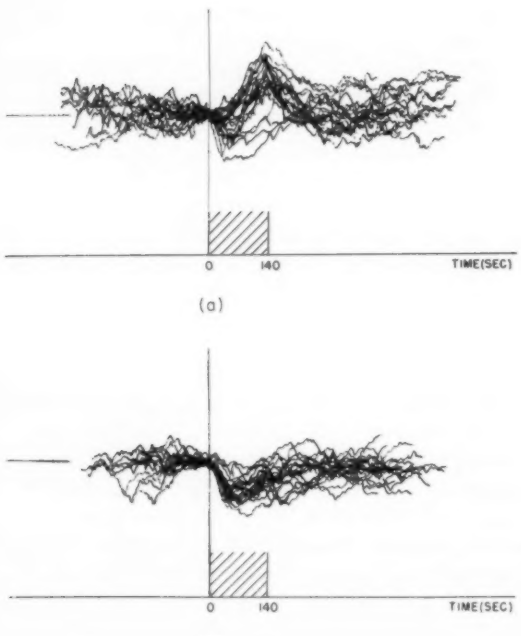

FIG. 2. (a) Superimposed electrometer recordings of 21 hydrogen runs. (b) Superimposed electrometer recordings of 19 helium runs.

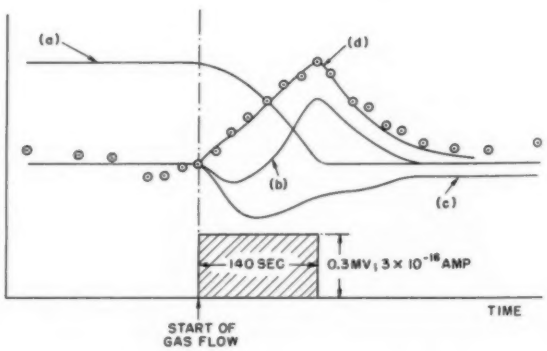

FIG. 3. (a) Observed pressure (arbitrary units) in the container as a function of time as the gas flows out. (b) Average voltage curve constructed from the data of Fig. 2(a). (c) Average voltage curve constructed from the data of Fig. 2(b). (d) Electrometer response to the flow, according to curve (a), of a uniformly charged gas from the container. Circles represent the difference between curves (b) and (c).

for much assistance with the apparatus.

*This work was supported in part by the U. S. Army Signal Corps, the Air Force Office of Scientific Research, and the Office of Naval Research.

[1]R. A. Lyttleton and H. Bondi, Proc. Roy. Soc. (London) A252, 313 (1959).

[2]V. W. Hughes, Phys. Rev. 105, 170 (1957).

[3]J. C. Zorn, G. E. Chamberlain, and V. W. Hughes, Bull. Am. Phys. Soc. 5, 36 (1960).

[4]A Piccard and E. Kessler, Arch. sci. phys. et nat. 7, 340 (1925).

[5]A. M. Hillas and T. E. Cranshaw, Nature 184, 892 (1959); see also H. Bondi and R. A. Lyttleton, Nature 184, 974 (1959), and A. M. Hillas and T. E. Cranshaw, Nature 186, 459 (1960).

[6]I. Shapiro and V. Estulin, Soviet Phys.-JETP 3(30), 626 (1957).

CLUSTER MODEL INTERPRETATION OF THE ISOTOPIC SPIN SELECTION RULE IN CERTAIN NUCLEAR REACTIONS

G. C. Morrison

Enrico Fermi Institute for Nuclear Studies, University of Chicago, Chicago, Illinois

(Received November 9, 1960)

In this note we wish to present results concerning the operation of the isotopic spin selection rule in nuclear reactions which have resulted from a study of some lithium-induced reactions. Experimental verification of such selection rules has previously been obtained from the study of (d,α)[1] and (α,d)[2] reactions, from the study of inelastic deuteron scattering,[3] and recently from the work of Halbert and Zucker[4] on the inelastic scattering of N^{14} by C^{12}. In the present work we have been concerned with the reactions $Li^6(Li^6, d)B^{10}$ and $Li^6(Li^7, t)B^{10}$ with particular reference to the reactions leading to the $T=1$, second excited state of B^{10} at 1.74 Mev. In the first reaction it was to be expected, since both Li^6 and the deuteron have $T=0$, that the probability of deuteron emission leading to the $T=1$ level in B^{10} would be reduced by virtue of the isotopic spin selection rule; the second reaction was studied for purposes of comparison.

In Fig. 1 the spectrum of deuterons observed at a laboratory angle of 9.5° from the reaction $Li^6(Li^6, d)B^{10}$ is presented. The positions of the levels in B^{10} are as calculated from the observed position of the deuterons leading to the first 1+ level in B^{10} and the variation of its position with the angle of observation. As can be seen from the observed spectrum, deuterons leading to the $T=1$ level in B^{10} are very much inhibited, and over the angular range where one could observe this deuteron group, the situation persisted. As discussed above, this result can be interpreted as confirmation of the isotopic spin selection rule. However, it is the purpose of this note to suggest that the observed inhibition may be considered on a different basis.

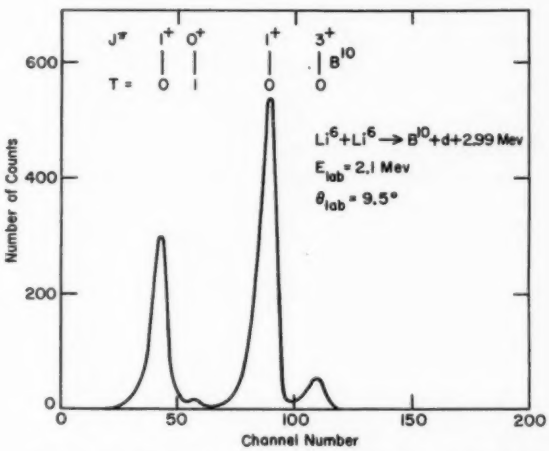

FIG. 1. The spectrum of deuterons observed in the reaction $Li^6(Li^6, d)B^{10}$ at a laboratory angle of 9.5° and incident energy of 2.1 Mev. The positions of the corresponding levels in B^{10} are indicated above.

As part of the reaction studies using lithium ions, evidence has been obtained that both the reactions (Li^6, d) and (Li^7, t) are favored and proceed in part by a stripping mechanism with capture of the alpha-particle substructure.[5] In the reaction $Li^6(Li^6, d)B^{10}$, if only the J^π of the final states in B^{10} are considered, there is no reason why the 0+ level should be reduced except possibly by a $(2J+1)$ weighting factor. However, we see from Fig. 1 that the deuterons leading to the 3+ level in B^{10} are reduced also relative to those leading to the 1+ levels. If now the situation is considered from the viewpoint of B^{10}

being formed as a result of the capture of an alpha particle by Li^6, the following considerations apply. The formation of B^{10} in a 1+ level can proceed by $l=0$ capture of the alpha particle, while the formation of the 3+ level can only proceed by at least $l=2$ capture and might be expected to be reduced as is observed. And now when we consider the formation of the $0+(T=1)$ level of B^{10} on this basis, there is no way by which an alpha particle ($J=0+$) can be captured by $Li^6(J=1+)$ to form a 0+ state.

Up to this point, the discussion has only been an alternative way of explaining the inhibition of the deuteron group leading to the $T=1$ level, since the usual one concerning isotopic spin conservation leads to the same conclusion. However, in the comparison study of the reaction $Li^6(Li^7,t)B^{10}$ essentially no tritons leading to the $T=1$ level were observed. In the reaction, there is now no restriction due to isotopic spin conservation which can inhibit the formation of the $T=1$ level in B^{10}. Likewise there is no consideration due to the available angular momentum for the reaction to proceed.

The spectrum of tritons observed at 14.5° from the reaction $Li^6(Li^7,t)B^{10}$ is shown in Fig. 2, with the calculated positions of the levels in B^{10} shown above. The similarity in the relative intensities of the tritons and deuterons leading to the same low-lying levels in B^{10} can be noted. That the second 1+ level in B^{10} is not more strongly excited may be due in part to the low Q value (-0.16 Mev) for the $Li^6(Li^7,t)B^{10}$ reaction leading to this level. With such small energy available in the center-of-mass system the transfer of an alpha particle to Li^8 may be inhibited by the Coulomb field, although it is realized that this argument also may account for some of the reduction observed in the tritons leading to the 0+ level where the Q value is only 0.25 Mev. A clarification of this point awaits detailed calculations involving the proposed reaction mechanism involving alpha-particle transfer. At this time, however, the most likely explanation of the inhibition of the triton group leading to the $T=1$ level appears to be the impossibility of Li^6 capturing an alpha particle to form a 0+ state of B^{10} as discussed for the $Li^6(Li^8,d)B^{10}$ reaction.

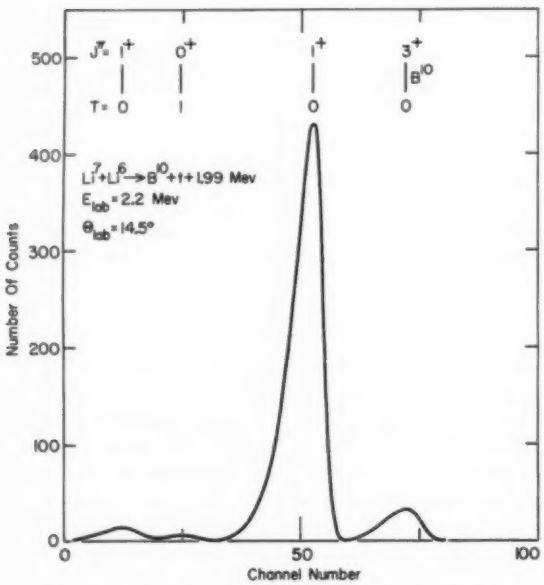

FIG. 2. The spectrum of tritons observed in the reaction $Li^6(Li^7,t)B^{10}$ at a laboratory angle of 14.5° and incident energy of 2.2 Mev. The positions of the corresponding levels in B^{10} are indicated above.

Of course this description of the reaction is just what the $T=1$ nature of the state implies insofar as this state in B^{10} corresponds to a nucleus with six neutrons and four protons or vice versa, where the two extra neutrons or protons are necessarily in a singlet state. Thus if one thinks of the $T=1$ level of B^{10} at 1.74 Mev as having the character of Be^8 plus a deuteron in the singlet $T=1$ state which is consistent with the 2-Mev difference in binding energy of the singlet and triplet states of the deuteron, the formation of this level when Li^6 captures an alpha particle would require a rearrangement of the deuteron in the target nucleus Li^8. That it is the $T=1$ state of the deuteron which is involved in both reactions studied and not a $T=1$ state arising from a Li^7+He^3 configuration can be seen from considerations of the nuclear masses involved which would predict a $T=1$ level of this nature at much higher excitation energies in B^{10}.

It would seem therefore that such heavy-particle stripping considerations together with such a "cluster" model[5] of the nucleus as discussed here are capable of explaining the observed isotopic spin conservation in the $Li^6(Li^8,d)B^{10}$ reaction in a very simple way. Furthermore one sees that in addition to the (Li^6,d) reaction, the (Li^6,α) reaction and the (α,d) and (d,α) reactions, at energies where heavy-particle stripping involving the transfer of a deuteron is expected to play an important reaction role, also fit into this scheme, since the observation of the isotopic spin selection rule involves a 0+ initial and final state and

the deuteron has spin 1. In addition, the conservation of isotopic spin observed in the inelastic scattering of deuterons, alpha particles, or more recently C^{12} ions from N^{14} can be understood as arising from the improbability of the deuteron in the target nucleus undergoing an internal spin flip to form its $T=1$ state.

It would appear then that at energies where stripping is expected to be important, one does not require the introduction of the formal concept of isotopic spin conservation to describe the inhibition observed in reactions leading to such 0+, $T=1$ levels. That isotopic spin selection rules are experimentally satisfied at high energies has also been pointed out by Wilkinson,[7] who suggests that the reason for their validity is the overlapping of many levels in the compound system which break up before isotopic spin mixing occurs. In this connection it would be of interest to examine the situation in a reaction leading to a higher $T=1$ level where $J\neq 0$, to see whether the transition is allowed or not. It will also be of interest to carry out a study of the reaction $B^{10}(Li^6,d)N^{14*}(T=1)$ and $B^{10}(Li^7,t)N^{14*}(T=1)$ to verify further the results obtained here. It can be pointed out that a study of the latter reaction in conjunction with the reaction $B^{10}(Li^7,He^3)C^{14}$(g.s.) should also provide a sensitive test of the relations between the cross sections predicted by the isotopic spin selection rules.

The author is grateful for the aid given by M. N. Huberman in carrying out the work, to L. Palmer and J. Erwood for dependable operation of the Van de Graaff accelerator, and to S. K. Allison for valuable discussions.

[1]C. P. Browne, Phys. Rev. 104, 1598 (1956).
[2]B. G. Harvey and J. Cerny, Bull. Am. Phys. Soc. 5, 230 (1960).
[3]See, for example, C. K. Bockelman, C. P. Browne, W. W. Buechner, and A. Sperduto, Phys. Rev. 92, 665 (1953).
[4]M. L. Halbert and A. Zucker, Second Conference on Reactions Between Complex Nuclei, Gatlinburg, May 2-4, 1960 [John Wiley & Sons, Inc., New York (to be published)].
[5]G. C. Morrison (to be published).
[6]K. Wildermuth and Th. Kanellopoulos, CERN Report 59-23, 1959 (unpublished).
[7]D. H. Wilkinson, Phil. Mag. 1, 379 (1956).

SEARCH FOR RESONANCE IN π-π INTERACTION IN π-N SCATTERING AT 0.96 Bev

J. G. Rushbrooke and D. Radojičić
Cavendish Laboratory, Cambridge, England
(Received November 21, 1960)

Photographs of interactions in a hydrogen bubble chamber exposed to the 0.96-Bev negative pion beam from the Brookhaven Cosmotron were kindly supplied by Professor Steinberger and have been measured and analyzed.[1] This Letter reports a detailed examination of 110 events of the type

$$\pi^- + p \rightarrow p + \pi^- + \pi^0$$

for evidence of a resonance in the pion-pion interaction.

Other photographs of the same exposure have been measured by Alles-Borelli, Bergia, Ferreira, and Waloschek[2] at Bologna, and some by Pickup, Ayer, and Salant[3] at Brookhaven. Center-of-mass momuntum spectra of the π^- and π^0 mesons from the above reaction were found[3,4] to be in reasonable accord with the extended isobaric nucleon model of Lindenbaum and Sternheimer,[4] which includes contributions from the $T'=\frac{1}{2}$ isobaric state (corresponding to the $T=\frac{1}{2}$ resonance in the π-N system at $T_\pi=600$ Mev) as well as from the $T'=3/2$ state.

Laboratory kinetic energy spectra of protons were found to possess a low-energy peak which has been interpreted by Bonsignori and Selleri[5] and Derado[6] as evidence for a strong pion-pion interaction. This interpretation is based on an estimate of the "pole part" of the pion-nucleon scattering cross section by the method of Chew and Low.[7] Their formula, valid when the square of the four-momentum transfer Δ^2 to the spectator nucleon approaches the unphysical limit $-\mu^2$, where μ is the pion mass, becomes in the case of the reaction considered,

$$\frac{\partial^2\sigma}{\partial\Delta^2\partial\omega^2}=\frac{f^2}{2\pi}\,\frac{\Delta^2/\mu^2}{(\Delta^2+\mu^2)^2}\,\frac{1}{q_{1L}^{\ 2}}\,\omega(\tfrac{1}{4}\omega^2-\mu^2)^{1/2}\sigma_{\pi\pi}(\omega), \tag{1}$$

where f^2 is the renormalized pion-nucleon coupling constant, q_{1L} the laboratory momentum of the incident pion, and $\sigma_{\pi\pi}(\omega)$ the total cross sec-

tion for scattering of the two pions at total energy ω (in their barycentric system). Bonsignori and Selleri argue that if $\sigma_{\pi\pi}$ is large enough the pole may be expected to dominate the first part of the physical zone, and suggest that formula (1) constitutes a reasonable approximation to the true matrix element in the region $\Delta^2 < 0.3M^2$, where M is the nucleon mass.

Upon integration over ω^2, formula (1) becomes

$$\frac{\partial\sigma}{\partial\Delta^2} = \frac{f^2}{2\pi}\frac{\Delta^2}{(\Delta^2+\mu^2)^2}\frac{1}{q_{1L}^{\ 2}} \times\int_{4\mu^2}^{\omega_{\max}^{(\Delta^2)}} \sigma_{\pi\pi}(\omega)(\omega^2/2\mu^2)(1-4\mu/\omega^2)^{1/2}d\omega^2, \quad (2)$$

where $\omega_{\max}(\Delta^2)$ is the upper limit obtained from the phase space diagram in the (Δ^2, ω^2) plane. Figure 1 shows experimental spectra of our results separately, and combined with those of the Bologna group, compared with predicted curves of[9] $\partial\sigma/\partial T$ from the statistical and isobar models,[9] and from Eq. (2) on the assumption that $\sigma_{\pi\pi}$ is constant. The striking low-T peak confirms that interactions of the incoming pion with a virtual meson emitted by the nucleon are significant in the low-Δ^2 region.

Qualitatively one would expect the observed low-energy spectrum to be only partially explained by this simple mechanism. Peierls[10] has recently predicted the inelastic $\pi^- - p$ branching ratios on the basis of a model in which final states are dominated by two types of final-state interaction: (a) between the two final-state pions in a state with $t_{\pi\pi}=1$, and (b) between a pion and the nucleon through the 33 resonance. According to this model, about two-thirds of the $(p\pi^-\pi^0)$ cross section involves mechanism (a). This can be regarded as an upper limit to the contribution of the simple picture described above. This agrees qualitatively with the point of view of Selleri,[11] who suggests that the reaction is initiated wholly by pion-pion interaction in the cloud, with a certain probability of their having no further interaction with the nucleon, which in the $(p\pi^-\pi^0)$ case is probably greater than 50%.

It is much more difficult to infer the presence of a resonance in $\sigma_{\pi\pi}$ from available data. Such a resonance in $\sigma_{\pi\pi}$ would be expected to produce a hump in a spectrum of events against ω^2/μ^2. A strong peak at $\omega^2/\mu^2 \approx 22$ is evident in the spectrum of all our events (solid histogram of Fig. 2), in disagreement with the predicted curves of the statistical and isobar models. Since isobar formation is known to occur,[1-3] it should be noted that this would yield a general background in ω^2/μ^2, above which our peak is still significant. Pickup, Ayer, and Salant[3] report a strong peak in their Q distribution for the $(\pi^-\pi^0)$ system at $Q=325$ Mev ($\omega^2/\mu^2=19$) after considering events with protons going backwards in the center-of-mass system.

It is proposed that valuable information on the existence and position of a resonance in $\sigma_{\pi\pi}$ could be obtained by resolving the available data into a number of separate regions of ω^2/μ^2, and considering spectra over Δ^2/μ^2 in each. This has been done and Fig. 3 compares experimental re-

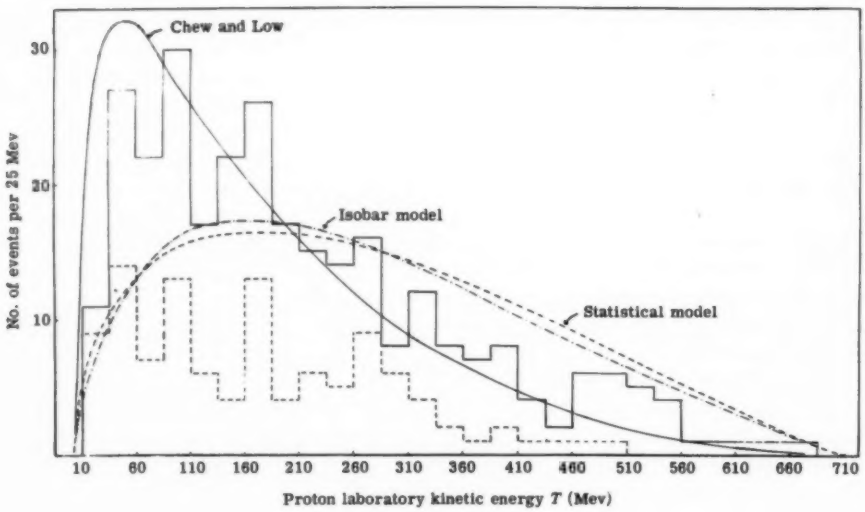

FIG. 1. Laboratory kinetic energy spectrum of the protons from the reaction $\pi^- + p \rightarrow \pi^- + \pi^0 + p$ at incident π^- kinetic energy 0.96 Bev. The histograms consist of Cambridge results alone (broken lines) and Cambridge and Bologna results combined (solid lines). The solid curve is obtained from the formula of Chew and Low [Eq. (2)], and the dashed curves give the results of the isobar model and the statistical model. The theoretical curves and the solid histogram are normalized to the same area.

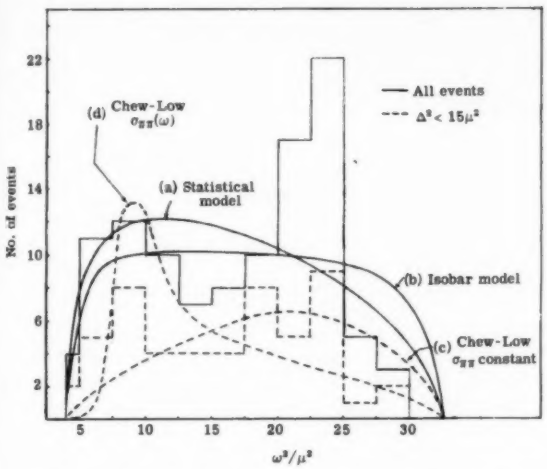

FIG. 2. Spectra of Cambridge events against ω^2/μ^2, where ω^2 is the square of the total energy of $(\pi^-\pi^0)$ in their barycentric system. The solid curves, derived from (a) statistical model and (b) isobar model, are normalized to the same area as the solid histogram which includes all events. Dashed curves were obtained by integrating the Chew-Low Eq. (1) over Δ^2 up to $\Delta^2 = 15\mu^2$, assuming (c) $\sigma_{\pi\pi}$ to be constant and (d) the Frazer-Fulco (reference 13) expression for $\sigma_{\pi\pi}(\omega)$, having $\omega_Y^2 = 8\mu^2$, $\Gamma = 0.4$; they are normalized to the area of the dashed histogram of events with $\Delta^2 < 15\mu^2$.

sults with the predictions[12] of the statistical model and of Chew and Low. The phase-space density for the $N\pi\pi$ system is

$$d\rho = \delta(p_2^2+\mu^2)\delta(q_2^2+\mu^2)\delta(k_2^2+M^2) \times \delta(p_2+q_2+k_2-p_1-k_1)dk_2dp_2dq_2,$$

where k_1 and k_2 are four-momenta of initial and final nucleons, and q_1, p_2, q_2 of the initial pion and two final pions, respectively. On integrating over superfluous variables, this becomes

$$d\rho = \frac{\pi^2}{2Mq_{1L}}(1-4\mu^2/\omega^2)^{1/2}d\omega^2 d\Delta^2, \qquad (3)$$

and therefore in the statistical model,

$$\frac{\partial\sigma}{\partial\Delta^2} = \text{const}\int_{\omega_{\min}^2}^{\omega_{\max}^2(\Delta^2)}(1-4\mu^2/\omega^2)^{1/2}d\omega^2. \qquad (4)$$

The strong low-Δ^2 peaking of the curves in each region obtained from Eq. (1) when integrated between the corresponding ω^2 limits is characteristic of the $\Delta^2/(\Delta^2+\mu^2)^2$ term which has a sharp maximum at $\Delta^2 = \mu^2$. This peaking is more marked than in the total spectrum against T

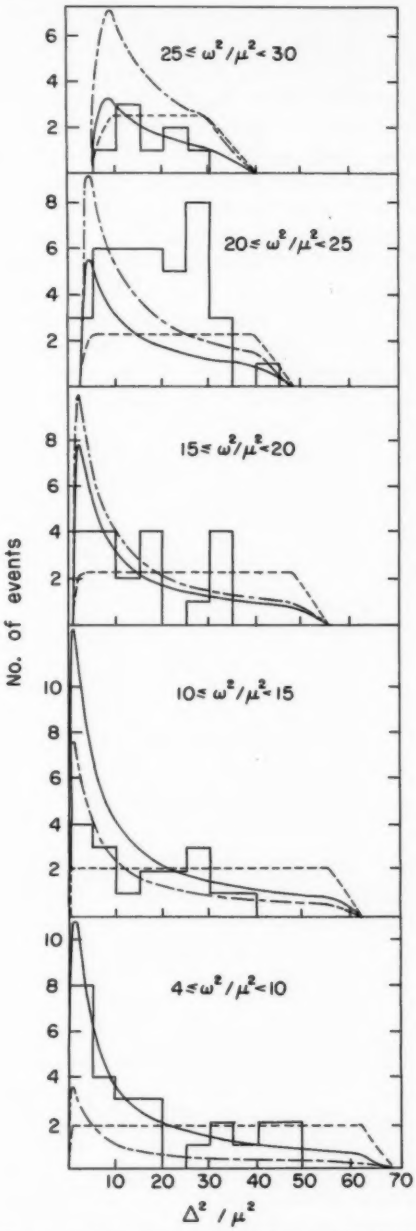

FIG. 3. Spectrum of Cambridge events divided into strips of ω^2/μ^2; the abscissae are expressed in units of Δ^2/μ^2. A solid curve was obtained by integrating the Chew-Low formula [Eq. (1)] between the limits of ω^2 shown, after inserting the Frazer-Fulco expression (reference 13) for $\sigma_{\pi\pi}(\omega)$, with $\omega_Y^2 = 8\mu^2$, $\Gamma = 0.4$. A dot-dashed curve is the same except that $\sigma_{\pi\pi}$ is assumed constant. A dashed curve gives the result of the statistical theory. Curves of each type are normalized to make the area under the total histogram of all events equal to the area under the curve obtained by integrating the corresponding expression over all values of ω^2.

(Fig. 1) and should be easier to recognize in practice. Recalling the possible peak at $\omega^2/\mu^2 \approx 22$ referred to above, there is no apparent resonance effect in the fourth ω^2 "strip" ($20 \leq \omega^2/\mu^2 < 25$), the fairly even distribution in Δ^2 being suggestive only of a two-body break-up into nucleon and "di-pion," to which the special assumptions of the Chew and Low theory are not appropriate. The low-Δ^2 peak in the lowest "strip" of ω^2 ($4 \leq \omega^2/\mu^2 < 10$) is perhaps significant, despite the meager statistics, and suggests the possibility of a resonance in or near this region of ω^2. Correspondingly a set of curves are shown incorporating into Eq. (1) the Frazer and Fulco[13] $t_{\pi\pi} = 1$ resonance expression, in this case with $\omega_\gamma^2 = 8\mu^2$, $\Gamma = 0.4$.[14,15]

The effect of such a resonance on the spectrum of events against ω^2/μ^2 can be estimated by integrating Eq. (1) over Δ^2 up to $\Delta^2 = 15\mu^2 \approx 0.3M^2$ from the lower limit given by the allowed region in phase space, i.e.,

$$\frac{\partial\sigma}{\partial\omega^2} = \frac{f^2}{2\pi q_{1L}^2}\,\sigma_{\pi\pi}(\omega)\,\frac{\omega^2}{2\mu^2}\,(1-4\mu^2/\omega^2)^{1/2} \times \int_{\Delta_{\min}^2(\omega^2)}^{\Delta_{\max}^2(\omega^2)} \frac{\Delta^2}{(\Delta^2+\mu^2)^2}\,d\Delta^2, \qquad (5)$$

and inserting the Frazer-Fulco $\sigma_{\pi\pi}(\omega)$. The resulting curve (d) can now be compared with the spectrum of events (broken histogram of Fig. 2) corresponding to a region in which the pion-pion interaction is known to be important from Fig. 1. A curve (c) obtained from Eq. (5) assuming $\sigma_{\pi\pi}$ to be a constant is also shown. The experimental evidence is inconclusive when looked at from this point of view.

It is difficult to see how a single Frazer-Fulco resonance of narrow width (i.e., $\Gamma = 0.4$) without a significant nonresonant contribution could fit all the above spectra, as the bulk of events would tend to be concentrated into a region of ω^2 near ω_γ^2, as may be seen in Fig. 2, curve (d) and from the solid curves of Fig. 3. Final-state interactions would tend to mask this effect, however. A quantitative test of this point could only be made by performing an experiment designed to detect low-energy proton recoils, when, with large enough statistics, spectra of the type shown in Fig. 3 should reveal the presence of a pole operating in any accessible region of ω^2/μ^2.

We wish to thank Professor S. B. Treiman and Dr. E. J. Squires for helpful discussion. One of us (J.G.R.) is grateful to the Royal Dutch/Shell Group for a research scholarship, and the other (D.R.) to the University of Cambridge for a Clerk Maxwell scholarship. We acknowledge with gratitude the guidance and support of Professor O. R. Frisch, and the assistance of our colleagues Dr. A. J. Oxley, D. V. Bugg, J. Zoll, and V. Barnes.

---

[1]D. Radojičić et al. (to be published).

[2]V. Alles-Borelli, S. Bergia, E. Perez Ferreira, and P. Waloschek, Nuovo cimento 14, 211 (1959).

[3]E. Pickup, F. Ayer, and E. O. Salant, Phys. Rev. Letters 4, 474 (1960).

[4]S. J. Lindenbaum and R. M. Sternheimer, Phys. Rev. Letters 5, 24 (1960).

[5]F. Bonsignori and F. Selleri, Nuovo cimento 15, 465 (1960).

[6]I. Derado, Nuovo cimento 15, 853 (1960).

[7]G. F. Chew and F. E. Low, Phys. Rev. 113, 1640 (1959).

[8]T, the recoil nucleon laboratory kinetic energy, is related to Δ^2 by $\Delta^2 = 2MT$.

[9]The isobar model curve shown refers to the conventional isobar model [R. M. Sternheimer and S. J. Lindenbaum, Phys. Rev. 109, 1723 (1958)], calculated on the assumption that the isobar decays isotropically in the c.m. system. The "extended" isobar model (reference 4) includes an admixture of cases in which the nucleon has greater c.m. kinetic energy as it stems from the decay of an isobar of larger mass; this results in a smaller proportion of nucleons of low laboratory kinetic energy.

[10]R. F. Peierls, Phys. Rev. Letters 5, 166 (1960).

[11]F. Selleri, CERN Report 8511/*TH*. 90 (to be published).

[12]The corresponding curve predicted by the isobar model (reference 9) may be shown to resemble the statistical curve in this case.

[13]W. R. Frazer and J. R. Fulco, Phys. Rev. Letters 2, 365 (1959); Phys. Rev. 117, 1609 (1960).

[14]A π-π resonance of this shape has the effect of moving the peak of the Chew-Low curve of Fig. 1 to a smaller value of T, though the general shape is preserved.

[15]The only other direct evidence concerning a pion-pion resonance is from an experiment involving meson production in proton-deuteron collisions [A. Abashian, N. E. Booth, and K. M. Crowe, Phys. Rev. Letters 5, 258 (1960)] which favors $\omega_\gamma^2 \approx 5\mu^2$, $\Gamma \sim 1.0$-2.0. A reasonable fit to nucleon charge structure is obtained with $\omega_\gamma^2 = 11.5\mu^2$, and to the anomalous magnetic moment with $\Gamma = 0.4$, though these parameters are not determined very precisely.

π^+- PROTON SCATTERING CROSS SECTIONS BY CHEW-LOW EXTRAPOLATION*

G. A. Smith,†‡ H. Courant, E. Fowler, H. Kraybill, J. Sandweiss, and H. Taft
Physics Department, Yale University, New Haven, Connecticut

and

Brookhaven National Laboratory, Upton, New York
(Received November 17, 1960)

The π^+-p interaction cross section has been determined up to the 1-2 Bev region by many workers.[1,2] A new method recently suggested by Chew and Low[3] allows one to infer the total π^+-p cross section at various energies by measuring the process $p+p\rightarrow p+n+\pi^+$ at a specific laboratory energy. In particular, consider the diagram of Fig. 1(a). In this diagram one of the protons emits a π^+ meson which then scatters on the other proton; the pion emitter recoils as a neutron. The basic physical principle in the Chew-Low technique is related to the location and residue of a pole in the transition amplitude of the process $p\rightarrow n+\pi^+$. This pole is located in the nonphysical region of negative kinetic energy of the recoiling spectator neutron. The value of the residue at this pole is shown to be directly related to the pion-proton cross section at a given pion-proton Q value. The value of this application of the Chew-Low technique to measure π^+-p cross sections is not in the actual measurement of the cross sections but rather as a test of the technique itself.

Chew and Low suggest the construction of the function

$$F(w^2,p^2)=2\pi\left(\frac{M_1}{M_2}\right)^2\frac{q_{1L}^{\,2}(p^2-p_0^{\,2})^2}{[\frac{1}{4}w^4-\frac{1}{2}w^2(M_1^{\,2}+\mu_2^{\,2})+\frac{1}{4}(M_1^{\,2}-\mu_2^{\,2})^2]^{1/2}}\frac{\partial^2\sigma(pn\pi^+)}{\partial p^2\partial w^2},$$

where w is the total energy of the proton and pion in their c.m. system and is related to their Q value by $w=Q+M_1+\mu_2$, p is the neutron recoil momentum, M_1 is the proton mass, M_2 is the neutron mass, μ_2 is the π^+ mass, q_{1L} is the laboratory momentum of the incident proton, and

$$p_0^{\,2}=-(M_2/M_1)[\mu_2^{\,2}-(M_2-M_1)^2].$$

For any fixed value of w^2, $\partial^2\sigma(pn\pi^+)/\partial p^2\partial w^2$ has a second order pole at $p^2=p_0^{\,2}$ and the value of the residue at this pole is just $F(w^2,p_0^{\,2})$. Thus a plot of $F(w^2,p^2)$ vs p^2 extrapolated to $p^2=-\mu_2^{\,2}$ (assuming $M_1=M_2$) will yield the residue which is related to the cross section in the following manner:

$$F(w^2,-\mu_2^{\,2})=-2f^2\sigma_{\pi^+p}(Q),$$

where f is the pion-nucleon coupling constant and $f^2\approx 0.08$. It should also be noted that the diagram of Fig. 1(b) is also possible in π^+ production. This process competes with that of Fig. 1(a) and will provide background to the process of interest; however, this background should not affect the value of the residue $F(w^2,-\mu_2^{\,2})$, where $w=Q+M_1+\mu_2$ is for π^+-p only.

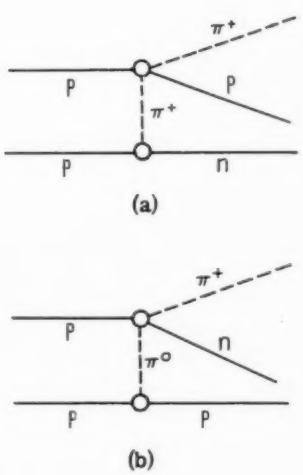

FIG. 1. Feynman diagrams considered in the Chew-Low analysis of $p+p\rightarrow p+n+\pi^+$.

The 20-inch liquid hydrogen bubble chamber of the Brookhaven Cloud Chamber group was exposed to a beam of 2.85-Bev protons from the Cosmotron. 790 examples of $p+p\rightarrow p+n+\pi^+$ have been identified in the analysis to date.[4] Each event was considered to be a possible candidate for the process of Fig. 1(a). Since the laboratory system and the rest system of the incident proton are completely equivalent in the proton-proton collision, the event was treated in that

system in which the neutron momentum was lower. Since one must determine accurately the value of $F(w^2, p^2)$ near $p^2 = 0$ to perform the extrapolation into the unphysical region of p^2, it is advantageous to select low neutron momenta.

Because of the extreme reduction of statistics by the $\partial^2\sigma(pn\pi^+)/\partial p^2 \partial w^2$ factor of $F(w^2, p^2)$, the final analysis was considered to be lacking sufficient statistics to measure more than two cross sections at different values of Q over rather wide intervals in p^2 and w^2. The two intervals selected were for $62 \leq Q \leq 226$ Mev where the π^+-p cross section peaks in the 3/2, 3/2 resonance at 154 Mev to about 200 mb, and $226 < Q \leq 793$ Mev where the π^+-p cross section falls from about 100 mb to 20 mb. The Chew-Low technique should measure some average cross section over each of these intervals. The results of this analysis are shown in Fig. 2.

Although the statistics make the extrapolation uncertain, on the basis of the least-squares linear and quadratic extrapolations shown in Fig. 2 the following conclusions seem to be justified: (a) One can clearly detect the difference between the cross section for the region $62 \leq Q \leq 226$ Mev and that which is found with the data in the region $226 < Q \leq 793$ Mev, and in addition these cross sections have approximately the correct relative magnitude. (b) The data are consistent with the fact that $\partial^2\sigma(pn\pi^+)/\partial p^2 \partial w^2$ must stay positive definite at least through $p^2 = (p^2)_{\min} \approx 0.005$ (Bev/c)^2.

So far as we know, this is the first Chew-Low extrapolation attempt, outside the deuteron case, where the answer has been known; in addition, it is felt that if a resonance exists in the π, π case which is as large as the 3/2, 3/2 π^+-p resonance, such an extrapolation should detect it.

We would like to take this opportunity to acknowledge the cooperation of Dr. Ralph P. Shutt and members of the Brookhaven Bubble Chamber group.

---

*Supported in part by the U. S. Atomic Energy Commission.

†Based on work submitted to the faculty of the Graduate School of Yale University by G. A. Smith in partial fulfillment of the requirements for the degree of Doctor of Philosophy.

‡Supported by the Socony Mobil Oil Company Fellowship in Physics, 1960-61.

[1]S. J. Lindenbaum, Annual Review of Nuclear Science (Annual Reviews Inc., Palo Alto, California, 1957), Vol. 7.

[2]J. C. Brisson, J. Detoef, P. Falk-Vairant, L. van Rossum, G. Valladas, and L. C. L. Yuan, Phys. Rev. Letters 3, 561 (1959). (Recent measurements in the region 382-872 Mev.)

[3]G. F. Chew and F. E. Low, Phys. Rev. 113, 1640 (1959).

[4]G. A. Smith, H. Courant, E. Fowler, H. Kraybill, J. Sandweiss, and H. Taft, Proceedings of the Tenth Annual Rochester Conference on High-Energy Nuclear Physics (to be published).

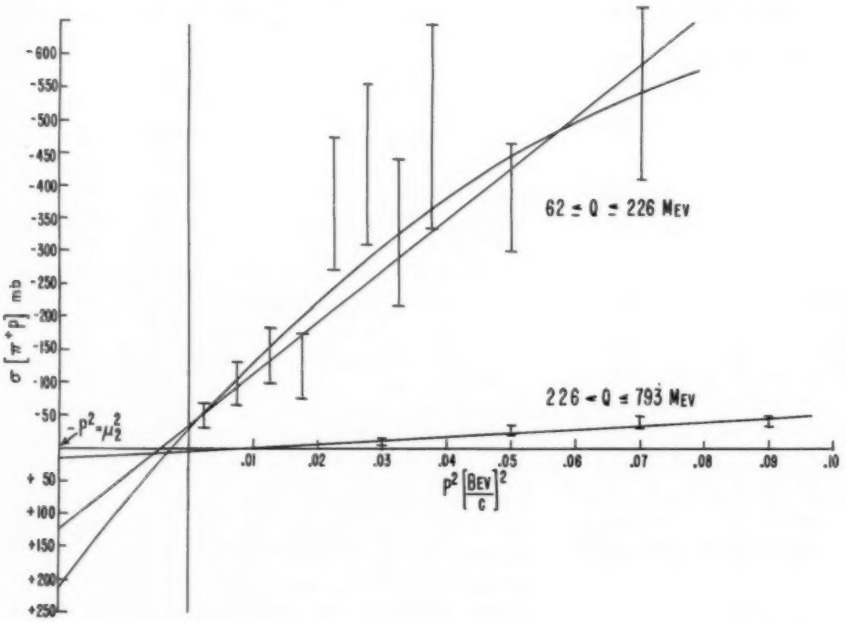

FIG. 2. Chew-Low plot with linear and quadratic least-squares extropolation.

NEUTRINO EMISSION FROM BLACK-BODY RADIATION AT HIGH STELLAR TEMPERATURES

Hong-Yee Chiu
The Institute for Advanced Study, Princeton, New Jersey

and

P. Morrison
Department of Physics and Newman Laboratory of Nuclear Studies, Cornell University, Ithaca, New York
(Received November 28, 1960)

That neutrino emission processes may affect the properties of matter at high temperatures, and hence stellar evolution, was first pointed out by Gamow and Schoenberg[1] and by Pontecorvo.[2] We list the known important neutrino emission processes as follows:

(*i*) The so-called "urca" process, in which neutrinos are emitted by nuclear transitions.[1,3,4] This process depends only upon the observed nucleon-neutrino coupling, while all those which follow take place only with a universal Fermi interaction.

(*ii*) Neutrino bremsstrahlung[2,5]:

$$e^- + (Z,A) - e^- + \nu + \bar{\nu} + (Z,A).$$

(*iii*) The photoneutrino or neutrino Compton effect[4]:

$$\gamma + e^- - e^- + \nu + \bar{\nu}.$$

We add two new processes, which are the subject matter of this note[6]:

(*iv*) Pair-annihilation neutrinos:

$$e^- + e^+ - \nu + \bar{\nu}.$$

(*v*) Photon-photon neutrinos:

1. $\gamma + \gamma - \nu + \bar{\nu}$,

2. $\gamma + \gamma - \gamma + \nu + \bar{\nu}$.

The energy lost from finite regions due to processes (*i*), (*ii*), and (*iii*) is not important for temperatures below 10^{10} °K. For most densities, and for temperatures around 10^9 °K, processes (*iv*) and (*v*) are considerably more rapid.

These last two processes involve direct neutrino emission from black-body radiation itself, mediated either by virtual electron-positron pairs or by the real pairs present in thermal equilibrium. In spite of the more complex graphs which describe processes (*v*), they reach importance comparable with the simple process (*iv*) since the available energy in the center-of-mass system is typically higher, at least in the region of $kT/mc^2 \ll 1$. The graphs for these processes are shown in Fig. 1; process $(v, 1)$ requires renormalization before it can be interpreted. An estimate of process $(v, 2)$ confirms the idea that it contributes to the energy loss rate about like process (*iv*) even though it is proportional to an additional three powers of 1/137.

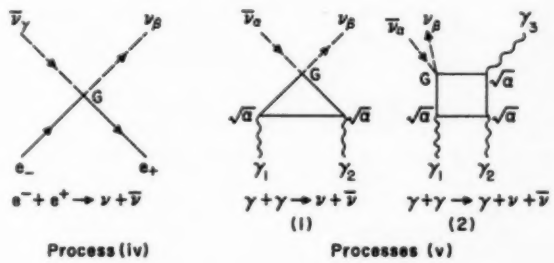

FIG. 1. Feynman diagrams for the processes considered here.

Only the simple process (*iv*), with its unique Feynman diagram, has been calculated exactly. The transition amplitude is proportional to $(\bar{\nu}e)(\bar{e}\nu)$ as in the theory of Feynman and Gell-Mann,[7] from which we take the Fermi coupling constant, G. Calculation of the cross section for the pair process in the center-of-mass system is elementary, and gives

$$\sigma_{iv} = 1.5\times10^{-45}(c/v_{\rm rel})(E_T^{\,2} - 1)\ \text{cm}^2,$$

where E_T is the total c.m. energy in units of m_0c^2, and $v_{\rm rel}$ is the relative velocity in the c.m. system. The number of electron pairs present at equilibrium is well known.[8] In the pure vacuum radiation field, where the initial proper mass density is zero, the positron density becomes

$$n_+^{\,v} = (1/\pi^2)(\hbar/m_0c)^{-3}f(\beta), \quad \beta = (m_0c^2/kT) \qquad (1)$$

and

$$f(\beta) = \int_0^\infty \exp[-\beta(1+x^2)^{1/2}]x^2dx$$

$$= \frac{1}{\beta}\int_0^\infty \exp[-\beta\cosh\theta]\cosh 2\theta d\theta$$

$$= K_2(\beta)/\beta. \qquad (2)$$

$K_2(\beta)$ is the modified Hankel function of second order.[9] The presence of nondegenerate matter expresses the density of positrons present at equilibrium, but does not affect the rate of production of positrons. The energy loss, however, depends only upon the production rate (and the equal annihilation rate), and is therefore independent of matter density, until degeneracy begins to affect the production of positron-electron pairs. For the nondegenerate case, then, the electron density does not matter; in the degenerate case, if also $n_- \gg n_+$, we have

$$n_+^{(d)} = n_+^{v} \exp(-E_F/kT);$$

E_F is the electron Fermi energy, including m_0c^2.

Note that

$$(1+\tfrac{1}{2}x^2) > (1+x^2)^{1/2} > x.$$

We find the approximations to (2):

$$f_\infty(\beta) = e^{-\beta}\int_0^\infty \exp[-\tfrac{1}{2}x^2\beta]x^2dx = (\tfrac{1}{4}\sqrt{\pi})(2/\beta)^{3/2}e^{-\beta}, \quad \beta \gg 1,$$

$$f_0(\beta) = \int_0^\infty \exp[-x\beta]x^2dx = 2/\beta^3, \quad \beta \ll 1. \quad (3)$$

The rate of loss of energy density is given by the integral

$$-\frac{dU}{dt} = \iint (E_- + E_+)\sigma_{iv} v_{\text{rel}} n_- n_+ d^3p_- d^3p_+,$$

where the subscripts refer to electron and positron quantities. Making such rough estimates as

$$E_- \cong E_+ \cong m_0c^2,$$

the integral can be approximated. We obtain

$$-dU/dt \cong 7.5\times10^{20}[f(\beta)]^2 \text{ ergs/cc-sec}, \quad \text{(nondegenerate)}$$

$$\cong 2.5\times10^{14}(\bar{Z}/\bar{A}) \exp(-E_F/kT) f(\beta), \quad \text{(degenerate)}$$

where $\bar{Z}$ and $\bar{A}$ are mean values of atomic number and atomic mass.

In stellar problems the energy loss rate is usually expressed not in terms of unit volume, but per gram of matter, for which the relations above must be modified to read

$$\epsilon = (1/\rho)(dU/dt) \text{ ergs/g-sec}.$$

We list in Table I a few values of ϵ for various processes of energy loss in the relevant temperature and density region. It is to be observed that processes of type (v), so far only roughly estimated, are not only independent of density but even of degeneracy of the material. Both processes (iv) and (v) are independent of chemical composition, apart from the effect of electron density on degeneracy.

The thermal energy content of matter at $T = 10^9$ °K is 10^{17} ergs/gram. Therefore the relaxation time for cooling by neutrino loss due to the processes we consider lies between 10^9 sec and 10^{15} sec. In any case, by the time T has reached 2×10^9 °K, the relaxation time is only of the order of 10^4 to 10^5 sec.

Temperatures of 2×10^9 °K or more are required by the current theories of element synthesis for elements beyond iron, and by the ideas of supernova collapse.[10-13] It seems that neutrino-loss processes change the means by which such temperatures may be reached, but

Table I. Rates of energy loss by neutrino emission.[a] Energy loss in ergs/gram-second, at a density of 10^6 g/cc.

Temperature (°K)	Process: Photoneutrino (*iii*)	Process: Annihilation (*iv*)	Process: Photon-photon (v,2) (approximate)	t_{cool} (sec)
5×10^8	10^2	$10^{0.7}$	$10^{3.5}$	10^{13}
1×10^9	$10^{4.2}$	$10^{7.4}$	10^7	10^9
2×10^9	$10^{8.6}$	$10^{11.6}$	10^{11}	10^5
2.5×10^9	$10^{10.4}$	$10^{12.6}$	10^{12}	10^4

[a]In the last column is entered the relaxation time in seconds for losing the full thermal energy content of the material by neutrino emission.

do not modify their effects.

The matter and thermal radiation in a stellar interior will remain in thermal equilibrium in spite of neutrino emission, provided that the energy loss rate is low enough to permit readjustment of the local near-equilibrium conditions. The virial theorem relates the thermal energy strictly to the gravitational energy while this remains true. Neutrino loss will therefore not result in reduced temperature but only in the contraction of the star, the gravitational energy making up for the neutrinos radiated. The central temperature will rise at a rate limited by neutrino emission, until the time for gravitational readjustment—roughly measured by the free-fall times of 1 to 100 seconds (depending on density)—becomes longer than the characteristic time of neutrino energy loss. Until central temperatures of about 3×10^9 °K are reached, the star which has begun to emit neutrinos will everywhere remain in a state of near equilibrium, and show increasingly rapid gravitational contraction. This final stage of stellar evolution is thus controlled by the consequences of the universal Fermi interaction, together with gravitational effects; nuclear processes do not play the determining role until the "phase change" from iron to helium is reached at 5×10^9-7×10^9 °K.

In view of the high neutrino emission rate, the first mark of supernovae might be high neutrino flux while the surface of the star has yet shown no sign of this sudden internal collapse. At $T=5\times10^9$ °K, the neutrino flux from such stars will amount to 10^{53} neutrinos of average energy 1 Mev per second. At a distance of 100 light years, the flux is around 10^{13}/cm^2-sec. This is detectable.[14] Therefore the establishment of a neutrino monitor station in terrestial or spatial laboratories may help us predict forthcoming supernovae.

It is a great pleasure to thank Professors R. F. Christy, F. J. Dyson, W. A. Fowler, T. Gold, Mr. M. Levine, and Dr. T. T. Wu for much discussion, and one of us thanks Professor J. R. Oppenheimer for the hospitality of the Institute for Advanced Study.

---

[1]G. Gamow and M. Schoenberg, Phys. Rev. 59, 539 (1941).

[2]B. M. Pontecorvo, J. Exptl. Theoret. Phys. (U.S.S.R.) 36, 1615 (1959) [translation: Soviet Phys.—JETP 9(36), 1148 (1959)].

[3]H. Y. Chiu, Ann. Phys. (to be published).

[4]H. Y. Chiu and R. Stabler (to be published).

[5]G. M. Gandel'man and V. S. Pianev, J. Exptl. Theoret. Phys. (U.S.S.R.) 37, 1072 (1959) [translation: Soviet Phys.—JETP 10(37), 764 (1960)].

[6]Compare G. Wataghin, Phys. Rev. 66, 149 (1944) (before universal Fermi interaction).

[7]R. P. Feynman and M. Gell-Mann, Phys. Rev. 109, 193 (1958).

[8]L. D. Landau and E. M. Lifshitz, Statistical Physics, translation by R. F. Peierls and R. E. Peierls (Pergamon Press Ltd, London, 1958), p. 325.

[9]Tabulation of $K_2(\beta)$ can be found, e.g., in G. N. Watson, Theory of Bessel Functions (Macmillan Company, New York, 1948), p. 737.

[10]S. A. Colgate and M. H. Johnson, University of California Radiation Laboratory Report UCRL-6097 (unpublished).

[11]E. M. Burbidge, G. R. Burbidge, W. A. Fowler, and F. Hoyle, Revs. Modern Phys. 29, 547 (1957).

[12]W. A. Fowler and F. Hoyle (to be published).

[13]A. G. W. Cameron, Astrophys. J. 130, 917 (1959).

[14]F. Reines and C. L. Cowan, Jr., Phys. Rev. 92, 830 (1953). The neutrino background due to the sun is estimated to be less than 10^{10}/cm^2-sec on earth.

TOTAL CROSS SECTIONS OF PROTONS WITH MOMENTUM BETWEEN 10 AND 28 Gev/c

A. Ashmore,* G. Cocconi, A. N. Diddens, and A. M. Wetherell
CERN, Geneva, Switzerland
(Received November 21, 1960)

A beam of protons elastically scattered by the internal aluminum target of the CERN proton synchrotron[1] (scattering angle ~25 mrad) has been used for counter measurements of proton cross sections on protons, neutrons, and complex nuclei.

The momentum of the proton beam was varied from 10 to 28 Gev/c by changing the operating energy of the accelerator and by isolating the elastic peak by means of magnetic selection. A typical momentum spectrum of the beam at 24-Gev operating energy is given in Fig. 1. It was obtained at ~80 m from the target, with a 1m magnet and four scintillators defining the incoming and outgoing beams (resolution of the system, $\Delta p/p \approx 5\%$). The spectra at other energies were similar to this one. No particles were found around the elastic peak when the field of the analyzing magnet was reversed, thus confirming that the particles detected at normal setting were indeed protons.

The cross-section measurements were made utilizing the protons around ($\pm 2.5\%$) the elastic peak. At 80 m from the target their intensity was, at all energies, $\sim 5\times10^{3}$ cm^{-2} pulse^{-1}, when 2×10^{11} protons per pulse were circulating in the accelerator ($\frac{1}{3}$ pulse sec^{-1} at the highest energy, 1 sec^{-1} at the lowest; duration of each pulse $\approx$ 30 msec).

The total cross sections on protons and neutrons were measured with a "good geometry" setup. After magnetic selection, the incoming beam was defined by two scintillators, each 1 cm in diameter, 10 m apart, and the beam attenuation was measured by a row of 5 scintillators, 2 cm in diameter, aligned with the first two and subtending, at the absorber, angles ranging from 2 to 10 mrad. The choice of these angles was dictated by the divergence of the beam, the expected multiple Coulomb scattering of the protons in the absorber (~1 radiation length thick), and the expected distribution of the elastically scattered protons (the characteristic angle of the nucleon shadow scattering at 25 Gev is ~10 mrad).

For the p-p cross section, attenuation measurements were carried out alternatively with a carbon and a polyethylene absorber. For the p-n measurements H_2O and D_2O were used. Conventional coincidence circuits with resolving times of $\sim 2\times10^{-8}$ sec measured simultaneously real and chance coincidences.

The total cross section was obtained, at each energy, by extrapolating to zero solid angle the attenuations measured with the various apertures. For angles small in comparison with those expected for shadow scattering, this extrapolation should be linear in a solid angle plot, and in fact at all energies the experimental points after correction for multiple scattering[2] and beam di-

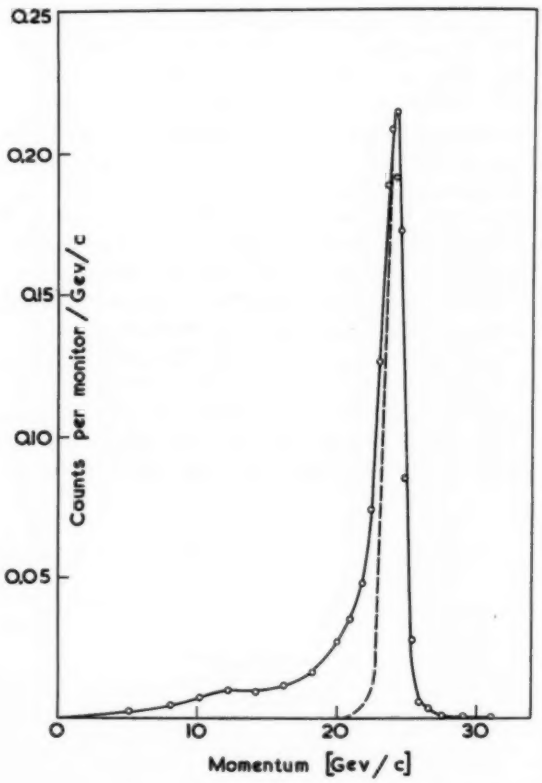

FIG. 1. Momentum spectrum of the external beam of protons elastically scattered in the target of the accelerator. Operating energy 24 Gev; Al target; scattering angle 25 mrad. The dashed line shows the shape expected for a monochromatic line of 24.2 Gev/c.

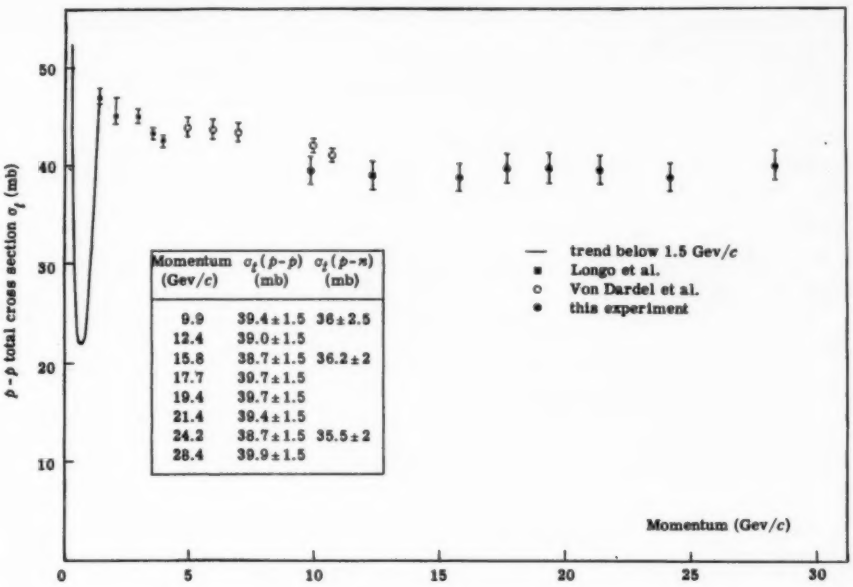

Momentum (Gev/c)	$\sigma_t(p\text{-}p)$ (mb)	$\sigma_t(p\text{-}n)$ (mb)
9.9	39.4±1.5	36±2.5
12.4	39.0±1.5	
15.8	38.7±1.5	36.2±2
17.7	39.7±1.5	
19.4	39.7±1.5	
21.4	39.4±1.5	
24.2	38.7±1.5	35.5±2
28.4	39.9±1.5	

FIG. 2. p-p and p-n total cross sections (diffraction scattering included) as a function of proton momentum. (Von Dardel et al., reference 4; Longo et al., reference 6.)

vergence did not deviate too much from a straight line. The slopes of these lines were, as expected, inversely proportional to the square of the proton momentum.[3]

The final results for the cross sections are given in Fig. 2, together with those of other authors. The correction for multiple Coulomb scattering and beam divergence was $\leq 4\%$, that for chance coincidence $\leq 4\%$. The errors quoted for our points are ~3 times larger than the purely statistical ones because of the contribution of the systematic errors introduced by these corrections and the extrapolation to zero solid angle. The relative values at different momenta should thus have errors smaller than those given in Fig. 2. Our values for the p-p cross sections are in good agreement, around 10 Gev/c, with those obtained by Von Dardel et al.[4] using a liquid hydrogen absorber, and at 24 Gev/c with that obtained with the CERN 30-cm hydrogen bubble chamber.[5] The striking feature of the data contained in Fig. 2 is the constancy, at around 40 mb, of the p-p cross section from 5 to 28 Gev/c.

Taking into account the shadowing of the neutron by the accompanying proton in the deuteron, it seems that the p-n cross section is essentially the same as the p-p cross section at the three momenta where measurements were performed.

At 24 Gev a "bad geometry" measurement of the cross section of protons on nuclei was performed. In this case only three scintillators were used after the absorber and subtended angles of 15, 20, and 30 mrad. At these angles the effect of the shadow scattering was small and the other corrections were negligible. A linear extrapolation to zero solid angle based on these three measurements was taken as an estimate of the absorption (total minus diffraction scattering) cross section. The results of this measurement are displayed in Fig. 3. It is remarkable how well an $A^{2/3}$ law fits the data, though for the

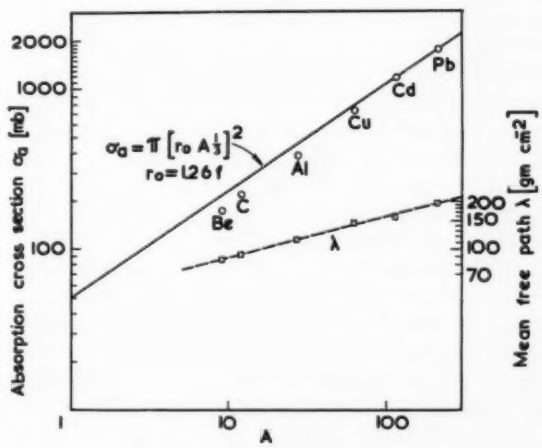

FIG. 3. Nuclear absorption cross sections and mean free paths of 24.2-Gev/c protons in various elements.

lightest elements a good deal of transparency could be expected.

We are extremely grateful to the Machine Group of the proton synchrotron for their very efficient operation of the accelerator at all energies, and at all times. We thank Mr. C. A. Stahlbrandt for his assistance with the electronics. One of us (A.A.) wishes to thank CERN for making his visit possible.

*On leave from Queen Mary College, University of London, London, England.

[1]This beam was initially proposed and studied by B. Dayton and H. Winzeler [B. Dayton, W. Koch, M. Nikolic, H. Winzeler, J. C. Combe, W. M. Gibson, W. O. Lock, M. Schneeberger, and G. Vanderhaeghe, Helv. Phys. Acta 33, 544 (1960)].

[2]R. M. Sternheimer, Rev. Sci. Instr. 25, 1070, 1954.

[3]Also the contribution of the secondaries generated by the interactions occurring in the absorber should be proportional to the solid angle. At our angles, however, this contribution was estimated to be small in comparison with the elastic scattering.

[4]G. Von Dardel, D. H. Frisch, R. Mermod, R. H. Milburn, P. A. Piroué, M. Vivargent, G. Weber, and K. Winter, Phys. Rev. Letters 5, 333 (1960).

[5]Private communication from the CERN bubble chamber and I. E. P. (Instrumentation for the Evaluation of Photographs) groups.

[6]M. J. Longo, J. A. Helland, W. N. Hess, B. J. Moyer, and V. Perez-Mendez, Phys. Rev. Letters 3, 568 (1959).

$\Lambda\pi$ RESONANCE AND POSSIBLE DETERMINATION OF THE KYN PARITIES*

Marc Ross†
Università di Roma, Rome, Italy

and

Gordon Shaw
University of California, La Jolla, California

(Received November 14, 1960)

Experiments by Alston et al.[1] and Ferro-Luzzi et al.[2] at Berkeley, observing the reaction

$$K^- + p \to \Lambda + \pi^- + \pi^+, \qquad (1)$$

have recently been reported which indicate a resonance in the $\Lambda+\pi$ system at about 1380-Mev total energy, i.e., 50 Mev below the threshold for $\bar{K}+N$. We propose that this resonance be described in terms of a quasi-bound state of the isotopic spin $I=1$, s-wave $\bar{K}N$ system. (The angular distribution indicates $J=\frac{1}{2}$ for the resonant system, in agreement with this proposal.) Using our effective-range formalism[3] we will first establish the compatibility of this description with present data. Then we suggest how better data will permit fuller use of the effective-range theory to make detailed tests of this association of the $\Lambda\pi$ resonance with the $\bar{K}N$ s state. Determination of the orbital angular momentum of the resonant $\Lambda\pi$ state (or the resonant $\Sigma\pi$ state that will also be present), and thus determination of the $K\Lambda N$ (or $K\Sigma N$) parity, is discussed.

This description can be decided by reference to the observed K^-+p reactions. Let us consider process (1) at a fixed high energy and examine those events where the π^+, say, has sufficiently high momentum so that it is definitely not associated with the Λ in this resonance. Such conditions were obtained in the experiment of Alston et al. We will speak in terms of the energy of the $\Lambda\pi^-$ system. We assume that the main production process near 1380 Mev involves two-body production of the π^+ and the resonant state, with the subsequent decay of the latter. Call the amplitude for this entire process T_{res}. In this picture, the quasi-bound $\bar{K}N$ system decays into $\Lambda+\pi$ (or $\Sigma+\pi$), the rapid energy dependence in T_{res} being associated with this decay. This dependence is characterized essentially by the two-body amplitude[4]

$$|k_N^{-1/2} T(\bar{K}+N \to \Lambda+\pi)| = \left[\operatorname{Im}\frac{1}{a_1}/(1+|\alpha|^2)\right]^{1/2} \left|\frac{1}{a_1}+ik_N\right|^{-1}, \qquad (2)$$

with $a_1(k_N)$ the $I=1$ $\bar{K}N$ complex scattering length, k_N the $\bar{K}N$ momentum, extended below threshold where $k \to i\kappa$ ($\kappa>0$) and $|\alpha|^2 = |T_1(N\Sigma)|^2/|T(N\Lambda)|^2$.

Thus the rapid energy dependence is given by

$$|T_{\text{res}}|^2 \propto \text{Im}\,\frac{1}{a_1(\kappa_N)} \times \left|\frac{1}{a_1(\kappa_N)} - \kappa_N\right|^{-2} [1+|\alpha(\kappa_N)|^2]^{-1}. \quad (3)$$

The form (3) is explicitly that given if the π^+ is considered to be "knocked off" the proton at first and to remain a "spectator."[5] Equation (3) yields, by the way, an infinite derivative in the cross section in the form of a step (not a cusp) at the $\bar{K}N$ threshold (for Rea positive). This seems to agree with observation.[1]

Now we need to know the energy dependence of $1/a_1(\kappa)$. Consider a system of n coupled two-body channels in a given state of J, J_z, I, parity, etc. Then the scattering amplitude can be written in the matrix form[3]

$$T = k^{l+\frac{1}{2}}(M - ik^{2l+1})^{-1}k^{l+\frac{1}{2}}, \quad (4)$$

where M is a real symmetric $(n\times n)$ matrix which is an even function of all the channel momenta k_i and $k^{l+\frac{1}{2}}$ has entries $(k^{l+\frac{1}{2}})_{ij} = \delta_{ij}k_i^{l_i+\frac{1}{2}}$ (where below the ith threshold $k_i \to i\kappa_i$, $\kappa > 0$). It was shown in reference 3 that analogously to the one-channel effective-range theory the diagonal elements are accurately given by an expression quadratic in k_i:

$$M_{ii}(E) = M_{ii}(E_0) + \tfrac{1}{2}c_{l_i}R_i^{1-2l_i}[k_i^2 - k_i^2(E_0)], \quad (5)$$

with $c_0 = 1$, $c_1 = -3$, etc., where R_i is the range of forces in channel i and E_0 is any convenient energy at which we make our expansion. In addition the nondiagonal elements M_{ij} are to a good approximation energy independent: $M_{ij}(E) \approx M_{ij}(E_0)$.

The s-wave $\bar{K}N$, $I=1$ state is coupled to two other channels ($\Sigma\pi$ and $\Lambda\pi$) so that in order to use the full formalism we need to know 6 "zero-range" parameters $M_{ij}(E_0)$. However, the rough low-energy data are only good enough to determine three $I=1$ "zero-range" parameters: a_1 and the $(\Sigma/\Lambda)_{I=1}$ ratio $|\alpha|^2$. Now as a first approximation we take k_Σ and k_Λ to be constant over the energy region of interest. Then

$$\frac{1}{a_1(\kappa_N)} = \frac{1}{a_1} + \tfrac{1}{2}R_N\kappa_N^2, \quad (6)$$

where R_N is the range of forces in the $\bar{K}N$ channel which we take to be $\mu_{\bar{K}N}^{-1} = 0.4\times10^{-13}$ cm. Among the scattering-length solutions of Dalitz and Tuan[6] only (a-) with

$$a_1 = (1.0+0.18i)\times10^{-13}\ \text{cm} \quad (7)$$

could yield a (narrow) resonance for $I=1$. It is very important to note that only by looking at the energy dependence of $a_1(\kappa_N)$, e.g., noting from (6) that $a_1 > R_N$, can we decide that the positive a_1 [of the (a-) solution as contrasted to the (b-) solution] is due to an attraction strong enough to bind in the $\bar{K}N$ channel and not a repulsion or a strong nondiagonal interaction (which will yield a positive Rea but not a narrow resonance).[3,4] Inserting (6) and (7) into (3), we find that $|T_{\text{res}}|^2$ is peaked at

$$\kappa_N = 260\ \text{Mev}/c,$$

whereas experimentally $\kappa_N \approx 180$ Mev/c, and the full width at half maximum is

$$\Delta\kappa = 120\ \text{Mev}/c,$$

whereas experimentally $\Delta\kappa \approx 130$ Mev/c. Some caution is called for in assessing this agreement since, besides our neglect of the energy dependence of k_Σ and k_Λ, (a) there is a direct or three-body amplitude interfering with T_{res} which may shift the peak position, although it should not disturb the width very much; (b) the scattering length (a-) used was based on too big an $|\alpha(k_N=0)|^2$. We note that our proposal predicts only an $I=1$ resonance: Association of the resonance with the KN channel rules out an $I=2$ resonance and the scattering-length solutions (based on present data) permit resonances in either $I=1$ or 0 but not both.

An important experiment needed to test our proposal in greater detail is the Coulomb interference study on elastic K^-+p scattering: Constructive interference would eliminate the scattering-length solutions with positive real part and invalidate our proposal. The present data[7] are close to giving an answer. More precise low-energy K^-+p reaction experiments performed at several energies, e.g., accurate determination of the $\Sigma^+\pi^-/\Sigma^-\pi^+$ ratio as a function of energy, would permit fuller use of the effective-range formalism (4) and (5). [A detailed survey is now in progress using this formalism to see just how much the effective-range terms can contribute to the K^-+p cross sections as well as the effects of the KYN parities; i.e., we are trying to determine how much we can tie down the quantities in (4) and (5) with a given accuracy of the K^-+p data.] We note that a large energy region above threshold as well as the entire resonance region

below $\kappa_N = 0$ is included in the range

$$R_i^2 |k_i^2 - k_i^2(\kappa_N = 0)| \leq 1$$

throughout which effective-range theory might be expected to be good.[3]

From associating the $\Lambda\pi$ resonance with the $\bar{K}N$ s state, it follows that if we can measure the orbital angular momentum of the $\Lambda\pi$ (or the resonant $\Sigma\pi$ state) the $K\Lambda N$ (or $K\Sigma N$) parity will be measured. One possibility of determining l_Λ is from the Λ polarization. Referring to (1), we measure θ from the perpendicular to the plane of production of the resonant $\Lambda\pi$ and the spectator particle, and consider $s_{1/2}$ and $p_{1/2}$ $\Lambda\pi$ systems. If P is the degree of polarization of the resonant systems, the Λ polarization is

$$s_{1/2}\text{: } P,$$

$$p_{1/2}\text{: } P(\cos^2\theta - \sin^2\theta).$$

Of course P depends on the production mechanism, angle, and energy: One may not readily find a situation with large P.

A different possibility is to look at the energy dependence of $|\alpha|^2$ over the resonance. The $\Sigma\pi$ threshold is very favorably located close to the resonance, so that with any detailed data, s- or p-wave resonances could be distinguished. The present data already provide some indication of the $K\Sigma N$ parity. Experimentally,[7] $|\alpha|^2$ is found to be roughly 1 at the $\bar{K}N$ threshold, whereas averaged over the resonant region,[1] $|\alpha|^2 \ll 1$. Theoretically, we have from (4),[8] in first approximation,

$$|\alpha|^2 \propto k_\Sigma^{2l_\Sigma+1} / k_\Lambda^{2l_\Lambda+1}. \quad (8)$$

Thus, from (8), we find that $|\alpha|^2$ decreases from its value at the $\bar{K}N$ threshold to that at the peak of the resonance by a factor of 2 for $l_\Sigma = l_\Lambda = 1$ (even KYN parities). On the other hand, if we consider $l_\Sigma = 0$, $|\alpha|^2$ remains essentially constant in this energy region, which may be in disagreement with experiment.

---

*This work was performed in part under the auspices of the U. S. Atomic Energy Commission.

†On leave from Indiana University, Bloomington, Indiana.

[1]M. Alston, L. W. Alvarez, P. Eberhard, M. L. Good, W. Graziano, H. K. Ticho, and S. G. Wojcicki, Proceedings of the Tenth International Rochester Conference on High-Energy Nuclear Physics, 1960 (to be published). We would like to thank Professor M. Good for informing us of these results.

[2]M. Ferro-Luzzi, J. P. Berge, J. Kirz, J. J. Murray, A. H. Rosenfeld, and M. Watson, Bull. Am. Phys. Soc. 5, 509 (1960).

[3]M. Ross and G. Shaw, Ann. Phys. (to be published).

[4]M. Ross and G. Shaw, Ann. Phys. 9, 391 (1960).

[5]T. Kotani and M. Ross, Nuovo cimento 14, 1282 (1959), see Eq. (59).

[6]R. Dalitz and S. Tuan, Ann. Phys. 10, 307 (1960), see footnote 14.

[7]L. Alvarez, Ninth International Conference on High-Energy Physics, Kiev, 1959 (to be published).

[8]Alternately, one can argue that the $\bar{K}N$ quasi-bound state would be characterized by a fixed probability ratio for $\Sigma\pi/\Lambda\pi$ in the region of interaction; (8) then follows from the small values of kr involved.

UNIFIED APPROACH TO HIGH- AND LOW-ENERGY STRONG INTERACTIONS ON THE BASIS OF THE MANDELSTAM REPRESENTATION*

G. F. Chew and S. C. Frautschi
Lawrence Radiation Laboratory and Department of Physics, University of California, Berkeley, California
(Received November 28, 1960)

We wish here to outline an approach to the theory of strong interactions, based on the Mandelstam representation, that treats high- and low-energy phenomena in a unified manner. Our approach, which will be described in detail elsewhere, extends somewhat the original program proposed by Mandelstam.[1] The most striking achievement thus far is the inference, from the observed constancy of high-energy total cross sections, that in the low-energy elastic region the P-wave interaction should be strong; at the same time, bound states or large low-energy phase shifts for $J \geq 2$ seem inconsistent with the theory. Furthermore, the divergence difficulty encountered by Chew and Mandelstam[2] in handling low-energy P resonances appears to be removed by the Pomeranchuk relation[3] between high-energy particle and antiparticle cross sections.

We use the pion-pion interaction to illustrate

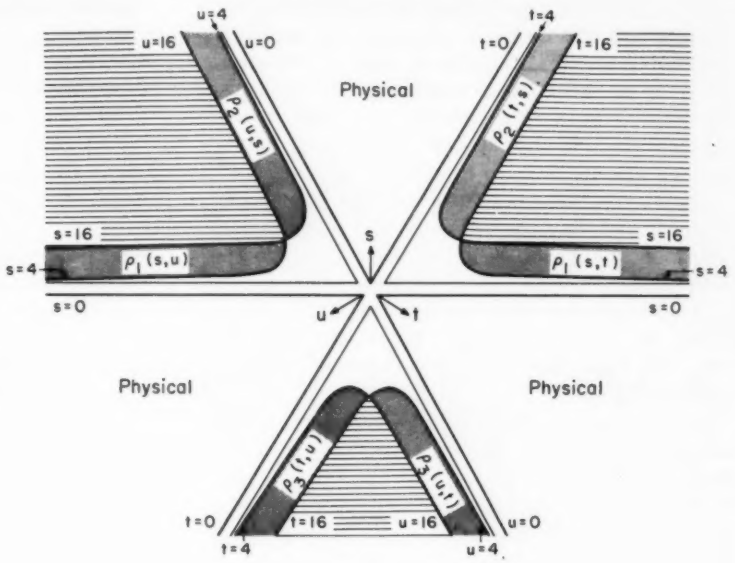

FIG. 1. The Mandelstam diagram for elastic $\pi\pi$ scattering. In a physical region the variable indicated is the square of the barycentric-system total energy—in pion mass units. The assignment of locations to ρ_1, ρ_2, and ρ_3 corresponds to the amplitude $A(s,t,u)$ of reference 4. Corresponding assignments for $B(s,t,u)$ and $C(s,t,u)$ are obtained by interchange of channel labels.[4]

our approach, although it will be clear that the essential features may be generalized. Figure 1 shows the Mandelstam diagram for $\pi\pi$ elastic scattering, where the variables s, t, and u have the usual meaning.[4] The wedge-shaped physical regions are labeled as such, and the shaded areas indicate where the double spectral functions fail to vanish. Our central assumption is that the double spectral functions in the heavily shaded areas dominate those parts of the physical regions whose distance from a boundary is of the order of magnitude of the width of the heavily shaded strips, i.e., 16 pion mass units (squared). This gives us a theory that covers not only low energies but arbitrarily high energies with low momentum transfer.

The above assumption seems a priori reasonable on the usual geometrical grounds, but in addition it is fortified by two empirical circumstances. First, total cross sections generally are largest in the low-energy elastic region. Second, diffraction peaks in elastic scattering are always observed in the forward direction at high energies. The latter means, for example, that near the right-hand boundary of the upper physical region in Fig. 1 (the s region) the quantity, $\mathrm{Im}A(s,t)$, for s large and fixed, falls off sharply as t decreases from zero (forward direction). The width of the diffraction peak in NN and πN scattering corresponds to $\Delta t \sim 20$, and it will be surprising if the same is not true for $\pi\pi$ scattering as well as for other strongly interacting particle combinations. Now, we have

$$\mathrm{Im}A(s,t) \sim \frac{1}{\pi}\int_4^\infty dt' \frac{\rho(t',s)}{t'-t},$$

so a t dependence of the kind required for diffraction implies a concentration of the double spectral function within a distance from the boundary of the order Δt. Such a concentration in the double spectral region labeled ρ_2 in Fig. 1, when applied to the t channel (the lower right-hand physical region), is in agreement with the first of the above-mentioned empirical circumstances, i.e., the largeness of total cross sections at low energy. We shall return to this point at the end of this Letter.

Fortunately, the double spectral functions in the heavily shaded areas are determined by relatively tractable elastic unitarity conditions, as first pointed out by Mandelstam[1] and recently re-emphasized by Cutkosky.[5] Because of space limitations we do not write these conditions here, although they will play a central role in actual dynamical calculations. Suffice it to say that in the $\pi\pi$ problem there are three distinct "strip" functions to be calculated, which we have indicated in Fig. 1 as ρ_1, ρ_2, and ρ_3. Each of these is determined exactly in the strip regions by an integral over bilinear combinations of absorptive parts of elastic amplitudes. It is only in the interior regions that inelastic amplitudes explicitly play a role.

In his original paper[1] Mandelstam stated the opinion that attempting to calculate the parts of the double spectral function on which we are now focusing attention is not worthwhile because inelastic effects are implied, in contradiction with the basic approximation, which is elastic. We believe that there is no inconsistency; the elastic unitarity condition is to be employed only where it is correct, in order to calculate double spectral functions in the strip regions. Inelastic scattering is not calculated completely, but that part occurring at low momentum transfers (implied, for example, in the s physical region in Fig. 1 by the existence of ρ_2) should be well approximated.

It is worthwhile digressing momentarily to relate these ideas to those recently expressed by Salzman and Salzman[6] and by Drell,[7] as well as by Pomeranchuk.[8] If we focus attention on the s physical region of Fig. 1, the double spectral function ρ_1 corresponds to diagrams in which only two particles are present in intermediate states but any number may be exchanged. In other words, ρ_1 is calculated from the Cutkosky diagram[5] shown in Fig. 2(a) and represents purely elastic effects in the s channel. On the other hand, ρ_2 is calculated from diagram 2(b), in which any number of particles are allowed in intermediate states but only two are exchanged (it is elastic in the t channel). Obviously, then, we are calculating here the diffraction scattering associated with inelastic transitions in which a single pion is exchanged. This is just the mechanism of Salzman and Salzman, Drell, and Pomeranchuk. We believe that our approach is more systematic, since it raises no questions it cannot answer about cross sections in unphysical regions; however, we can only discuss total cross sections and elastic scattering, not the distribution of inelastic events.

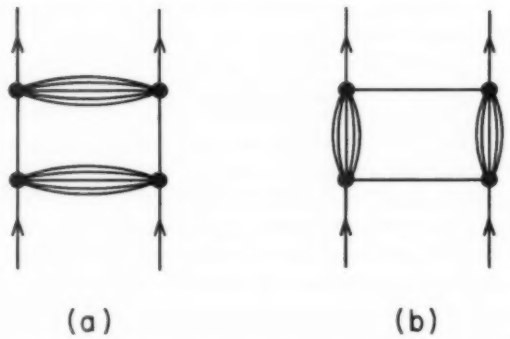

FIG. 2. The two Cutkosky diagrams needed to calculate the double spectral functions in the strip regions.

Returning to the main argument, we now consider a second postulate: that total cross sections for strongly interacting particles asymptotically approach constants at very high energies. Even within the scheme of approximation proposed here we believe that our combined requirements of unitarity and analyticity are inconsistent with total cross sections that increase indefinitely with energy. In any event, such a situation seems nonsensical and would, we believe, be impossible if unitarity were completely enforced. On the other hand, there are almost certainly solutions, such as the S-dominant solutions discussed by Chew, Mandelstam, and Noyes,[9] for which the asymptotic behavior of the double spectral functions implies a total cross section vanishing strongly at infinity. This alternative also we reject as unreasonable, feeling that a characteristic of strong interactions is a capacity to "saturate" the unitarity condition at high energies for those states that overcome the centrifugal barrier. Such a saturation should lead to a constant total cross section.

We add a final related postulate, that the first diffraction peak approaches a constant limiting shape at very high energies, and thus we arrive at the general assumption[10]:

$$\lim_{\substack{s\to\infty \\ -20\lesssim t<0}} \mathrm{Im}A(s,t)\to sf(t). \tag{1}$$

From Fig. 1, this is equivalent to

$$\lim_{\substack{s\to\infty \\ -20\lesssim t<0}} \frac{1}{\pi}\int \frac{\rho_2(t',s)}{t'-t}\,dt'\to sf(t), \tag{2}$$

which seems unnatural unless

$$\lim_{\substack{s\to\infty \\ 4<t\lesssim 20}} \rho_2(t,s)\to s\rho_2{}^L(t). \tag{3}$$

Although limit (3) cannot be said to follow strictly from limit (1), we adopt (3) as the basis for further argument. Similar reasoning can be employed for $\rho_1(t,s)$ and $\rho_3(t,s)$ to define $\rho_1{}^L(t)$ and $\rho_3{}^L(t)$. Then we borrow Pomeranchuk's argument[3] about consistency of the fixed t dispersion relations to conclude that

$$\rho_2{}^L(t)=\rho_3{}^L(t). \tag{4}$$

This equality corresponds to the statement that the total $(\pi^+\pi^-)$ and $(\pi^+\pi^+)$ cross sections become asymptotically the same.

It is important to remark that the behaviors (3) and (4) appear to be consistent in the strip regions with the integral unitarity conditions which are to be used to calculate the double spectral functions. Thus we believe that we shall be able to find solutions of our equations satisfying these conditions. How many free parameters are present in such solutions we shall not know until further study has been made of the consistency of our equations in the interior regions where they are not exact and where a cutoff probably will be needed.

We close by pointing out that condition (3), when the substitution law is invoked, implies that amplitudes at low energy are asymptotically proportional to t as $t\to\infty$. Thus, regardless of how many parameters are allowed, S-dominant solutions are ruled out and a strong interaction in the P wave (and no higher waves) is implied.[11] [At the same time, condition (4) appears to eliminate the inconsistency encountered by Chew and Mandelstam[2] when they attempted to ignore the double spectral functions in a consideration of P-dominant solutions.] It seems, therefore, that one has in these considerations the beginning of an understanding of why strong interactions are so uniform in their manifestations: One may conjecture that the defining characteristic of strong interactions is that they are "as strong as possible." The consequence from such a statement of a constant behavior for cross sections at high energies has always been plausible. Now we see that at low energies it appears inconsistent with general principles to have interactions so strong as to produce resonances or bound states for $J \geq 2$. The "strongest possible" interaction should, however, produce large low-energy P phase shifts. There remains an open question, of course, as to what extent one can determine the precise interaction strength on the basis of the "strip approximation" proposed here.

---

*This work was supported in part by the U. S. Atomic Energy Commission and in part by the National Science Foundation.

[1]S. Mandelstam, Phys. Rev. 112, 1344 (1958).

[2]G. F. Chew and S. Mandelstam, University of California Lawrence Radiation Laboratory Report UCRL-9126, March, 1960 (unpublished).

[3]I. Pomeranchuk, J. Exptl. Theoret. Phys. (U.S.S.R.) 34, 725 (1958) [translation: Soviet Phys.-JETP 34(7), 499 (1958)].

[4]G. F. Chew and S. Mandelstam, Phys. Rev. 119, 467 (1960). It will be assumed that the reader is familiar with the general principles discussed in this reference as well as in reference 1.

[5]R. E. Cutkosky, Phys. Rev. Letters 4, 624 (1960).

[6]F. Salzman and G. Salzman, Phys. Rev. Letters 5, 377 (1960).

[7]S. Drell, Phys. Rev. Letters 5, 342 (1960).

[8]I. Pomeranchuk, paper presented at the Tenth International Rochester Conference on High-Energy Nuclear Physics, 1960 (to be published).

[9]G. F. Chew, S. Mandelstam, and H. P. Noyes, Phys. Rev. 119, 478 (1960).

[10]The statements in this paragraph are uncertain with respect to logarithmic factors. Only the powers of s are to be taken seriously.

[11]In reference 1 Mandelstam discusses the relation between asymptotic behavior in t and the strength of interaction. Two papers on potential scattering by T. Regge, Nuovo cimento 14, 951 (1959), and University of Rochester Physics Department preprint, NYO-9266, 1960 (unpublished), are also very enlightening. Regge shows that the amplitude behaves like t^α, where α increases as the strength of an attractive interaction grows. For partial waves such that $l \leq \alpha$, there may be bound states or resonances, corresponding to the necessity for subtractions in the Mandelstam representation in these low-l states. For $l > \alpha$, subtractions are not needed and bound states or resonances are correspondingly absent. Although Regge's work is confined to potential scattering, we feel confident of the generality of this connection between asymptotic behavior in t and the maximum l that interacts strongly. When spin is present, of course, the connection will be slightly more complicated.

NEW APPROACH TO PERTURBATION THEORY IN QUANTUM ELECTRODYNAMICS

Ivo Bialynicki-Birula*
University of Rochester, Rochester, New York
(Received November 4, 1960)

It has been pointed out many times that the infinite results in the perturbation approach to quantum field theory may be due to the singular character of the solution at zero value of the coupling constant. In this note we want to prove that this does happen. Our procedure is to calculate exactly the S matrix as far as this singular dependence on the coupling constant is concerned and to apply perturbation expansion to the remaining nonsingular dependence. All results turn out to be finite[1] in every order of perturbation theory as long as the coupling constant is kept finite. The measurable results do not depend critically on the coupling constant (and are the same as those obtained with the use of the ordinary renormalized perturbation theory), but the renormalization constants do.

We will discuss our procedure in the case of quantum electrodynamics. Our starting point is the ordinary Lagrangian,

$$\mathfrak{L}(x) = \bar{\psi}(i\gamma\cdot\partial - m_0)\psi - \tfrac{1}{2}A_{\mu,\nu}A^{\mu,\nu} - e_0\bar{\psi}\gamma\cdot A\psi, \quad (1)$$

and we will not make any changes in the theory. Next we divide[2] this Lagrangian into the free part and the interaction part in a different way from the usual one, namely,

$$\mathfrak{L}_0(x) = \bar{\psi}(i\gamma\cdot\partial - m)\psi - \Lambda^{-2}\bar{\psi}(i\gamma\cdot\partial - m)^3\psi - \tfrac{1}{2}A_{\mu,\nu}A^{\mu,\nu}, \quad (2)$$

$$\mathfrak{L}_I(x) = -e_0\bar{\psi}\gamma\cdot A\psi - (\delta m)\bar{\psi}\psi + \Lambda^{-2}\bar{\psi}(i\gamma\cdot\partial - m)^3\psi, \quad (3)$$

where Λ is a constant, whose role will become clear later. The free equations for the electron field can be solved exactly and they lead to a propagator having the Pauli-Villars structure,

$$S(p) = (m - \gamma\cdot p)^{-1}\left[1 - \Lambda^{-2}(m - \gamma\cdot p)^2\right]^{-1} = (m - \gamma\cdot p)^{-1} - \tfrac{1}{2}(m+\Lambda-\gamma\cdot p)^{-1} - \tfrac{1}{2}(m-\Lambda-\gamma\cdot p)^{-1}. \quad (4)$$

An indefinite metric appears in the world of virtual particles only and all observable (final and initial) states are characterized by a positive-definite metric in every order of perturbation theory. Let us now assume that

$$\Lambda^{-1} = E_{\max}^{-1} e_0^{2(N+1)},$$

where N is the highest order of perturbation theory, and $E_{\max}$ is the highest energy of the initial and final particles that we are interested in. The S matrix can now be expanded into a power series in e_0, and all terms are now finite provided the dependence of the electron propagator on e_0 is treated exactly. The additional term in the interaction Lagrangian can always be neglected in perturbation theory if the energies of initial and final particles are finite, which means that this procedure cannot give answers concerning the limiting high-energy behavior. When the energies of the initial or final particles tend to infinity the additional term in the interaction Lagrangian cannot be treated by perturbation theory. All renormalization constants appear to have a singular dependence on the coupling constant of logarithmic type and they cannot be expanded into a power series in e_0. All measurable quantities are given by a power series in e which is at least asymptotic.

The procedure outlined above can be applied to all nonrenormalizable theories as well as to renormalizable ones. A more detailed account will be published elsewhere.

---

*On leave of absence from Warsaw University, Warsaw, Poland.

[1]We will not discuss the infrared divergencies here.

[2]There are, of course, many ways of dividing the initial Lagrangian which give the same answer.

INVESTIGATION OF THE FIVE-POINT FUNCTION*

L. F. Cook, Jr.,† and Jan Tarski‡
Lawrence Radiation Laboratory, University of California, Berkeley, California
(Received November 18, 1960)

In this Letter we wish to describe and discuss the results of an investigation concerning the singularities of Feynman amplitudes for production processes.

Our investigation was motivated by three considerations. First, experiments[1] are being conducted in which five-particle processes are analyzed for the purpose of studying the π-π interaction,[2] and, in particular, the conjectured π-π resonance.[3] It is intended to extrapolate the data in at least one of these experiments (see Fig. 1), and a knowledge of the singularities of the amplitude is necessary to interpret properly the results of such an extrapolation. Second, such production amplitudes are of interest in themselves, and, also, are needed for the purpose of studying the three-particle intermediate states in dispersion theory. Third, Cutkosky has pointed out that the Feynman amplitude containing five external momenta joined by a single internal loop has simple poles, which correspond to all the internal momenta on the mass shell.[4] It is thus of interest to know whether these poles can be useful in theoretical analyses, and whether they have direct experimental effects; e.g., such poles could be near the pole indicated in Fig. 1.[5]

In our investigation we restricted ourselves to single-loop diagrams without crossed lines, and in addition, we considered in detail the corresponding amplitudes for only four specific processes and for only one configuration of momenta for each process. Our reasons for considering only such diagrams are as follows: On the one hand, it can be easily shown that our general conclusions are not affected by the analytic properties of the amplitudes which correspond to crossed diagrams, or to diagrams with a simpler internal structure. We may also note that the study of crossed diagrams does not lead to any new complications, and the simpler diagrams can be readily analyzed on the basis of previous studies.[6,7] On the other hand, diagrams with a more complicated internal structure yield singularities which are further removed from the region of interest. Moreover, it has been shown that in some cases the essential features of such more complicated diagrams are also present in the single-loop diagrams for a given process,[8] and a similar conclusion may well be valid for production processes.

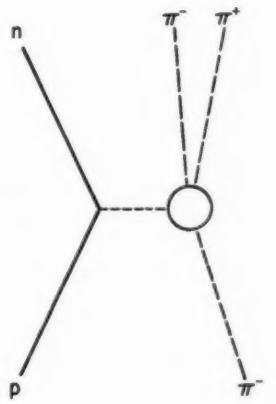

FIG. 1. The diagram associated with a single-particle pole in the amplitude $\langle N2\pi|N\pi\rangle$. An extrapolation to this pole is expected to give information about the π-π interaction.

We considered specific processes with specific configurations of momenta because a more general analysis seems to require a considerable amount of additional study. We felt that such a more general analysis could be more effectively carried out after a preliminary investigation has been made.

The amplitudes which we considered in detail correspond to the diagrams of Fig. 2. Diagrams (a) and (b) are relevant to two of the experiments used for a study of the π-π interaction. Diagram (c) is pertinent for a possible experimental investigation of the five-point poles. Since there are no single-particle poles in the amplitude $\langle d\,2\pi|d\,\pi\rangle$ analogous to that indicated in Fig. 1, it is likely that any behavior indicative of a pole is due to the five-point poles. Finally, diagram (d) is relevant in the study of the deuteron form factor.[9] We shall refer to the processes and the amplitudes of these diagrams as processes and amplitudes (a) - (d), respectively.

We now consider a general Feynman amplitude, M_s, corresponding to diagram (e) of Fig. 2, with momenta and masses as indicated. Such an amplitude is a function of ten kinematical invariants, p_{ij}^2, $i<j$, where the p_{ij} are defined by

$$p_{ij}=p_{i,i+1}+\cdots+p_{j-1,j}. \qquad (1)$$

(Spin dependence is irrelevant for our discussion.

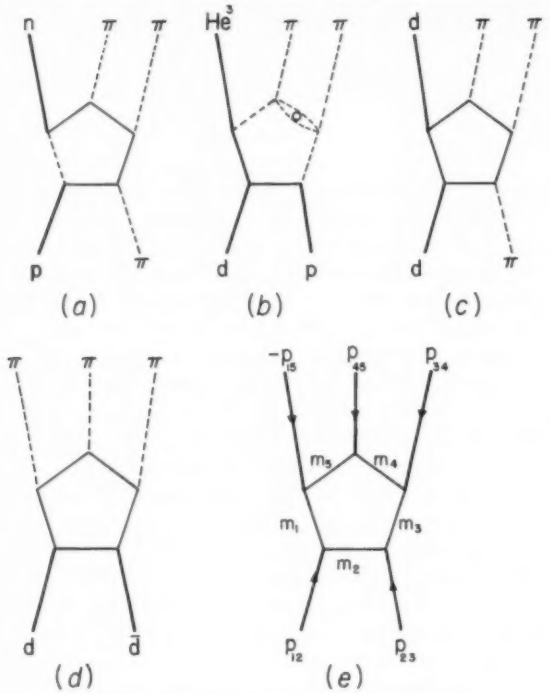

FIG. 2. Single-loop diagrams for production processes. Diagrams (a) - (d) correspond to the amplitudes which were studied in detail, and diagram (e) shows the labeling of the lines. In diagram (b) we assume that two of the internal pions are in resonance and behave as a single particle of mass $3.5m_\pi$. [This diagram has been suggested by R. J. Eden, Proceedings of the Tenth Annual Rochester Conference on High-Energy Nuclear Physics, 1960 (to be published)].

We also assume that each m_i is different from zero.) It is also convenient to introduce quantities x_{ij} defined by

$$p_{ij}^2 = m_i^2 + m_j^2 + 2m_i m_j x_{ij} \quad \text{for } i<j, \tag{2a}$$

$$x_{ji} = x_{ij}, \quad x_{ii} = -1. \tag{2b}$$

We form the matrix (x_{ij}), and we are able to describe concisely the possible locations of all the singularities of M_s by the following theorem[10]: Every singularity of M_s lies on a hypersurface (in the space of the complex invariants) defined by setting the determinant of a principal minor of the matrix (x_{ij}) equal to zero.

The various types of singularities, corresponding to the various hypersurfaces, can be given a simple physical interpretation: The order of a given principal minor equals the number of internal momenta on the mass shell. In particular, the five-point poles lie on the hypersurface $\det(x_{ij}) = 0$. In case of other singularities, there are internal momenta which do not affect the singularities. The singularities can then be identified with those of appropriate contracted diagrams. (A diagram is contracted by removing one or more internal lines and joining the endpoints of each removed line. The result is a diagram with fewer vertices.) It should be emphasized that every singularity lies on some such hypersurface, but the converse statement does not hold. In fact, the difficulty of the problem lies in determining which of these points are regular and which are singular on a suitably defined physical sheet.

The complete details of our investigation will be submitted for publication in the near future, but a brief summary can be given here. For convenience we consider two of the invariants as (complex) variables, and the others as parameters. We first choose such values for the parameters that there is a region in the real plane of the two variables where the amplitude is real and analytic. For this choice of parameters the singularities (for the two variables) can be readily obtained. We next vary the parameters to their physical values and follow the displacement of these singularities as the variation is done.[6,7]

We stated in the foregoing that we considered in detail only four processes and only one configuration of momenta for each process. We used the labeling shown in diagram (e) of Fig. 2 for the other diagrams, and we selected the following configuration in the center-of-mass system:

$$p_{12} = (E_{12}, q, 0, 0); \; -p_{34} = (E_{34}, 0, -\tfrac{1}{2}p, p),$$

$$p_{23} = (E_{23}, -q, 0, 0); \; -p_{45} = (E_{45}, 0, -\tfrac{1}{2}p, -p),$$

$$p_{15} = (E_{15}, 0, p, 0). \tag{3}$$

This configuration corresponds to momenta p_{12} and p_{23} incoming, and the others outgoing. Furthermore, we used the following incident laboratory energies: for process (a), $T_\pi = 670$ Mev; for process (b), $T_p = 648$ Mev; for process (c), $T_\pi = 650$ Mev; and for process (d), $T_{\bar{d}} = 500$ Mev. [For processes (a) and (b), these energies are used in the experiments.] These incident energies and Eqs. (3) now determine all the invariants.

Some of our results are given in Fig. 3. This figure shows singularities in the complex p_{25}^2 plane, for each of the amplitudes (a) and (d). [Amplitudes (b) and (c) are described briefly in the sequel.] We chose the p_{25}^2 plane to display

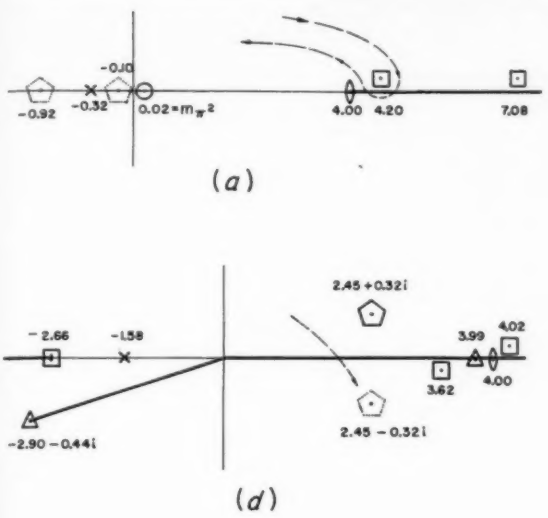

FIG. 3. Singularities in the p_{25}^2 planes associated, respectively, with diagrams (a) and (d) of Fig. 2. The values refer to the nucleon mass as a unit. See text for explanation of details.

our results in order to compare the location of the five-point poles and other singularities of amplitude (a) with the pole indicate in Fig. 1, which occurs at $p_{25}^2=m_\pi^2$. For amplitude (d), the quantities of interest are the distances from the singularities to the region over which the amplitude is integrated, since these distances are important in determining the effect of the singularities. The distances in the p_{25}^2 plane between the singularities and the location given by the value of p_{25}^2 in the physical process are illustrative, for a first orientation. The values of the other invariants are the actual physical values. However, we made the following exception: Process (d) is relevant for a study of the deuteron form factor, for which the amplitude $\langle 3\pi|d\bar{d}\rangle$ is needed in an unphysical region, and with regard to this we somewhat arbitrarily reduced the value of p_{13}^2 to $10m_\pi^2$.

On the diagrams of Fig. 3 the crosses show the values of p_{25}^2 associated with the physical processes. The circle in diagram (a) indicates the pole implied by Fig. 1. Other geometrical figures indicate in an obvious way the various types of singularities related to the single-loop diagrams. In particular, the pentagons indicate the five-point poles, and the figures formed by two arcs indicate the thresholds for the production of two real nucleons; to these singularities correspond diagrams with lines 1, 3, and 4 contracted. Dotted lines indicate that a given pole lies on an unphysical sheet, and that a continuation along the indicated path will lead to the pole. (Other singularities on unphysical sheets are not displayed.) Figures which are slightly removed from the real axis indicate that the points are singular in the limit $\mathrm{Im}\,p_{25}^2\to 0$, but the limit must be taken from the indicated half-plane. In this connection we may note that all the singularities other than the five-point poles (and the single-particle pole) are branch points, logarithmic or square-root, and cuts must be prescribed which connect them and the point at infinity. Such branch cuts are shown on the diagrams of Fig. 3.

The properties of singularities of amplitudes (b) and (c) do not differ greatly from those of the singularities of amplitude (a), and for this reason we do not give separate diagrams for these amplitudes. In particular, the five-point poles are located on an unphysical sheet, and in fact near the physical region, as in Fig. 3(a). However, amplitudes (b) and (c) differ from amplitude (a) in having vertex-type singularities (anomalous thresholds). Such singularities are present in amplitude (d), but not in amplitude (a). [We also note that the complete amplitude for process (b) has a single-particle pole at $p_{25}^2=m_N^2$. We recall that in the amplitude for process (c) there is no such pole.]

The possible effects of a pole depend upon its residue as well as its distance from the relevant region, and we remark here that Cutkosky[4] has given a method of determining the residues of the five-point poles. A further discussion of the residues, however, is planned for a separate communication.

We now turn to a brief discussion of our results. Of immediate interest are the results for processes (a) and (b). Our investigation suggests very strongly that the five-point poles and the other singularities of amplitudes (a) and (b), respectively, have no noticeable direct effect on these processes. This conclusion is based on calculations for only special configurations of momenta, but even if moderate changes in these configurations are made, the essential aspects of the arrangement of the singularities should remain as in Fig. 3(a). Further, even if for some extreme configurations of momenta the amplitude should be markedly affected by the singularities, the contribution to the cross section of such configurations would not be great.

We also remark that the five-point poles have very little direct effect for process (c), for the chosen configuration of momenta. In contrast to the remarks in the preceding paragraph, it is of interest to determine whether certain extreme configurations exist for which the amplitude is noticeably affected by the five-point poles. Such effects could be experimentally measured, and the absence of a single-particle pole would simplify the theoretical interpretation.

Finally, for process (d) (with the unphysical value $p_{13}^2 = 10m_\pi^2$), we notice that there is a five-point pole on the physical sheet, and it can be expected to stay there for moderate changes of the configurations of momenta. Since the distances from the singularities, including the pole, to the region of interest are such that their effect on the amplitude can be significant, a further study of this process is suggested. On the other hand, a preliminary calculation suggests that the amplitude $\langle 3\pi | N\overline{N}\rangle$ has no singularities other than the normal thresholds near the region of interest; in particular, the relevant five-point poles lie on an unphysical sheet. Thus it appears that these other (anomalous) singularities can be ignored in the study of the three-pion contribution to the nucleon form factor.

In conclusion, we should like to make one general observation which may be of interest. Studies of the vertex and scattering amplitudes[6] have shown that the presence of external particles which are near instability leads to singularities other than the normal thresholds. This pattern of behavior is also illustrated by our results regarding the amplitudes relevant in the nucleon and deuteron form factors, viz., in the latter case the anomalous singularities are on the physical sheet.

We are grateful to Professor R. J. Eden for encouragement and advice, and we are indebted to Dr. D. L. Judd for hospitality extended to us at the Lawrence Radiation Laboratory, where most of this work was carried out. One of us (J.T.) would like to thank Professor J. R. Oppenheimer for hospitality at the Institute for Advanced Study during the completion of this work.

---

*This work was done in part under the auspices of the U. S. Atomic Energy Commission.

†Present address: Palmer Physical Laboratory, Princeton University, Princeton, New Jersey.

‡Present address: The Institute for Advanced Study, Princeton, New Jersey.

[1]E. Segrè et al.; L. Alvarez et al.; V. Perez-Mendez et al.: experiments in progress at Lawrence Radiation Laboratory, Berkeley. A. Abashian, N. E. Booth, and K. M. Crowe, Phys. Rev. Letters 5, 258 (1960).

[2]G. F. Chew and F. E. Low, Phys. Rev. 113, 1640 (1959). For a general theory of the π-π interaction see G. F. Chew and S. Mandelstam, Phys. Rev. 119, 467 (1960).

[3]W. R. Frazer and J. R. Fulco, Phys. Rev. Letters 2, 365 (1959).

[4]R. E. Cutkosky, J. Math. Phys. 1, 429 (1960). It is also implicit in the work of L. D. Landau [Nuclear Phys. 13, 181 (1959)] that these singularities of production amplitudes are simple poles.

[5]This possibility was first pointed out to one of us by S. B. Treiman (private communication).

[6]R. Karplus, C. M. Sommerfield, and E. H. Wichmann, Phys. Rev. 111, 1187 (1958); 114, 376 (1959).

[7]J. Tarski, J. Math. Phys. 1, 149 (1960).

[8]See, e.g., R. J. Eden, Phys. Rev. 119, 1763 (1960).

[9]Bose statistics and conservation laws imply that the process $d + \overline{d} \rightleftharpoons 2\pi \rightleftharpoons \gamma$ is forbidden, and thus the lowest mass intermediate pion contribution to the deuteron form factor is associated with diagram (d) of Fig. 2. We may also note that the process $d + \overline{d} \rightleftharpoons N + \overline{N} \rightleftharpoons \gamma$ has an anomalous threshold, and for this reason it actually constitutes the lowest mass contribution.

[10]See Appendix B of reference 7. We note that in the second part of reference 6 and in reference 7 quantities y_{ij} were used, where $y_{ij} = -x_{ij}$, rather than the x_{ij}. The x_{ij} preserve the signs of the quantities p_{ij}^2, and were first used by S. Mandelstam.

ABSTRACTS

In this section are printed the abstracts of Articles that have been forwarded to The American Institute of Physics for publication in THE PHYSICAL REVIEW. In quoting information obtained from this section before the appearance of the corresponding Article, reference should be made to "Physical Review (to be published)" rather than to this Journal.

PERTURBATION THEORY FOR AN INFINITE MEDIUM OF FERMIONS. II. Abraham Klein, University of Pennsylvania, Philadelphia, Pennsylvania (Received October 13, 1960).

New forms of the linked-cluster expansion for the ground-state energy of a normal spherical system are given in terms of the exact single-particle propagator and of the associated self-energy operator. These forms are shown to be stationary with respect to variations of the latter quantities. A new concise proof of the Hugenholtz-Van Hove theorem on single-particle energies is then possible. The variational principle also explains the insensitivity of recent binding energy calculations to the choice of single-particle energies. It is shown how all results may be extended to systems with anisotropic features.

PERTURBATION THEORY FOR AN INFINITE MEDIUM OF FERMIONS. III. DERIVATION OF THE LANDAU THEORY OF FERMI LIQUIDS. Abraham Klein, University of Pennsylvania, Philadelphia, Pennsylvania (Received October 13, 1960).

The methods employed in the previous papers of this series for the ground-state energy of a normal Fermion system are extended to finite temperatures. The basic assumption is that the density matrix of the actual system in thermodynamic equilibrium can be derived by adiabatic transformation from the density matrix of a system of noninteracting particles at the same temperature, volume, and chemical potential. However, the spectrum of the noninteracting system must be dependent on the intensive parameters. The self-consistency of the scheme is exhibited by demonstrating that the effective potential characterizing this system can be related to the self-energy operator of the actual system. Two equivalent versions of the theory are derived. In one of these the basic equations are precisely those of the Landau theory of Fermi liquids with the difference, however, that all quantities are given explicitly from first principles.

COULOMB SCATTERING OF POLARIZED ELECTRONS. W. R. Johnson, T. A. Weber, and C. J. Mullin, University of Notre Dame, Notre Dame, Indiana (Received August 19, 1960).

An approximate analytical expression for the spin-dependent cross section for Coulomb scattering, valid to order $(\alpha Z)^4$, is developed. The development is based on a modification of the Sommerfeld-Maue wave function. The $(\alpha Z)^2$ and $(\alpha Z)^3$ terms in the resulting cross section are identical with the corresponding terms found by the second Born approximation. The $(\alpha Z)^4$ term is verified by analytically summing the corresponding term in the Mott series. Graphs, comparing the approximate analytical expressions for both the cross section and asymmetry function with exact numerical results, are included.

CYCLOTRON RADIATION FROM RELATIVISTIC PARTICLES WITH AN ARBITRARY VELOCITY DISTRIBUTION. Ludwig Oster, Laboratory of Marine Physics, Yale University, New Haven, Connecticut (Received October 5, 1960).

A formula is derived which represents the spectral and angular behavior of cyclotron radiation emitted by a relativistic particle moving in a constant magnetic field and having arbitrary velocity components parallel and perpendicular to the field. This formula is used to describe the emission of an assembly of particles having a Maxwellian distribution function. All broadening mechanisms of practical importance—collisions, relativistic mass variability, and Doppler effects—are included and discussed.

ANALYTIC PROPERTIES OF SINGLE-PARTICLE PROPAGATORS FOR MANY-FERMION SYSTEMS. J. M. Luttinger, Columbia University, New York, New York (Received October 11, 1960).

Certain general properties of single-particle propagators for a system of interacting fermions are derived. In addition, the properties of the proper self-energy part $G_k(\zeta)$ which were used

in previous work on the ground-state energy and on the Fermi surface are established. In particular, the fact that to all orders of perturbation theory in the interaction, $\mathrm{Im}G_k(x - i0^+)$ behaves like $C_k(x - \mu)^2$ ($C_k > 0$) for x very near μ, is proved.

EFFECT OF ELECTRON EXCHANGE ON THE DISPERSION RELATION OF PLASMONS. Oldwig von Roos and Jonas S. Zmuidzinas, Jet Propulsion Laboratory, California Institute of Technology, Pasadena, California (Received October 5, 1960).

A calculation of the influence of electron exchange on the dispersion relation of a high-density electron gas at 0°K is described. The result is compared with those obtained by various authors using different methods.

CORRECTION TO THE DEBYE-HÜCKEL THEORY. John G. Trulio and Stephen G. Brush, Lawrence Radiation Laboratory, University of California, Livermore, California (Received October 13, 1960).

The correction to the equation of state of a classical electron gas is calculated by the method of Abe. The results are compared with those recently obtained by a different method by Bowers and Salpeter.

SOLUTION OF THE FUNCTIONAL DIFFERENTIAL EQUATION FOR THE STATISTICAL EQUILIBRIUM OF A CRYSTAL. Robert M. Lewis and Joseph B. Keller, Institute of Mathematical Sciences, New York University, New York, New York (Received October 13, 1960).

The s-particle distribution functions ($s = 1, 2, \cdots$) of classical equilibrium statistical mechanics are determined for a crystal, as power series in the temperature. They are obtained by solving Bogolyubov's functional differential equation. From the distribution functions, the thermodynamic functions of a crystal are computed as power series in the temperature. The leading terms in these series are the usual classical results which are customarily derived by assuming that the potential energy is a quadratic function of the particle displacements. The further terms, which depend upon the nonquadratic or anharmonic terms in the potential, provide corrections to the usual results, which become more important as the temperature increases. If only a few terms in the series are used, the results will be valid at temperatures low compared to some characteristic temperature of the crystal, e.g., the melting temperature. Since they are based on classical mechanics, the results are valid only at temperatures high compared to the Debye temperature.

The series expansions of the distribution functions and thermodynamic functions may be viewed as the low-temperature analogs of the virial expansions, which are low-density expansions. As in the case of the virial expansions, all the terms are determined explicitly in analytic form, but their actual evaluation is difficult.

DEFECTS IN IRRADIATED SILICON. I. ELECTRON SPIN RESONANCE OF THE Si-*A* CENTER. G. D. Watkins and J. W. Corbett, General Electric Research Laboratory, Schenectady, New York (Received October 7, 1960).

The Si-*A* center is a major, radiation-damage defect produced in "pulled" silicon by a room temperature irradiation. As a result of studies described in this paper (I), and the following one (II), it is concluded that this center is a lattice vacancy with an oxygen atom impurity bridging two of the four broken bonds associated with the vacancy. Spin resonance and electrical activity arise from an electron trapped in the other two bonds. In this paper (I), the spin resonance studies are described. A molecular orbital treatment of the trapped electron wave function satisfactorily accounts for the observed g tensor, as well as the hyperfine interaction observed with neighboring 4.7% abundant Si^{29} nuclei. Study of the changes in the spectrum of a sample subjected to uniaxial stress are also described. Under stress, the amplitudes of the individual resonance components (which correspond to different orientations of the defect in the crystal) are observed to change. This results from (1) electronic redistribution of the trapped electrons among the defects, and (2) thermally activated reorientation of the defects themselves under the applied stress. These two effects are separated and a quantitative study of their magnitudes and signs, as well as their rates, is given. The results confirm many of the important microscopic features of the model.

DEFECTS IN IRRADIATED SILICON. II. INFRARED ABSORPTION OF THE Si-*A* CENTER. J. W. Corbett, G. D. Watkins, R. M. Chrenko, and R. S. McDonald, General Electric Research Laboratory, Schenectady, New York (Received October 7, 1960).

The Si-*A* center is a major, radiation-damage defect produced in "pulled" silicon by room temperature irradiation. In this paper (II), we present the infrared measurements which, in conjunction with the spin resonance measurements of the preceding paper (I), establish the identity of the Si-*A* center. A new infrared absorption band is observed at 12 μ in electron-irradiated silicon. This band is shown to be a vibrational band of impurity oxygen in the lattice. Macroscopic and microscopic correlations between the 12μ band and the spin resonance of the Si-*A* center are presented. The macroscopic correlations are of production rate, recovery, etc. The microscopic correlations derive from the absorption of polarized infrared radiation by samples of various crystallographic orientations, subjected to a uniaxial, compressive stress. Partial alignment of the defects is induced by the stress and is detected as a dichroism in the 12μ band. This alignment is compared to the corresponding alignment studies in the spin-resonance measurements in paper I. It is shown that the kinetics and magnitude of the response to the stress are the same for the defects observed in both types of measurements. This shows that the 12μ band arises from the Si-*A* center and establishes the configuration of the oxygen in the defect. These results, together with the results of paper I, allow us to conclude that the Si-*A* center is a lattice vacancy with an oxygen atom bridging two of the four broken bonds associated with the vacancy. The remaining two bonds can trap an electron, giving rise to the spin resonance spectrum of the defect. The identification of the Si-*A* center indicates that the vacancy is mobile in a room-temperature irradiation.

ELECTRICAL PROPERTIES OF *n*-TYPE GaSb. Alan J. Strauss, Lincoln Laboratory, Massachusetts Institute of Technology, Lexington, Massachusetts (Received October 3, 1960).

The electrical conductivity and Hall coefficient of *n*-type GaSb doped with Se or Te have been measured, in most cases at 77°K and 300°K, for samples with net donor concentrations between about 6×10^{16} cm^{-3} and 2×10^{18} cm^{-3}. In general, the data are consistent with the two-band model which Sagar has proposed for the conduction band of GaSb, but systematic differences are observed between the properties of Se-doped and Te-doped samples. It seems likely that these differences are associated with impurity conduction of the metallic type. For the Te-doped samples, the electron mobility at 77°K apparently varies in an anomalous manner with increasing impurity concentration.

EFFECT OF STATIC STRAINS ON DIFFUSION. L. A. Girifalco and H. H. Grimes, Lewis Research Center, National Aeronautics and Space Administration, Cleveland, Ohio (Received September 16, 1960; revised manuscript received November 7, 1960).

A theory is developed that gives the diffusion coefficient in strained systems as an exponential function of the strain. This theory starts with the statistical theory of the atomic jump frequency as developed by Vineyard. The parameter determining the effect of strain on diffusion is related to the changes in the interatomic forces with strain. Comparison of the theory with published experimental results for the effect of pressure on diffusion shows that the experiments agree with the form of the theoretical equation in all cases within experimental error.

ULTRASONIC ATTENUATION IN NORMAL METALS AT LOW TEMPERATURES. A. B. Bhatia and R. A. Moore, University of Alberta, Edmonton, Canada (Received September 6, 1960; revised manuscript received October 24, 1960).

Expressions for the attenuation α_d and α_t of plane dilatational and shear sound waves are obtained by solving the Boltzmann transport equation for the electron distribution function f without assuming the existence of a relaxation time τ for the collision term in this equation. Instead the collision integral is considered to arise explicitly from the interaction of electrons with thermal phonons and impurities. Making the usual "ideal metal" assumptions, it is found that the attenuation in general depends on a set of effective relaxation times τ_{LM} which are associated with the various terms in the expan-

sion of f in a series of spherical harmonics $Y_{LM}(\theta, \phi)$; the τ_{LM} are independent of the subscript M, and hence the same set $\{\tau_L\}$ determines both α_d and α_t. Explicit expressions for τ_L are derived.

For the case of all τ_L equal to one another and equal to τ, say, the analytical expressions for α_d and α_t obtained here are the same as those of Pippard. However, usually the τ_L are not equal to one another. It is then found that when $\lambda >> l$ (λ is the wavelength of the sound wave and l a mean free path of the electrons), τ in Pippard's expressions must be replaced by τ_2 and, contrary to what is usually assumed, α would not be in general proportional to the electrical conductivity σ ($\sigma \propto \tau_1$). When $\lambda << l$, the attenuation, with one exception, is independent of $\{\tau_L\}$ and is the same as that given by Pippard. For $\lambda \sim l$, and the τ_L not equal to one another, α may be calculated numerically if the ratios τ_L/τ_1 are known; the results of one such calculation show that the deviations from Pippard's analytical expressions are at most about 20%, provided τ in the latter is identified as τ_2.

Lastly, the possible influence of electron-electron collisions on attenuation is briefly discussed.

DOMAIN CONFIGURATIONS ABOUT NONMAGNETIC PARTICLES IN IRON. William D. Nix and Robert A. Huggins, Department of Materials Science, Stanford University, Stanford, California (Received October 3, 1960).

The closure domain configuration about a nonmagnetic particle in iron is considered in terms of magnetostatic, interfacial wall, and magnetostrictive energies. Equations for the total energy of the domain configuration and the value of the geometrical parameter θ have been derived. The effects of particle size and shape are considered.

BLEACHING AND RECOVERY OF F CENTERS IN KCl. Loretta E. Silverman* and L. I. Grossweiner, Department of Physics, Illinois Institute of Technology, Technology Center, Chicago, Illinois (Received October 12, 1960).

F centers in KCl are optically bleached at room temperature with a minimum light energy of 20.1 ± 1.0 ev per F center. The F band is recovered on further room-temperature x-raying with a minimum energy of 69 ± 5 ev per F center. The increase in the M and R bands during optical bleaching of the F band is nullified upon the recovery of the F band by further x-raying. The recovery kinetics are second-order in the number of optically bleached F centers with a rate-constant of $(7.9 \pm 0.8) \times 10^{-20}$ cm^3/F center-sec. The rate law requires an energy transfer from the bulk lattice and is consistent with an exciton mechanism.

*Present address: Electronics Research Division, Armour Research Foundation, Technology Center, Chicago, Illinois.

CROSS-RELAXATION AND CONCENTRATION EFFECTS IN RUBY. Roy W. Roberts, Melabs, Palo Alto, California, James H. Burgess, Stanford University, Palo Alto, California, and Harold D. Tenney, Melabs, Palo Alto, California (Received October 13, 1960).

Cross relaxation effects in ruby maser crystals are treated by introduction of a cross-relaxation probability in the rate equations. Detailed solutions have been obtained for several specific processes and compared to recent experiments. It is shown that cross relaxation can improve maser performance even in the absence of impurity doping. Pulse experiments at 0.06% and 0.14% chromium ion concentrations in a ruby traveling-wave maser are interpreted in terms of a five-spin process in addition to a four-spin process.

PHOTOCONDUCTIVITY OF SILVER CHLORIDE CRYSTALS UNDER PULSED X-RAY IRRADIATION. Alwin E. Michel,* Department of Engineering Physics, Cornell University, Ithaca, New York (Received October 5, 1960).

The photoconductivity produced by irradiation with 0.2-μsec x-ray pulses was studied in AgCl as a function of temperature (80 - 280°K), x-ray intensity and penetration, field strength, and crystal preparation, in order to obtain information about lifetimes and mobilities of electrons and holes. The measurements of electron lifetimes (~1μsec) and mobilities in air-grown crystals are in agreement with those reported in the literature. The photoconductive response can be described by assuming deep electron traps throughout the volume of the crystal and possibly a disturbed surface layer. No hole motion is observed

below 250°K; above that temperature the schubweg per unit field is estimated at 5×10^{-8} cm²/v.

The electron lifetime in crystals grown and annealed in He is much smaller than in the air grown samples. Assuming the same mobility in both samples, the lifetime at 80°K is 3×10^{-9} sec. At higher temperatures the pulses show long tails, and between 200 and 280°K the saturation time varies exponentially with $1/T$. It is assumed that there exist shallow traps (~0.08 ev) in a thin surface region which otherwise has a long electron lifetime as compared to the bulk of the crystal. Measurements on crystals doped with 20 ppm of Cu^+ indicate that the Cu^+ ions do not act as effective electron traps. On the other hand, the presence of 1 ppm of Ni ions reduces the lifetime at 30°K to less than 3×10^{-11} sec, indicating a capture cross section of the Ni ion larger than 300 A².

*Present address: IBM Research Laboratory, Poughkeepsie, New York.

DEGENERACY IN Ag_2Te. C. Wood, V. Harrap, and W. M. Kane, Research Division, Philco Corporation, Philadelphia, Pennsylvania (Received August 24, 1960; revised manuscript received November 8, 1960).

The Hall coefficient, resistivity, and Seebeck coefficient of n- and p-type specimens of Ag_2Te have been measured over the temperature range from 55 to 300°K. These results indicate that the compound is highly degenerate over the whole temperature range studied. Calculations were made of the effective masses, mobility ratios, and energy gap and gave order-of-magnitude values.

SURFACE STRUCTURES AND PROPERTIES OF DIAMOND-STRUCTURE SEMICONDUCTORS. D. Haneman,* Barus Physics Laboratory, Brown University, Providence, Rhode Island (Received October 6, 1960).

Low-energy electron-diffraction and secondary electron emission measurements have been made on (111) and (11$\bar{1}$) surfaces of GaSb and (100) surfaces of InSb. To account for the diffraction patterns observed both for these materials and previously for Ge and Si, a general model for (111) surfaces of diamond-structure semiconductors is proposed. Every second atom, counting along alternate close-spaced rows, is raised with respect to its neighbors, being bonded to the sublayer by three p bonds while the "dangling bond" is s-type. The remaining three-fourths of the surface atoms have dangling p bonds and are bonded to the sublayer by trigonal sp^2-type bonds.

The Ga or (11$\bar{1}$) face of GaSb has maximum sticking coefficients of 10^{-5} and 10^{-4} for oxygen and CO_2, respectively, these values being 10 times greater than those found for the Sb or (111) face. Multilayer adsorption of oxygen takes place on all the surfaces measured. The oxygen can be removed by heat treatment alone. Evidence is presented to show that diffusion of oxygen into the bulk is an important mechanism for regenerating the clean surfaces by heat treatment. Carbon dioxide adsorbs on GaSb so as to show structure. It apparently deposits as an unbroken molecule, and, unlike oxygen, does not build up several layers.

*Now at Physics Department, University of New South Wales, Sydney, Australia.

FRIEDEL SUM RULE FOR A SYSTEM OF INTERACTING ELECTRONS. J. S. Langer, Carnegie Institute of Technology, Pittsburgh, Pennsylvania, and V. Ambegaokar,* Westinghouse Research Laboratories, Pittsburgh, Pennsylvania (Received October 3, 1960).

The Friedel sum rule is derived for a system of interacting electrons in a periodic potential.

*Present address: Institute for Theoretical Physics, Copenhagen, Denmark.

ABSORPTION SPECTRA OF F_2^-, Cl_2^-, Br_2^-, AND I_2^- IN THE ALKALI HALIDES. C. J. Delbecq, W. Hayes,* and P. H. Yuster, Argonne National Laboratory, Argonne, Illinois (Received October 12, 1960).

After x-ray irradiation at liquid nitrogen temperature, holes are trapped by forming F_2^- molecule ions in LiF; Br_2^- molecule ions in KBr containing one of the impurities Ag^+, Tl^+, Pb^{++}, or NO_2^-; and I_2^- molecule ions in KI containing one of the impurities listed above. An investigation of the optical and paramagnetic resonance spectra of crystals containing F_2^-, Br_2^-, and I_2^- centers leads to an identification of the optical transitions of these centers. The polarizations and relative intensities of the optical absorptions in the X_2^-

molecule ion series are discussed with reference to the energy level scheme to be expected for such a species.

*Now at the Clarendon Laboratory, Oxford, England.

SURFACE MOBILITY OF COPPER IONS ON CUPROUS OXIDE. Rudolf Frerichs and Irving Liberman, Northwestern University, Evanston, Illinois (Received September 9, 1960; revised manuscript received November 7, 1960).

This paper reports on the motion of Cu^+ ion vacancies on the surface of cuprous oxide at room temperature under the application of an electric field. The measurement of the mobility of the Cu^+ vacancies was made by means of a "time of flight" procedure. The formation of luminescent centers is the unique property of Cu^+ vacancies that makes them directly observable. The mobility of the Cu^+ vacancies at room temperature is about 10^{-11} cm^2/volt-sec. The variation of the mobility with temperatures between 28°C and 55°C is observed. From these data the constants of the diffusion equation $D = D_0 \exp(\Delta H/RT)$ are computed: $D_0 = 5\times10^{-7}$ cm^2 sec, $\Delta H = 8100$ calories. The low values obtained for these constants show that the ionic current follows low-resistance paths formed by the crystal grain boundaries or along the surface of the crystal.

TUNNELING CURRENT IN ESAKI DIODES. Clayton Wilson Bates, Jr., Solid-State Physics Group, AVCO Research and Advanced Development Division, Wilmington, Massachusetts (Received October 4, 1960).

The integral giving the net tunneling current flowing across the junction in an Esaki diode,

$$I = A\int_{E_c}^{E_v} \{f_c(E) - f_v(E)\}\, Z\rho_c(E)\rho_v(E)dE,$$

is evaluated under the normal assumptions that $(\xi_c - E_c)$ and $(E_v - \xi_v)$ are of the order of $2kT$. The resulting expression is

$$I = -\frac{A''(E_v - E_c)^2(1 - e^{qV/kT})}{(m+n)e^{a/2} + (1+e^{qV/kT})},$$

where A'' is an arbitrary constant and m, n, and a are functions of the Fermi levels on both sides of the junction, the location of the band edges, and the absolute temperature. This expression is plotted as a function of the applied voltage for temperatures of 200°K, 300°K, and 350°K for donor and acceptor concentrations of 10^{19} cm^{-3} and 1.6×10^{19} cm^{-3}, respectively. The resulting curves compare quite favorably with those of Esaki.

ELECTRIC FIELD GRADIENTS IN DILUTE ALLOYS OF SILVER. C. A. Giffels,* G. W. Hinman, and S. H. Vosko,† Department of Physics, Carnegie Institute of Technology, Pittsburgh, Pennsylvania (Received August 31, 1960).

The directional correlation of the gamma rays emitted in the decay of Cd^{111} has been measured with the cadmium embedded in the cubic silver lattice in order to observe the electric field gradients produced by various solute atoms. The alloys studied contained small concentrations of cadmium, indium, tin, antimony, or germanium. The results were compared to various theories of screening and were found to be in agreement with a $\cos(2kr+\phi)/r^3$ falloff of shielding charge, where k is the wave number at the Fermi surface. This work corroborates recent results of Rowland by an independent method.

*Now at Bell Telephone Laboratories, Whippany, New Jersey.

†Now at McMaster University, Hamilton, Ontario, Canada.

EXCITONS AND PLASMONS IN SUPERCONDUCTORS. A. Bardasis and J. R. Schrieffer, University of Illinois, Urbana, Illinois (Received October 13, 1960).

The Anderson-Rickayzen equations of motion for a superconductor derived within the random phase approximation (RPA) are used to investigate the collective excitations of superconductors. A spherical harmonic expansion is made of the two-body interaction potential $V(\vec{k},\vec{k}')$, and a spectrum of excitations whose energies lie within the energy gap 2Δ is obtained. These excitations may be characterized by the quantum numbers L and M involved in the potential expansion. For an L-state exciton to exist, the L-wave part of the potential must be attractive at the Fermi surface. Odd-L excitons have unit spin and may be considered as spin waves. For s-state pairing

in the superconducting ground state, the plasmon mode corresponds to the $L=0$ exciton whose energy is strongly modified by the long-range Coulomb interaction. For a general potential several bound states may exist for given L and M. If the L-wave potential is stronger than the s-wave part of the potential, the system is unstable with respect to formation of L-state excitons. In this case, the ground state is formed with L-state pairing, special cases of which are the p-state pairing considered by Fisher and the d-state pairing proposed recently by several authors for the ground state of He^3 and nuclear matter. Corrections to the Anderson-Rickayzen equations are discussed which lead to a new set of exciton states if the L-wave potential is repulsive. These excitons are interpreted as bound electron-hole pairs, as opposed to the particle-particle excitons present with an attractive L-wave potential.

OPTICAL CONSTANTS OF SILVER. E. A. Taft and H. R. Philipp, General Electric Research Laboratory, Schenectady, New York (Received October 10, 1960).

The optical constants for electrolytically polished silver samples were determined from normal-incidence reflectance data in the spectral region 2 to 10 ev. The sharp minimum in the curve for k near 3.8 ev, which is associated with the onset of interband transitions, is deeper than in previous results. A second minimum is observed near 9.2 ev, which is approximately the calculated energy for simple free-electron plasma oscillations.

OPTICAL-MODEL ANALYSIS OF LOW-ENERGY ELECTRON-HYDROGEN SCATTERING. B. A. Lippmann and H. M. Schey, Lawrence Radiation Laboratory, University of California, Livermore, California (Received September 30, 1960).

The electron-hydrogen scattering problem is reduced to an equivalent one-body problem by the use of an optical-model potential. Two effects are examined quantitatively: the influence of the Pauli principle and the elastic scattering in the triplet state. For a long-range optical potential, the effect of the Pauli principle is small; however, for a short-range optical potential, the Pauli principle changes the zero-energy cross section by an order of magnitude.

The elastic scattering results, though in agreement with many previous calculations, are disappointing. It is argued that this is due to an inconsistent application of the optical model, and that a more consistent use of the optical model is equivalent to (and therefore provides a derivation for) the heuristic procedure, used by Martin, Seaton, and Wallace, which yields scattering lengths close to the Rosenberg, Spruch, and O'Malley bounds.

IONIZATION CROSS SECTIONS FOR PROTONS ON HYDROGEN GAS IN THE ENERGY RANGE 0.15 TO 1.10 Mev. J. W. Hooper, Engineering Experiment Station and School of Electrical Engineering, Georgia Institute of Technology, Atlanta, Georgia and E. W. McDaniel, D. W. Martin, and D. S. Harmer, Engineering Experiment Station and School of Physics, Georgia Institute of Technology, Atlanta, Georgia (Received September 23, 1960).

Measurements have been made of the ionization cross section for protons incident on hydrogen gas in the energy range 0.15 - 1.10 Mev. The experimental cross section in this region can be represented by $\sigma_i = (3.45 \pm 0.20)E^{-(0.870 \pm 0.005)} \times 10^{-17}$ cm^2/molecule, where E is the incident proton energy in Mev. The experimental results are in excellent agreement with a Born approximation calculation, which is discussed.

DETECTION OF DOUBLE RESONANCE BY FREQUENCY CHANGE: APPLICATION TO Hg^{201} Robert H. Kohler, Department of Physics and Research Laboratory of Electronics, Massachusetts Institute of Technology, Cambridge, Massachusetts (Received September 27, 1960).

A new type of double-resonance experiment that depends on wavelength effects rather than on polarization effects is discussed. Incident polarized light is replaced by incident light of wavelength coincident with just one component of the structure to be measured. The analyzer is replaced by a cell of gas that absorbs just that same component and lets the others pass. Magnetic resonance from the excited component to one of the others is monitored by increases in the light transmitted through the absorbing gas. This experiment requires that the Doppler width be smaller than the structure.

This method was first applied to measure the hyperfine structure of the $^3P_1$ state of Hg^{201}. The incident light and absorbing gas were both supplied by separated Hg^{198}, whose resonance line coincides naturally with one component of the Hg^{201} hyperfine structure. Measurement of Hg^{201} is discussed in detail. These hfs intervals were found: $f(\frac{1}{2} \rightarrow \frac{3}{2}) = 7551.613 \pm 0.013$ Mc/sec, and $f(\frac{3}{2} \rightarrow \frac{5}{2}) = 13\,986.557 \pm 0.008$ Mc/sec. The magnetic dipole and electric dipole interaction constants, calculated without quadratic hfs corrections, are $a = -5454.569 \pm 0.003$ Mc/sec, and $b = -280.107 \pm 0.005$ Mc/sec.

Means for applying the method when there is no isotope coincidence are given. This new method is compared with the polarization technique and is found to give signal-to-noise ratios that are orders of magnitude higher.

MICROWAVE SPECTRUM OF CHLORINE DIOXIDE. I. ROTATIONAL ASSIGNMENT. R. F. Curl, Jr., and James L. Kinsey,* Department of Chemistry, Rice University, Houston, Texas, John G. Baker,† Department of Physical Chemistry, Cambridge University, Cambridge, England, James C. Baird,‡ George R. Bird,‖ and Robert F. Heidelberg, Department of Chemistry, Rice University, Houston, Texas, and T. M. Sugden, D. R. Jenkins, and C. N. Kenney, Department of Physical Chemistry, Cambridge University, Cambridge, England (Received October 13, 1960).

The microwave spectrum of chlorine dioxide has been investigated and several rotational transitions assigned. The resulting rotational constants (in Mc/sec) are:

$Cl^{35}O_2$: $A = 52\,072$, $B = 9952$, $C = 8332$;

$Cl^{37}O_2$: $A = 50\,725$, $B = 9952$, $C = 8295$.

These constants are limited in precision by the presence of hyperfine structure which has been only approximately treated. The structural parameters of chlorine dioxide as obtained from the rotational constants are $r_{Cl\text{-}O} = 1.473 \pm 0.01$ A; $\angle O\text{-}Cl\text{-}O = 117° 36' \pm 1°$. Approximate hyperfine constants are given.

*Present address: Department of Chemistry, University of California, Berkeley, California.

†Present address: Bristol University, Bristol, England.

‡Present address: California Research Corporation, Richmond, California.

‖Present address: Polaroid Corporation, Cambridge, Massachusetts.

α^3 CORRECTIONS TO HYPERFINE STRUCTURE IN HYDROGENIC ATOMS. Daniel E. Zwanziger,* Columbia University, New York, New York (Received August 26, 1960).

The α^3 term in the ratio of the hyperfine splitting in the $2S$ state of the one-electron atom to the hyperfine splitting in the $1S$ state is recalculated, and a new theoretical value for this ratio is obtained which is in agreement with the experimental value, thereby eliminating a previously reported discrepancy. The calculation consists in the evaluation of the low-momentum parts, of order α^3hfs, of the expression for the lowest order radiative level shift in the bound interaction representation with external Coulomb and magnetic dipole fields. By rearranging the terms so as to display the gauge invariance of the matrix elements with respect to the external potentials, considerable simplicity is achieved, and the formulas are easily interpreted as a generalization of the expression for the lowest order Lamb shift. The contribution from soft photon intermediate states is obtained by an extension of the method developed by Schwartz and Tiemann for evaluating the Bethe logarithm, and an Appendix contains a tabulation of twelve analogous integrals which were integrated numerically, and which may be of use elsewhere. The calculated value of the ratio is $\frac{1}{8}(1.000\,034\,5 \pm 0.000\,000\,2)$ which agrees with the experimental values for hydrogen: $\frac{1}{8}(1.000\,034\,6 \pm 0.000\,000\,3)$, and deuterium: $\frac{1}{8}(1.000\,034\,2 \pm 0.000\,000\,6)$.

*Now at the University of California, Berkeley, California.

LOW-ENERGY PROTONS PRODUCED IN THE DEUTERON BOMBARDMENT OF NUCLEI. E. W. Hamburger,* B. L. Cohen, and R. E. Price, University of Pittsburgh, Pittsburgh, Pennsylvania (Received July 5, 1960).

When nuclei are bombarded by fast deuterons a continuous spectrum of protons is observed at energies corresponding to $Q < -2.2$ Mev. The shape and angular distribution of this continuum were studied for several targets, from Li to Au, with 14.8-Mev deuterons. The angular distributions are strongly peaked at or close to 0° for light elements; for heavy elements the peak broadens and moves to ~50°. The energy spectrum shows a peak which, with increasing angle, moves to lower energies for light elements, and moves

to higher energies for heavy elements. All features of the results are explained using a semiclassical theory in which the deuteron is broken up in the external field of the nucleus. The breakup occurs at or near the nuclear surface for light elements, but quite far out from it in heavy elements. Observed cross sections are far larger than theoretical predictions for either Coulomb or nuclear breakup.

*Now at Departamento de Fisica, Faculdade de Filosofia, Ciencias e Letras, Universidade de Sao Paulo, Sao Paulo, Brazil.

NEUTRON-NEUTRON SCATTERING LENGTH. Kirk W. McVoy,* Lawrence Radiation Laboratory, University of California, Livermore, California, and Brandeis University, Waltham, Massachusetts (Received August 29, 1960).

The final-state interaction of the two neutrons from the reaction $\pi^- + d \rightarrow 2n + \gamma$ has a pronounced and distinctive effect on the momentum spectrum of the outgoing particles. In particular, the neutron spectrum is sharply peaked in the neighborhood of 2 Mev, with a shape that is quite sensitive to the strength of the *nn* interaction. In the region of this peak, the relative neutron-neutron momentum is so small that the *nn* interaction is completely characterized by its scattering length. Hence it is proposed that a measurement of the shape of the neutron spectrum from this reaction may provide a convenient means of measuring the neutron-neutron scattering length. Neutron spectra are calculated in an impulse approximation, for several assumed values of the scattering length. It appears from their shapes that, in this way, present neutron-detection techniques should be capable of determining the scattering length to within 25%.

*Present address: Brandeis University, Waltham, Massachusetts.

NEW APPLICATION OF DELAYED COINCIDENCE TECHNIQUES FOR MEASURING LIFETIMES OF EXCITED NUCLEAR STATES: Ca^{42} AND Sc^{47}. P. C. Simms, N. Benczer-Koller,* and C. S. Wu, Columbia University, New York, New York (Received October 11, 1960).

A new application of the delayed coincidence technique for measuring short nuclear lifetimes has been developed which is basically similar to the well-known prompt comparison method. Systematic errors can be reduced and greater accuracy obtained for nuclei which exhibit both a prompt and a delayed event. A transistorized time-to-amplitude converter was used. The mean life of the second excited state of Ca^{42}[$(4.8 \pm 0.3) \times 10^{-10}$ sec] and the first excited state of Sc^{47}($< 5 \times 10^{-12}$ sec) were measured. Also the mean life of the first excited state of Hg^{198} [$(3.5 \pm 0.5) \times 10^{-11}$ sec] was determined by the usual self-comparison method.

*Present address: Department of Physics, Rutgers University, New Brunswick, New Jersey.

LONGITUDINAL POLARIZATION OF O^{14} POSITRONS. J. C. Hopkins,* J. B. Gerhart, F. H. Schmidt, and J. E. Stroth,† Department of Physics, University of Washington, Seattle, Washington (Received October 3, 1960).

The longitudinal polarization of positrons from the pure Fermi transition of O^{14} has been studied by the method of Bhabha scattering. A prismatic beta-ray spectrometer selected 1.0-Mev positrons which then were focussed by a solenoidal magnetic lens on a Supermendur foil magnetized by the lens. Scattered positrons and recoil electrons were detected in fast coincidence. The scattering asymmetry observed upon reversal of the lens magnetic field was $(4.16 \pm 0.80)\%$ which corresponds to positron longitudinal polarization $+(0.97 \pm 0.19)v/c$.

*Now at Los Alamos Scientific Laboratory, Los Alamos, New Mexico.

†Now at San Jose State College, San Jose, California.

ASYMMETRIC FISSION OF BISMUTH. T. T. Sugihara and J. Roesmer,* Jeppson Laboratory of Chemistry, Clark University, Worcester, Massachusetts, and J. W. Meadows, Jr.,† Cyclotron Laboratory, Harvard University, Cambridge, Massachusetts (Received August 24, 1960; revised manuscript received November 7, 1960).

An asymmetric mode of mass division in the mass region 66-73 has been observed in the fission of Bi^{209} with 36-Mev protons. About 0.3% of the fissions contribute to this mode. At 58 Mev no evidence for asymmetric fission (< 0.05% of total fissions) as a separate mode could be found. The fission cross sections at 36 and 58 Mev are 1.9 and 11.3 mb, respectively. The narrowness of the 36-Mev asymmetric peak leads to the sug-

gestion that the asymmetric fission of bismuth results from the fission of a single nuclear species and from a closed-shell effect, similar to the fine structure observed in low-energy fission of heavy elements. This asymmetric fission is considered to occur from states of relatively high excitation energy. However, the possibility of asymmetric fission also occurring from states of low excitation energy, whether following neutron evaporation or as a consequence of an inelastic proton interaction, cannot be ruled out. The symmetric fission observed with both 36- and 58-Mev protons is consistent with the results obtained by Fairhall in the fission of bismuth with 22-Mev deuterons.

*Present address: Nuclear Science and Engineering Corporation, Pittsburgh, Pennsylvania.

†Present address: Argonne National Laboratory, Argonne, Illinois.

NEUTRON TRANSFER TO EXCITED STATES IN N^{15} IN THE REACTION $N^{14}(N^{14}, N^{13})N^{15}$. Kenneth S. Toth, Oak Ridge National Laboratory, Oak Ridge, Tennessee (Received September 9, 1960).

The neutron-transfer reaction, $N^{14}(N^{14}, N^{13})N^{15}$, was investigated from 6° to 60° c.m. with 28-Mev N^{14} ions accelerated in the Oak Ridge 63-inch cyclotron. Circular strips of aluminum foil, each encompassing a known angular increment, were used to stop the radioactive N^{13} (10-min). Excited states in N^{13} are unstable with respect to proton emission; the first excited state in N^{15} is 5.28 Mev above ground. Therefore, N^{13} nuclei resulting from transfers to the ground state of N^{15} are at least 5 Mev more energetic than those resulting from transfers to N^{15} excited states. The two groups of N^{13} particles were distinguished by placing suitable absorbers in front of the aluminum catcher foils. It was found that transfers to excited states become more abundant relative to ground-state transfers as the incident N^{14} energy is lowered.

BETA-GAMMA DIRECTIONAL CORRELATIONS IN THE DECAY $Sb^{124} \rightarrow Te^{124}$. Helmut Paul,* Physics Department, Purdue University, Lafayette, Indiana (Received October 10, 1960).

We have measured the β-γ directional correlations involving the 1.6-Mev β group of Sb^{124} and the second excited 2^+ state (at 1325 kev) of Te^{124}. Both of the γ rays (0.72 and 1.32 Mev) de-exciting this state were used. For the 0.72-Mev γ ray, the results for the coefficient ϵ in $W(\theta) = 1 + \epsilon P_2(\cos\theta)$ are: $\epsilon = 0.20 \pm 0.02$, 0.18 ± 0.02, 0.19 ± 0.03, and 0.22 ± 0.06 for β energies of 1.02, 1.16, 1.30, and 1.44 ± 0.07 Mev, respectively. For the 1.32-Mev γ ray, we find $\epsilon = -0.28 \pm 0.08$ for a β-energy range of 1.0-1.6 Mev. From these results, the mixing ratio for the 0.72-Mev γ ray is $\delta = +0.8^{+0.7}_{-0.2}$. It is shown that the 1.6-Mev β transition must be due, at least partly, to the B_{ij} matrix element. Assuming $u = x = 0$ (in Kotani's notation), our data can be fitted by either $Y/z = 0.04$ (i.e., an essentially unique transition), or $Y/z = 1.2$.

*Present address: Studiengesellschaft für Atomenergie, Lenaugasse 10, Wien VIII, Austria.

LIQUID-DROP NUCLEAR MODEL WITH HIGH ANGULAR MOMENTUM. Robert Beringer and W. J. Knox, Department of Physics, Yale University, New Haven, Connecticut (Received October 10, 1960).

The equilibrium shapes of rotating liquid drops are calculated in the spheroidal approximation. The solutions are prolate forms for high angular momenta such as are produced in compound nuclei resulting from heavy-ion bombardments. This is thought to account for the angular and energy distributions observed in heavy-ion-induced fission and light-particle evaporation.

MEASUREMENT AND INTERPRETATION OF NEUTRON TOTAL CROSS SECTIONS OF CARBON, CALCIUM, AND LEAD. R. M. Wilenzick, G. E. Mitchell,* K. K. Seth, and H. W. Lewis, Duke University, Durham, North Carolina (Received August 29, 1960).

The neutron total cross sections of carbon, calcium, and lead have been determined in the energy region 200-960 kev using a time-of-flight technique. The observed cross section for carbon has been analyzed in terms of the effective-range theory as well as the bound-level contribution with results which agree very well with those obtained by the (d,p) stripping experiments. Also it is concluded that the upper limit for the total width of the "proposed" resonance at 610 kev is 100 ev. For calcium and lead the

data are analyzed for resonance parameters. It is found that the s-wave strength function for Ca^{40} increases rapidly with increasing energy. It is concluded also that the course of the Pb cross sections can be explained only by the presence of a broad ($\theta_\lambda^2 = 0.05$) s-wave resonance in Pb^{208}, at $E_n = 515 \pm 15$ kev with resonance width $\Gamma_n = 100 \pm 15$ kev.

*Now at Florida State University, Tallahassee, Florida.

MEASUREMENT OF DEUTERON POLARIZATION PRODUCED BY d-α SCATTERING AT 1.07 Mev. Lee G. Pondrom* and J. W. Daughtry, Aeronautical Research Laboratories, Wright-Patterson Air Force Base, Ohio (Received October 13, 1960; revised manuscript received November 10, 1960).

Elastic scattering from He^4 gas in the energy region of the 1.07-Mev resonance has been used to polarize deuterons. After scattering through 30° in the laboratory by the polarizer, the polarization of the deuteron beam has been analyzed by the reaction $He^3(d,p)He^4$ near 400 kev. This was accomplished by observing protons at 0° and 90°, and measuring the dependence of the counting rate ratio on the deuteron polarization. $He^3(d,p)He^4$ is well described in this energy region by a single-level Breit-Wigner formula, and therefore has a predictable sensitivity to deuteron polarization. The experimental results are consistent with the magnitude of the polarization component $\langle T_{20} \rangle$ calculated from the d-α phase-shift analysis.

*Now at Physics Department, Columbia University, New York, New York.

ANALYSIS OF K-MESON PRODUCTION BY $\bar{p}$ ANNIHILATION. T. F. Hoang,* Lawrence Radiation Laboratory, University of California, Berkeley, California (Received August 22, 1960; revised manuscript received November 17, 1960).

The production of K and π mesons in $\bar{p}$-p annihilations is compared for antiprotons of 1-Bev/c momentum and antiprotons at 480-Mev kinetic energy. By modifying the Fermi model by assuming a π-π resonant state with a mass slightly greater than two pion masses, good agreement with the results is obtained and the interaction volume Ω_π is no longer too large. An isobaric state with a mass greater than or equal to three pion masses is ruled out.

*Now at Laboratoire de Physique, Ecole Polytechnique, Paris, France.

ANTIPROTON ANNIHILATIONS IN PROPANE. Sulamith Goldhaber, Gerson Goldhaber, Wilson M. Powell, and Rein Silberberg, Lawrence Radiation Laboratory and Department of Physics, University of California, Berkeley, California (Received September 1, 1960).

An experiment to study the $\bar{p}$ annihilation process at 1.05 Bev/c was performed with the Lawrence Radiation Laboratory 30-in. propane bubble chamber. It was observed that the K-meson production in annihilation events rises sharply with the increase in energy, namely from $(4 \pm 1)\%$ for annihilations at or near "rest" to $(8 \pm 1)\%$. On the other hand, the pion multiplicity was not observed to increase appreciably with the increase of available energy. We have found a pion multiplicity of 5.0 ± 0.2. These numbers are discussed in this paper and compared with existing models for the $\bar{p}$ annihilation process. It is pointed out that with further increase in bombarding energy, different models may differ appreciably in the above quantities.

We have observed a $\bar{p}$-H annihilation cross section of 51 ± 10 mb and a $\bar{p}$-C annihilation cross section of 368 ± 60 mb at 1.05 Bev/c $\bar{p}$ momentum. Crude determinations of the $\bar{p}$ charge-exchange process—which turns out to be forward peaked—and of $\bar{p}$ inelastic-scattering events leading to pion production are also discussed.

HEAVY NUCLEI IN THE PRIMARY COSMIC RADIATION AT PRINCE ALBERT, CANADA. II. H. Aizu,* Y. Fujimoto, S. Hasegawa, M. Koshiba,† I. Mito,‡ J. Nishimura, and K. Yokoi,‡ Institute for Nuclear Study, University of Tokyo, Tanashi, Tokyo, Japan, and Marcel Schein,‖ Department of Physics, Enrico Fermi Institute for Nuclear Studies, University of Chicago, Chicago, Illinois (Received August 19, 1960; revised manuscript received November 4, 1960).

The investigation of the low-energy primary cosmic radiation has been extended to include the heavier elements of $Z \geq 9$; the light elements Li, Be, and B; and α particles. The results of a previous paper on carbon, nitrogen, and oxy-

gen have also been confirmed with better statistics. The energy spectra of all these components show a general similarity in shape. A possible deviation of the light-element spectrum from this similarity is discussed. The abundances of various elements in the low-energy region of 200 to 700 Mev per nucleon are essentially the same as observed in the higher energy region.

*Department of Physics, Rikkyo University, Tokyo, Japan; now at Department of Physics, Northwestern University, Evanston, Illinois.

†Now at Department of Physics, University of Chicago, Chicago, Illinois, on leave of absence from University of Tokyo, Tokyo, Japan.

‡College of General Education, University of Tokyo, Komaba, Tokyo, Japan.

‖Deceased.

DEMONSTRATION OF QUANTUM MECHANICS IN THE LARGE. T. B. Day, University of Maryland, College Park, Maryland (Received September 22, 1960).

An example is given which demonstrates in a straightforward and dramatic manner that when two particles like $(K^0+\overline{K}^0)$ or (2γ) are created simultaneously, the probabilities involved in observing any further events related to their simultaneous creation must be calculated quantum-mechanically and are correlated, even for macroscopic distances in absorbing media. In particular, a correlation in the polarizations of the two γ rays from positronium annihilation as a function of the thickness of magnetized iron through which they are passed is pointed out by way of a proposed experiment.

SHELL-MODEL CALCULATIONS OF THE HYPERFINE EFFECT IN μ-MESON CAPTURE. H. Überall,* Carnegie Institute of Technology, Pittsburgh, Pennsylvania (Received October 14, 1960).

Numerical values for the difference in μ-meson capture rates from the two hyperfine states of a mesonic atom are obtained for F^{19}, Al^{27}, and P^{31}, employing the simple Mayer-Jensen version of the shell model for Al^{27} and P^{31}, and a more accurate version for F^{19}. In all these cases, we get considerably larger values than those found in previous estimates, thus rendering experiments more feasible. In view of the consequences of atomic conversion on the observation of the capture rate differences, conversion effects in the rate and asymmetry of μ-meson decay electrons are discussed also.

*Present address: Harrison M. Randall Laboratory of Physics, University of Michigan, Ann Arbor, Michigan.

MODEL OF HYPERON DECAY. L. Wolfenstein, Carnegie Institute of Technology, Pittsburgh, Pennsylvania (Received October 7, 1960).

The vanishing of the asymmetries in the decays $\Sigma^- \to n+\pi^-$ and $\Sigma^+ \to n+\pi^+$ are explained in a model in which all Σ decays occur via virtual K-meson decays. The model then predicts a Λ-decay asymmetry of similar magnitude but opposite sign to that of $\Sigma^+ \to p+\pi^0$. Certain other predictions of this model are discussed.

INELASTIC SCATTERING OF A Σ^- HYPERON WITH AN EMULSION NUCLEUS. H. E. Fisk and D. J. Prowse, Physics Department, University of California, Los Angeles, California (Received October 3, 1960).

During a systematic study of fast hyperons resulting from the nuclear capture of K^- mesons, an event has been found which is interpreted as the elastic scattering of a Σ^- hyperon by a bound neutron. The reaction kinematics are insufficient to determine the nature of the nuclear potential for Σ^- hyperons but it appears that when about 10 of these events have been found and analyzed, it will be possible to infer the sign of the potential from the general effect it will have on the observable kinematics of the events.

MOMENTUM SPECTRUM OF MUONS. W. Pak,* S. Ozaki,† B. P. Roe,‡ and K. Greisen, Laboratory of Nuclear Studies, Cornell University, Ithaca, New York (Received October 12, 1960).

The momentum spectrum has been measured with a magnetic spectrometer for cosmic-ray particles incident vertically and at 68° zenith angle, in the range 2 to 70 Bev/c. The apparatus discriminates strongly against all particles but muons. The vertical muon spectrum is found to be in good agreement with the results reported by Pine et al. and by Ashton et al. No comparable data at 68° have been published. Assuming

muon creation to occur entirely through pion decay, a single-pion production spectrum accounts for the muon spectra at both zenith angles. The muon positive excess at energies of 8 to 50 Bev has also been obtained. The results, while in general agreement with those of other workers, confirm the expected tendency for the positive excess to decrease with energy.

*Now at Stevens Institute of Technology, Hoboken, New Jersey.

†Now at Osaka City University, Osaka, Japan.

‡Now at University of Michigan, Ann Arbor, Michigan.

NEUTRAL LEPTON CURRENTS AND NEUTRINO DETECTION. R. W. King, Physics Department, Purdue University, Lafayette, Indiana (Received October 6, 1960).

The interactions of neutrinos with complex nuclei are explored assuming the existence of a neutral lepton current.

ELASTIC SCATTERING OF 146-Mev POLARIZED PROTONS BY DEUTERONS. Herman Postma* and Richard Wilson, Cyclotron Laboratory, Harvard University, Cambridge, Massachusetts (Received October 7, 1960).

The polarization and differential cross section of 146-Mev protons elastically scattered by deuterons have been measured in the center-of-mass angular range from 3.9° to 170°. A description of the liquid deuterium target and detection apparatus which permitted the measurement of the elastic events over these angles is given. At small angles the proton was energy-analyzed; at large angles the recoil partner of the proton, the deuteron, was identified and energy-analyzed. Although the energy resolution of ±1.7 Mev and the angular resolution of ±2.0° were sufficient to separate quasi-elastic events from elastic events at most angles, they were insufficient to resolve unambiguously the 2.3-Mev inelastic events resulting from the formation of virtual deuterons. The measured cross section is in qualitative agreement with cross sections at neighboring energies; no comparison of measured polarizations is possible due to the lack of other experiments. The cross sections and polarization for angles less than 80° c.m. are well fitted by the Kerman, McManus, and Thaler theory using the Gammel and Thaler nucleon-nucleon potential description. The energy and angular dependence of the large-angle pickup cross section proposed by Chew and Goldberger agree well with experiment; however, the small measured positive polarization is not predicted by this theory, and probably indicates destructive interference between the direct and the pickup scattering.

*Now at Oak Ridge National Laboratory, Oak Ridge, Tennessee.

SYMMETRY OF THE ND^{-1} SOLUTIONS FOR COUPLED SCATTERING AMPLITUDES. J. D. Bjorken, Institute of Theoretical Physics, Stanford University, Stanford, California and M. Nauenberg, Institute for Advanced Study, Princeton, New Jersey (Received October 11, 1960).

A proof is given that the ND^{-1} matrix solutions for coupled scattering amplitudes are symmetric if the discontinuity of the scattering matrix across the unphysical cut is symmetric.

AUTHOR INDEX TO VOLUME 5

References with (E) are to Errata

ABASHIAN, ALEXANDER, NORMAN E. BOOTH, and KENNETH M. CROWE. Possible anomaly in meson production in $p+d$ collisions 258

ALLEN, T. K., GEORGE A. PAULIKAS, and ROBERT V. PYLE. Instability of a positive column in a magnetic field 409

ALSTON, MARGARET, LUIS W. ALVAREZ, PHILIPPE EBERHARD, MYRON L. GOOD, WILLIAM GRAZIANO, HAROLD K. TICHO, and STANLEY G. WOJCICKI. Resonance in the $\Lambda\pi$ system 520

ALVAREZ, LUIS W. (see Alston, Margaret) 520

AMATI, D., B. VITALE, and A. STANGHELLINI. Some considerations on the recently found evidence for a $\pi\Lambda$ resonance 524

AMELINCKX, S. and P. DELAVIGNETTE. Dislocation loops due to quenched-in point defects in graphite 50

ANDERSON, A. C., H. R. HART, JR., and J. C. WHEATLEY. Self-diffusion coefficient and nuclear susceptibility of liquid He^3 133

ANDERSON, P. W. and P. MOREL. Generalized Bardeen-Cooper-Schrieffer states and aligned orbital angular momentum in the proposed low-temperature phase of liquid He^3 136; 282(E)

ANTONČÍK, EMIL (see Tauc, Jan) 253

ASCARELLI, GIANNI. Interaction of high-energy phonons in germanium 367

ASHMORE, A., G. COCCONI, A. N. DIDDENS, and A. M. WETHERELL. Total cross sections of protons with momentum between 10 and 28 Gev/c 576

AYER, F. (see Pickup, E.) 161

BALL, JAMES S. Effect of the pion-pion resonance on the negative-positive ratio 73

BARDIN, R. K., C. A. BARNES, W. A. FOWLER, and P. A. SEEGER. ft value of O^{14} and the universal Fermi interaction 323

BARNES, C. A. (see Bardin, R. K.) 323

——— (see Nordberg, M. E.) 321

BARTON, J. C. Resonant scattering of antineutrinos 514

BAUMGARTNER, E., L. BROWN, P. HUBER, H. RUDIN, and H. R. STRIEBEL. Source of polarized deuterons and the verification of alignment with the $T(d,n)He^4$ reaction 154

BEARD, DAVID B. Interaction of the solar plasma with the earth's magnetic field 89

BEHRENDS, R. E. and A. SIRLIN. Possible existence of $\Delta Q = -\Delta S$ decays 476

BENCZER-KOLLER, N. (see Wu, C. S.) 432

BERNSTEIN, JEREMY and STEVEN WEINBERG. Partially conserved currents and the K' meson 481

BERNSTEIN, RICHARD B. (see Hostettler, Hans U.) 318

BERTRAM, W. J., JR., R. A. REITER, T. A. ROMANOWSKI, and R. B. SUTTON. Observation of the "isotope effect" in the nuclear capture of negative muons by chlorine 61

BIALYNICKI-BIRULA, IVO. New approach to perturbation theory in quantum electrodynamics 584

BIERSTEDT, P. E. (see Kepler, R. G.) 503

BIRGE, ROBERT W. and WILLIAM B. FOWLER. Proton helicity from Λ decay 254

BISI, A., G. FAINI, E. GATTI, and L. ZAPPA. Positron lifetime in metals 59

BLACKIE, R. F., A. ENGLER, and J. H. MULVEY. Estimate of the neutral π-meson lifetime 384

BLOOM, STEWART D., LLOYD G. MANN, and JOHN A. MISKEL. Isotopic spin conservation and beta-gamma circular polarization correlation in A^{41} and Sc^{46} 326

BLUM, H. (see Holton, W. C.) 197

BLUMBERG, W. E., J. EISINGER, V. JACCARINO, and B. T. MATTHIAS. Correlations between superconductivity and nuclear magnetic resonance properties 149

———, J. EISINGER, V. JACCARINO, and B. T. MATTHIAS. Nuclear magnetic resonance in scandium and lanthanum metal 52

BOLEF, D. I. (see Ruby, S. L.) 5

BOLLHAGEN, HEINS (see Carr, Thomas D.) 418

BOND, W. (see Collins, R. J.) 303

BOORSE, H. A., A. T. HIRSHFELD, and H. LEUPOLD. Difference in lattice specific heats in the normal and super-

conducting phases 246
BOOTH, NORMAN E. (see Abashian, Alexander) 258
BOUCHIAT, M. A., T. R. CARVER, and C. M. VARNUM. Nuclear polarization in He^3 gas induced by optical pumping and dipolar exchange 373
BOWCOCK, J., W. N. COTTINGHAM, and D. LURIÉ. π-π scattering, nucleon structure, and π-N scattering 386
BOYLE, A. J. F., D. ST. P. BUNBURY, and C. EDWARDS. Polarization of the conduction electrons in the ferromagnetic metals 553
BOZORTH, R. M., A. J. WILLIAMS, and D. D. DAVIS. Critical field for superconductivity in niobium-tin 148
BREIT, G., M. H. HULL, JR., K. LASSILA, and H. M. RUPPEL. Form of the one-pion exchange potential 274
BROUT, R. Collective oscillations and giant density fluctuations 193
BROWN, L. (see Baumgartner, E.) 154
BROWN, L. M. and F. CALOGERO. Effects of pion-pion interaction in electromagnetic processes 116(E)
BROWN, R. N., J. G. MAVROIDES, M. S. DRESSELHAUS, and B. LAX. Interband magnetoreflection in bismuth. II. Low fields 243
BROWN, R. W., P. WESSEL, and E. P. TROUNSON. Plasmon reradiation from silver films 472
BRYAN, R. A. (see Saylor, D. P.) 266
BUCHSBAUM, S. J. Ion resonance in a multicomponent plasma 495
BUMILLER, F., M. CROISSIAUX, and R. HOFSTADTER. Electron scattering from the proton 261
—— (see Hofstadter, R.) 263
BUNBURY, D. ST. P. (see Boyle, A. J. F.) 553
BURKHARDT, H. (see Gomez, R.) 170
BUTTERWORTH, J. Nuclear spin-lattice relaxation in vanadium metal 305

CABIBBO, N. and R. GATTO. Consistency of the $K^+ - \pi^+ + \pi^0 + \gamma$ rate with the $\Delta T = \frac{1}{2}$ rule 382
—— and R. GATTO. Symmetry between muon and electron 114
CALAWA, A. R., R. H. REDIKER, B. LAX, and A. L. McWHORTER. Magneto-tunneling in InSb 55
CALOGERO, F. (see Brown, L. M.) 116(E)
CARR, THOMAS D., ALEX G. SMITH, and HEINS BOLLHAGEN. Evidence for the solar corpuscular origin of the decameter-wavelength radiation from Jupiter 418
CARVER, T. R. (see Bouchiat, M. A.) 373
CASELLA, R. C. Toroidal energy surfaces in crystals with wurtzite symmetry 371
CHAMBERS, R. G. Shift of an electron interference pattern by enclosed magnetic flux 3
CHAUDHURY, MANUJENDRA LAL. Non-local potential and alpha-decay barrier penetrability 205
CHESTER, MARVIN. Evidence for a configurational emf in a conducting medium 91
CHEW, G. F. and S. C. FRAUTSCHI. Unified approach to high- and low-energy strong interactions on the basis of the Mandelstam representation 580
CHIDLEY, B. G. (see Reiter, R. A.) 22
CHILDS, CHARLES B. and LAWRENCE SLIFKIN. Room-temperature dislocation decoration inside large crystals 502
CHIU, HONG-YEE and P. MORRISON. Neutrino emission from black-body radiation at high stellar temperatures 573
CHYNOWETH, A. G., R. A. LOGAN, and P. A. WOLFF. Effect of Landau levels upon tunnel currents in indium antimonide 548
——, G. H. WANNIER, R. A. LOGAN, and D. E. THOMAS. Observation of Stark splitting of energy bands by means of tunnelling transitions 57
CLARK, K. C. (see Young, Robert A.) 320
CLASS, C. M. (see Durham, F. E.) 202
CLOGSTON, A. M. (see Matthias, B. T.) 542
COCCONI, G. (see Ashmore, A.) 576
COCCONI, V. T., T. FAZZINI, G. FIDECARO, M. LEGROS, N. H. LIPMAN, and A. W. MERRISON. Precise measurements of the mean lives of μ^+ and μ^- mesons in carbon 19
COCHRAN, D. R. F. (see Dash, J. G.) 152
—— (see Nagle, D. C.) 364
COENSGEN, F. H., W. F. CUMMINS, W. E. NEXSEN, JR., and A. E. SHERMAN. Evidence of containment of a 3-kev deuterium plasma 459
COHEN, B. L. (see Mead, J. B.) 105
COHEN, MORREL H. and L. M. FALICOV. Effect of spin-orbit splitting on the Fermi surfaces of the hexagonal-close-packed

metals 544
COLEMAN, P. J., JR., LEVERETT DAVIS, and C. P. SONETT. Steady component of the interplanetary magnetic field: Pioneer V 43
COLGATE, STIRLING A. and MONTGOMERY H. JOHNSON. Hydrodynamic origin of cosmic rays 235
COLLINS, R. J., D. F. NELSON, A. L. SCHAWLOW, W. BOND, C. G. B. GARRETT, and W. KAISER. Coherence, narrowing, directionality, and relaxation oscillations in the light emission from ruby 303
COOK, L. F., JR. and JAN TARSKI. Investigation of the five-pion function 585
CORENZWIT, E. (see Matthias, B. T.)
COTTINGHAM, W. N. (see Bowcock, J.) 542
COURANT, H. (see Smith, G. A.) 386
CRAIG, P. P. (see Dash, J. G.) 571
CRAWFORD, J. H., JR. and C. M. NELSON. Defect interactions in irradiated calcium-doped potassium chloride 314
CROISSIAUX, M. (see Bumiller, F.) 261
——— (see Hofstadter, R.) 263
CROWE, KENNETH M. (see Abashian, Alexander) 258
CUMMINS, W. F. (see Coensgen, F. H.) 459

DASH, J. G., R. D. TAYLOR, P. P. CRAIG, D. E. NAGLE, D. R. F. COCHRAN, and W. E. KELLER. Mössbauer effect in Fe^{57} at very low temperatures 152
DAVIS, D. D. (see Bozorth, R. M.) 148
DAVIS, LEVERETT (see Coleman, P. J., Jr.) 43
DAY, T. B. and G. A. SNOW. Capture of K^- mesons from high S orbitals in helium 112
DAYBELL, M. (see Gomez, R.) 170
DELAVIGNETTE, P. (see Amelinckx, S.) 50
DEPATIE, DAVID (see Reppy, John D.) 541
DERR, V. E., J. J. GALLAGHER, R. E. JOHNSON, and A. P. SHEPPARD. Microwave emission from an optically pumped atomic system 316
DERRICK, M. (see Fields, T. H.) 69
DEVONS, S., G. GIDAL, L. M. LEDERMAN, and G. SHAPIRO. Muon mass and charge by critical absorption of mesonic x rays 330
DeWIRE, J. W. (see Feldman, M.) 435
DIDDENS, A. N. (see Ashmore, A.) 576
DIEBOLD, R. E. (see Kilner, J. R.) 518
DRELL, S. D. Pion parameters from high-energy inelastic interactions 342
——— Production of particle beams at very high energies 278
——— and F. ZACHARIASEN. Observation of π-π resonance in pion production 66
DRESSELHAUS, M. S. (see Brown, R. N.) 243
DURHAM, F. E., D. H. RESTER, and C. M. CLASS. Electric-monopole-enhanced $2^{+\prime} \rightarrow 2^+$ transitions in Th^{232} and U^{238} 202

EBERHARD, PHILIPPE (see Alston, Margaret) 520
EDEN, RICHARD J. Proof of the Mandelstam representation in perturbation theory 213
EDWARDS, C. (see Boyle, A. J. F.) 553
EISINGER, J. (see Blumberg, W. E.) 52
——— (see Blumberg, W. E.) 149
ELLIOTT, R. J., B. R. HEAP, D. J. MORGAN, and G. S. RUSHBROOKE. Equivalence of the critical concentrations in the Ising and Heisenberg models of ferromagnetism 366
ENGLER, A. (see Blackie, R. F.) 384
ENGLERT, F. Theory of a Heisenberg ferromagnet in the random phase approximation 102
ERICSON, TORLEIF. Fluctuations of nuclear cross sections in the "continuum" region 430
ERIKSSON, K. E. and A. PETERMAN. High-energy behavior of cross sections in quantum electrodynamics 444
ERNST, FREDERICK, J. Reaction $\mu + N \rightarrow e + N'$: Intermediate Boson theory 478

FAINI, G. (see Bisi, A.) 59
FAIRBANK, HENRY A. (see Walker, E. J.) 139
FALICOV, L. M. (see Cohen, Morrel H.) 544
FAN, C. Y., PETER MEYER, and J. A. SIMPSON. Experiments on the eleven-year changes of cosmic-ray intensity using a space probe 272
———, PETER MEYER, and J. A. SIMPSON. Rapid reduction of cosmic-radiation intensity measured in interplanetary space 269
FAN, H. Y. (see Fisher, P.) 195
FAZZINI, T. (see Cocconi, V. T.) 19
FEHER, G., J. C. HENSEL, and E. A. GERE. Paramagnetic resonance absorption from acceptors in silicon 309
———, R. PREPOST, and A. M. SACHS. Muonium formation in semiconductors 515

——— (see Hensel, J. C.) 307
FELDMAN, M., V. HIGHLAND, J. W. DeWIRE, and R. M. LITTAUER. Double pion photoproduction 435
FETKOVICH, J. G. (see Fields, T. H.) 69
FIDECARO, G. (see Cocconi, V. T.) 19
FIELDS, T. H., G. B. YODH, M. DERRICK, and J. G. FETKOVICH. Cascade time of π^- in liquid hydrogen 69
FINGER, G. (see Reik, H. G.) 423
FISHER, P. and H. Y. FAN. Absorption spectra and Zeeman effect of copper and zinc impurities in germanium 195
FOWLER, E. (see Smith, G. A.) 571
FOWLER, W. A. (see Bardin, R. K.) 323
FOWLER, WILLIAM B. (see Birge, Robert W.) 254
FRANKL, D. R. (see Levinger, B.) 12
FRAUENFELDER, H. (see Nagle, D. E.) 364
FRAUTSCHI, S. C. Sensitivity of low-energy pion-nucleon scattering to a pion-pion resonance 159
——— (see Chew, G. F.) 580
FREEMAN, A. J. and R. E. WATSON. Contribution of the Fermi contact term to the magnetic field at the nucleus in ferromagnets 498
FRIEDLÄNDER, E. M. Pion cloud effects and the two-center model of cosmic-ray jets 212
FRISCH, D. H. (see von Dardel, G.) 333

GABRIEL, J. R. (see Powell, M. J. D.) 145
GALLAGHER, J. J. (see Derr, V. E.) 316
GARRETT, C. G. B. (see Collins, R. J.) 303
GATES, DUANE C. (see Swanson, William P.) 336
——— (see Swanson, William P.) 339
GATTI, E. (see Bisi, A.) 59
GATTO, R. (see Cabibbo, N.) 114
——— (see Cabibbo, N.) 382
GIAEVER, IVAR. Electron tunneling between two superconductors 464
——— Energy gap in superconductors measured by electron tunneling 147
GIBSON, GORDON, WILLIAM C. JORDAN, and EUGENE J. LAUER. Containment of positrons in a mirror machine 141
GIDAL, G. (see Devons, S.) 330
GLOVER, R. E., III and M. D. SHERRILL. Changes in superconducting critical temperature produced by electrostatic charging 248
GOLDENBERG, H. M., D. KLEPPNER, and N. F. RAMSEY. Atomic hydrogen maser 361
GOLDSTEIN, LOUIS. Thermal properties of solid He^4 104
GOMEZ, R., H. BURKHARDT, M. DAYBELL, H. RUDERMAN, M. SANDS, and R. TALMAN. Evidence against the existence of the B^0 meson 170
GOOD, MYRON L. (see Alston, Margaret) 520
GOODINGS, D. A. and V. HEINE. Contribution of exchange polarization of core electrons to the magnetic field at the nucleus of Fe 370
GOTOW, KAZUO and ERNST HEER. p-p phase shift solutions and depolarization scattering parameter at 210 Mev 111
GRAZIANO, WILLIAM (see Alston, Margaret) 520
GREEN, T. S. Evidence for the containment of a hot, dense plasma in a Theta pinch 297

HAGEDORN, R. Deuteron production in high-energy collisions 276
HALL, JOHN J. (see Koenig, Seymour H.) 550
HAM, F. S., G. W. LUDWIG, G. D. WATKINS, and H. H. WOODBURY. Spin Hamiltonian of Co^{2+} 468
HAND, L. N. Electron-proton scattering at 900 Mev and 135° 168
HART, H. R., JR. (see Anderson, A. C.) 133
HAVENS, W. W., JR. (see Rush, J. J.) 507
HEAP, B. R. (see Elliott, R. J.) 366
HEDGCOCK, F. T. Magnetic susceptibility of the two phases of lithium at low temperatures 420
HEER, ERNST (see Gotow, Kazuo) 111
HEINE, V. (see Goodings, D. A.) 370
HENSEL, J. C. and G. FEHER. Valence band parameters in silicon from cyclotron resonances in crystals subjected to uniaxial stress 307
——— (see Feher, G.) 309
HERLOFSON, N. Diffusion of particles in the earth's radiation belts 414
HESS, WILMOT N. and ARTHUR J. STARNES. Measurement of the neutron flux in space 48
HIGHLAND, V. (see Feldman, M.) 435
HILLMAN, PETER, H. TYREN, and TH. A. J. MARIS. Momentum distribution of protons in individual nuclear shells 107

HINTZ, NORTON M. (see Meyer, Verena) 207
HIRSHFELD, A. T. (see Boorse, H. A.) 246
HOFSTADTER, R., F. BUMILLER, and M. CROISSIAUX. Splitting of the proton form factors and diffraction in the proton 263
——— (see Bumiller, F.) 261
HOH, F. C. Plasma stability and boundary condition 75(E)
HOLTON, W. C., H. BLUM, and C. P. SLICHTER. Hyperfine structure of the *F* center in LiF 197
HONIG, A. and R. LEVITT. Shallow impurity traps and electron transfer dynamics in *n*-type silicon at liquid helium temperatures 93
HOPFIELD, J. J. (see Thomas, D. G.) 505
HOSTETTLER, HANS U. and RICHARD B. BERNSTEIN. Observation of quantum effects in the scattering of a monoenergetic Li beam by a crossed Hg beam 318
HUBER, P. (see Baumgartner, E.) 154
HUGHES, V. W., D. W. McCOLM, K. ZIOCK, and R. PREPOST. Formation of muonium and observation of its Larmor precession 63
HULL, M. H., JR. (see Breit, G.) 274

IKEGAMI, H. (see Takayama, K.) 238

JACCARINO, V., B. T. MATTHIAS, M. PETER, H. SUHL, and J. H. WERNICK. Magnitude and sign of the conduction electron polarization in rare-earth metals 251
———, M. PETER, and J. H. WERNICK. Nuclear magnetic resonance in α and β manganese 53
——— (see Blumberg, W. E.) 52
——— (see Blumberg, W. E.) 149
JACOB, GERHARD and TH. A. J. MARIS. Investigation of medium and heavy nuclei by quasi-free proton-proton scattering 210
JENKINS, THOMAS L. (see Swanson, William P.) 336
——— (see Swanson, William P.) 339
JOHNSON, MONTGOMERY H. (see Colgate, Stirling A.) 235
JOHNSON, R. E. (see Derr, V. E.) 316
JOHNSTON, D. F. (see Powell, M. J. D.) 145
JORDAN, WILLARD C. (see Gibson, Gordon) 141
JOSEPHSON, VERNAL. Instability mechanisms in transverse pinches 416

KAISER, W. (see Collins, R. J.) 303
KATZ, E. (see Read, P. L.) 466
KELLER, W. E. (see Dash, J. G.) 152
KENNEY, ROBERT W. (see Swanson, William P.) 336
——— (see Swanson, William P.) 339
KEPLER, R. G., P. E. BIERSTEDT, and R. E. MERRIFIELD. Electronic conduction and exchange interaction in a new class of conductive organic solids 503
KEYES, R. J. (see Lax, B.) 241
KEYES, ROBERT W. and PETER J. PRICE. Additional spin resonance spectrum in antimony-doped germanium 473
KILNER, J. R., R. E. DIEBOLD, and R. L. WALKER. Photoproduction of negative pions from hydrogen at forward angles 518
KING, JOHN G. Search for a small charge carried by molecules 562
KLEIN, MARTIN J. and RAYMOND D. MOUNTAIN. Thermal expansion coefficient of solid He^3 363
KLEPPNER, D. (see Goldenberg, H. M.) 361
KOENIG, SEYMOUR H. and JOHN J. HALL. Low-temperature transport in "split *p*-germanium" 550
KOHN, WALTER and STEPHEN J. NETTEL. Giant fluctuations in a degenerate Fermi gas 8
KRAMER, GUSTAV. *P*-wave phase shifts at 210 Mev and the photodisintegration of the deuteron 439
KRAYBILL, H. (see Smith, G. A.) 571

LANE, C. T. (see Reppy, John D.) 541
LASSILA, K. (see Breit, G.) 274
LAUER, EUGENE J. (see Gibson, Gordon) 141
LAX, B., J. G. MAVROIDES, H. J. ZEIGER, and R. J. KEYES. Infrared magnetoreflection in bismuth. I. High fields 241
——— (see Brown, R. N.) 243
——— (see Calawa, A. R.) 55
LEDERMAN, L. M. (see Devons, S.) 330
LEE, Y. K. (see Wu, C. S.) 432
LEGROS, M. (see Cocconi, V. T.) 19
LEUPOLD, H. (see Boorse, H. A.) 246
LEVINGER, B. and D. R. FRANKL. Power-induced shifts of cyclotron resonances in the valence band of germanium 12
LEVITT, R. (see Honig, A.) 93

LÉVY, MAURICE. Range of proton-antiproton annihilation 380
LEVY, R. A. Resonant spin-spin interaction between donors and acceptors in silicon 425
LINDENBAUM, S. J. and R. M. STERNHEIMER. Extension of the isobaric nucleon model for pion production in pion-nucleon and nucleon-nucleon collisions 24
LIPMAN, N. H. (see Cocconi, V. T.) 19
LITTAUER, R. M. (see Feldman, M.) 435
LOGAN, R. A. (see Chynoweth, A. G.) 57
——— (see Chynoweth, A. G.) 548
LOVE, H. M. (see McCracken, G. M.) 201
LUDWIG, G. W. and H. H. WOODBURY. Electronic structure of transition metal ions in a tetrahedral lattice 98
——— (see Ham, F. S.) 468
——— (see Woodbury, H. H.) 96
LURIÉ, D. (see Bowcock, J.) 386

MANN, LLOYD G. (see Bloom, Stewart D.) 326
MARIS, TH. A. J. (see Hillman, Peter) 107
——— (see Jacob, Gerhard) 210
MARSHAK, R. E. (see Saylor, D. P.) 266
MATTHIAS, B. T., M. PETER, H. J. WILLIAMS, A. M. CLOGSTON, E. CORENZWIT, and R. C. SHERWOOD. Magnetic moment of transition metal atoms in dilute solution and their effect on superconducting transition temperature 542
——— (see Blumberg, W. E.) 52
——— (see Blumberg, W. E.) 149
——— (see Jaccarino, V.) 251
——— (see Nagle, D. E.) 364
MAVROIDES, J. G. (see Brown, R. N.) 243
——— (see Lax, B.) 241
McCOLM, D. W. (see Hughes, V. W.) 63
McCRACKEN, G. M. and H. M. LOVE. Diffusion of lithium through tungsten 201
McCRACKEN, K. G. (see Palmeira, R. A. R.) 15
McWHORTER, A. L. (see Calawa, A. R.) 55
MEAD, J. B. and B. L. COHEN. Regularities of (d, α) reactions in heavy elements 105
MELKANOFF, M. A., D. J. PROWSE, D. H. STORK, and H. K. TICHO. $T=0$ K^+-nucleon phase shifts based on the optical model 108
MERMOD, R. (see von Dardel, G.) 333
MERRIFIELD, R. E. (see Kepler, R. G.) 503
MERRISON, A. W. (see Cocconi, V. T.) 19
MEYER, LOTHAR and F. REIF. Scattering of thermal energy ions in superfluid liquid He by phonons and He^3 atoms 1
MEYER, PETER (see Fan, C. Y.) 269
——— (see Fan, C. Y.) 272
MEYER, PH., J. PRENTKI, and Y. YAMAGUCHI. Determination of the relative Σ-Λ parity and of the ratio of asymmetry coefficients α_Λ to α_0 in hyperon decay from the pion-hyperon resonance 442
MEYER, VERENA and NORTON M. HINTZ. Charged particle and total reaction cross sections for protons at 9.85 Mev 207
MILBURN, R. H. (see von Dardel, G.) 333
MISKEL, JOHN A. (see Bloom, Stewart D.) 326
MIYAZAKI, S. (see Takayama, K.) 238
MOREL, P. (see Anderson, P. W.) 136; 282(E)
MORGAN, D. J. (see Elliott, R. J.) 366
MORINIGO, F. B. (see Nordberg, M. E.) 321
MORRISON, G. C. Cluster model interpretation of the isotopic spin selection rule in certain nuclear reactions 565
MORRISON, P. (see Chiu, Hong-Yee) 573
MOTTELSON, BEN R. and J. G. VALATIN. Effect of nuclear rotation on the pairing correlation 511
MOUNTAIN, RAYMOND D. (see Klein, Martin J.) 363
MULVEY, J. H. (see Blackie, R. F.) 384
MURTHY, V. RAMA. Isotopic composition of silver in an iron meteorite 539

NAGLE, D. E., H. FRAUENFELDER, R. D. TAYLOR, D. R. F. COCHRAN, and B. T. MATTHIAS. Temperature dependence of the internal field in ferromagnets 364
——— (see Dash, J. G.) 152
NAUENBERG, MICHAEL. Extrapolation method to determine differential scattering cross sections of unstable particles 438
NELSON, C. M. (see Crawford, J. H., Jr.) 314
NELSON, D. F. (see Collins, R. J.) 303
NETTEL, STEPHEN J. (see Kohn, Walter) 8
NEXSEN, W. E., JR. (see Coensgen, F. H.) 459
NICOL, JAMES, SIDNEY SHAPIRO, and PAUL H. SMITH. Direct measurement of the superconducting energy gap 461
NOMURA, K. C. Optical activity in tellurium 500
NORDBERG, M. E., F. B. MORINIGO, and C. A. BARNES. Comparison of the β-α angular correlations in Li^8 and B^8 321

O'MALLEY, THOMAS F. (see Spruch, Larry) 375

PALIK, E. D. (see Teitler, S.) 546
PALMEIRA, R. A. R. and K. G. McCRACKEN. Observation of a short-lived cosmic-ray solar flare increase with a high-counting-rate meson detector 15
PAULIKAS, GEORGE A. (see Allen, T. K.) 409
PEIERLS, RONALD F. Isotopic spin dependence of the pion-nucleon higher resonance 166
PELLAM, J. R. Evidence of the nature of rotating liquid helium 189; 282(E)
PETER, M. (see Jaccarino, V.) 53
——— (see Jaccarino, V.) 251
——— (see Matthias, B. T.) 542
PETERMAN, A. (see Eriksson, K. E.) 444
PICKUP, E., F. AYER, and E. O. SALANT. Single pion production in 0.96-Bev $\pi^- - p$ interactions 161
PINCUS, P. Theory of magnetic resonance in αFe_2O_3 13
PIROUÉ, P. A. (see von Dardel, G.) 333
PONTINEN, R. E. and T. M. SANDERS, JR. New electron spin resonance spectrum in antimony-doped germanium 311
POWELL, M. J. D., J. R. GABRIEL, and D. F. JOHNSTON. Ground-state splitting for d^5 ^6S ions in a cubic field 145
PRENTKI, J. (see Meyer, Ph.) 442
PREPOST, R. (see Feher, G.) 515
——— (see Hughes, V. W.) 63
PRICE, PETER J. (see Keyes, Robert W.) 473
PROWSE, D. J. (see Melkanoff, M. A.) 108
PYLE, ROBERT V. (see Allen, T. K.) 409

RADOJIČIĆ, D. (see Rushbrooke, J. G.) 567
RAMA MURTHY, V. Isotopic composition of silver in an iron meteorite 539
RAMSEY, N. F. (see Goldenberg, H. M.) 361
READ, P. L. and E. KATZ. Ionic Hall effect in sodium chloride 466
REDIKER, R. H. (see Calawa, A. R.) 55
REIF, F. (see Meyer, Lothar) 1
REIK, H. G., H. RISKEN, and G. FINGER. Theory of hot-electron effects in many-valley semiconductors in the region of high electric field 423
REITER, R. A., T. A. ROMANOWSKI, R. B. SUTTON, and B. G. CHIDLEY. Precise measurements of the mean lives of μ^+ and μ^- mesons in carbon 22
——— (see Bertram, W. J., Jr.) 61
REPPY, JOHN D., DAVID DEPATIE, and C. T. LANE. Helium II in rotation 541
RÉSIBOIS, P. Approach to equilibrium in quantum systems 411
RESTER, D. H. (see Durham, F. E.) 202
RISKEN, H. (see Reik, H. G.) 423
RIVIERE, A. C. and D. R. SWEETMAN. Dissociation of H_2^+ and He^- by electric fields 560
ROMANOWSKI, T. A. (see Bertram, W. J., Jr.) 61
——— (see Reiter, R. A.) 22
ROSENBERG, LEONARD (see Spruch, Larry) 375
ROSS, MARC and GORDON SHAW. $\Lambda\pi$ resonance and possible determination of the *KYN* parities 578
RUBY, S. L. and D. I. BOLEF. Acoustically modulated γ rays from Fe^{57} 5
RUDERFER, MARTIN. First-order terrestrial ether drift experiment using the Mössbauer radiation 191
RUDERMAN, H. (see Gomez, R.) 170
RUDIN, H. (see Baumgartner, E.) 154
RUPPEL, H. M. (see Breit, G.) 274
RUSH, J. J., T. I. TAYLOR, and W. W. HAVENS, JR. Proton motions in ammonium halides by slow neutron cross-section measurements 507
RUSHBROOKE, G. S. (see Elliott, R. J.) 366
RUSHBROOKE, J. G. and D. RADOJIČIĆ. Search for resonance in π-π interaction in π-N scattering at 0.96 Bev 567
RYTER, CH. Direct measurement of the electron density at the nucleus in metallic lithium at liquid helium temperature 10

SACHS, A. M. (see Feher, G.) 515
SALAM, ABDUS and J. C. WARD. $\Delta I = \frac{1}{2}$ rule 390
SALANT, E. O. (see Pickup, E.) 161
SALZMAN, FREDA and GEORGE SALZMAN. Single-virtual-boson-exchange interaction in high-energy collisions 377
SALZMAN, GEORGE (see Salzman, Freda) 377
SANDERS, T. M., JR. (see Pontinen, R. E.) 311
SANDS, M. (see Gomez, R.) 170
SANDWEISS, J. (see Smith, G. A.) 571
SAYLOR, D. P., R. A. Bryan, and R. E. MARSHAK. Boundary condition model for proton-proton scattering 266
SCHAWLOW, A. L. (see Collins, R. J.) 303
SEEGER, P. A. (see Bardin, R. K.) 323
SELOVE, W. Generalized isobar model,

and the pionic form factor of the nucleon 163
SHAPIRO, G. (see Devons, S.) 330
SHAPIRO, SIDNEY (see Nicol, James) 461
SHAW, GORDON (see Ross, Marc) 578
SHEARD, F. W. and J. M. ZIMAN. Thermal conductivity of isotopic mixtures of solid helium 138
SHEPPARD, A. P. (see Derr, V. E.) 316
SHERMAN, A. E. (see Coensgen, F. H.) 459
SHERRILL, M. D. (see Glover, R. E., III) 248
SHERWOOD, R. D. (see Matthias, B. T.) 542
SHONLE, JOHN I. Negative pion-proton elastic scattering at 600 to 750 Mev 156
SIGNELL, PETER S. Quantitative evidence of one-pion exchange effects in p-p scattering 474
SIMMS, P. (see Wu, C. S.) 432
SIMPSON, J. A. (see Fan, C. Y.) 269
——— (see Fan, C. Y.) 272
SINGER, S. F. Latitude and altitude distribution of geomagnetically trapped protons 300
SIRLIN, A. (see Behrends, R. E.) 476
SLICHTER, C. P. (see Holton, W. C.) 197
SLIFKIN, LAWRENCE (see Childs, Charles B.) 502
SMITH, ALEX G. (see Carr, Thomas D.) 418
SMITH, G. A., H. COURANT, E. FOWLER, H. KRAYBILL, J. SANDWEISS, and H. TAFT. π^+-proton scattering cross sections by Chew-Low extrapolation 571
SMITH, PAUL H. (see Nicol, James) 461
SNOW, G. A. (see Day, T. B.) 112
SONETT, C. P. Coupling of the solar wind and the exosphere 46
——— (see Coleman, P. J., Jr.) 43
SOROKIN, P. P. and M. J. STEVENSON. Stimulated infrared emission from trivalent uranium 557
SPRUCH, LARRY, THOMAS F. O'MALLEY, and LEONARD ROSENBERG. Modification of effective-range theory in the presence of a long-range potential 375
STANGHELLINI, A. (see Amati, D.) 524
STARNES, ARTHUR J. (see Hess, Wilmot N.) 48
STEINMANN, WULF. Experimental verification of radiation of plasma oscillations in thin silver films 470
STERNHEIMER, R. M. (see Lindenbaum, S. J.) 24
STEVENSON, M. J. (see Sorokin, P. P.) 557
STORK, D. H. (see Melkanoff, M. A.) 108
STRIEBEL, H. R. (see Baumgartner, E.) 154
SUHL, H. (see Jaccarino, V.) 251
SUTTON, R. B. (see Bertram, W. J., Jr.) 61
——— (see Reiter, R. A.) 22
SWANSON, WILLIAM P., DUANE C. GATES, THOMAS L. JENKINS, and ROBERT W. KENNEY. Photoproduction of charged mesons from deuterium and the π^-/π^+ ratio 336
———, DUANE C. GATES, THOMAS L. JENKINS, and ROBERT W. KENNEY. Total cross section for $\gamma + n - \pi^- + p$ near threshold by Chew-Low extrapolation 339
SWEETMAN, D. R. (see Riviere, A. C.) 560

TAFT, H. (see Smith, G. A.) 571
TAKAYAMA, K., H. IKEGAMI, and S. MIYAZAKI. Plasma resonance in a radio-frequency probe 238
TALMAN, R. (see Gomez, R.) 170
TARSKI, JAN (see Cook, L. F., Jr.) 585
TAUC, JAN and EMIL ANTONČÍK. Optical observation of spin-orbit interaction in germanium 253
TAYLOR, R. D. (see Dash, J. G.) 152
——— (see Nagle, D. E.) 364
TAYLOR, T. I. (see Rush, J. J.) 507
TEITLER, S. and E. D. PALIK. Voigt effect in semiconductors 546
THOMAS, D. E. (see Chynoweth, A. G.) 57
THOMAS, D. G. and J. J. HOPFIELD. Direct observation of exciton motion in CdS 505
THOULESS, D. J. and J. G. VALATIN. Rotating self-consistent fields and rotational states of nuclei 509
TICHO, HAROLD K. (see Alston, Margaret) 520
——— (see Melkanoff, M. A.) 108
TOWNES, C. H. Sensitivity of microwave spectrometers using maser techniques 428
TROUNSON, E. P. (see Brown, R. W.) 472
TUBIS, ARNOLD and JACK L. URETSKY. Interpretation of the Berkeley anomaly in high-energy p-d collisions 513
TURNER, E. H. Interaction of phonons and spin waves in yttrium iron garnet 100
TYREN, H. (see Hillman, Peter) 107

URETSKY, JACK L. (see Tubis, Arnold) 513

VALATIN, J. G. (see Mottelson, Ben R.) 511
——— (see Thouless, D. J.) 509

VARNEY, ROBERT N. Mobility of hydrogen ions 559
VARNUM, C. M. (see Bouchiat, M. A.) 373
VITALE, B. (see Amati, D.) 524
VIVARGENT, M. (see von Dardel, G.) 333
von DARDEL, G., D. H. FRISCH, R. MERMOD, R. H. MILBURN, P. A. PIROUÉ, M. VIVARGENT, G. WEBER, and K. WINTER. Total cross sections for p, $\bar{p}$, $K^{\pm}$, and $\pi^{\pm}$ on hydrogen between 3 and 10 Gev/c 333

WALKER, E. J. and HENRY A. FAIRBANK. Thermal conductivity of solid He^3 139
WALKER, R. L. (see Kilner, J. R.) 518
WANNIER, G. H. (see Chynoweth, A. G.) 57
WARD, J. C. (see Salam, Abdus) 390
WATKINS, G. D. (see Ham, F. S.) 468
WATSON, R. E. (see Freeman, A. J.) 498
WEBER, G. (see von Dardel, G.) 333
WEINBERG, STEVEN (see Bernstein, Jeremy) 481
WERNICK, J. H. (see Jaccarino, V.) 53
——— (see Jaccarino, V.) 251
WESSEL, P. (see Brown, R. W.) 472
WETHERELL, A. M. (see Ashmore, A.) 576
WHEATLEY, J. C. (see Anderson, A. C.) 133
WILLIAMS, A. J. (see Bozorth, R. M.) 148
WILLIAMS, H. J. (see Matthias, B. T.) 542
WINTER, K. (see von Dardel, G.) 333
WOJCICKI, STANLEY G. (see Alston, Margaret) 520
WOLFF, P. A. (see Chynoweth, A. G.) 548
WONG, HOW-SEN. Effective-range formula for photopion production from pions 70
WOODBURY, H. H. and G. W. LUDWIG. Vacancy interactions in silicon 96
——— (see Ham, F. S.) 468
——— (see Ludwig, G. W.) 98
WU, C. S., Y. K. LEE, N. BENCZER-KOLLER, and P. SIMMS. Frequency distribution of resonance line versus delay time 432

YAGODA, HERMAN. Star production by trapped protons in the inner radiation belt 17
YAMAGUCHI, Y. (see Meyer, Ph.) 442
YODH, G. B. (see Fields, T. H.) 69
YOUNG, ROBERT A. and K. C. CLARK. Rate of the three-body atomic oxygen reaction for the excitation of the airglow OI (5577 A) line 320

ZACHARIASEN, F. (see Drell, S. D.) 66
ZAPPA, L. (see Bisi, A.) 59
ZEIGER, H. J. (see Lax, B.) 241
ZIMAN, J. M. (see Sheard, F. W.) 138
ZIOCK, K. (see Hughes, V. W.) 63

520
548

70

96
468
98

432

17
442
69

320

66
59
241
138
63